



UNIVERSITY OF PISA  
DEPARTMENT OF VETERINARY SCIENCES  
Ph.D. in Veterinary Sciences

Kristina Tekavec

**MORPHOLOGICAL AND  
IMMUNOHISTOCHEMICAL CHARACTERISTICS  
OF CANINE NERVE SHEATH TUMORS**

Doctoral dissertation

Academic year 2021/22





UNIVERSITY OF PISA  
DEPARTMENT OF VETERINARY SCIENCES  
Ph.D. in Veterinary Sciences

Doctoral dissertation

**MORPHOLOGICAL AND  
IMMUNOHISTOCHEMICAL CHARACTERISTICS  
OF CANINE NERVE SHEATH TUMORS**

Candidate: Kristina Tekavec, DVM

Supervisor: Prof. Carlo Cantile, DVM, Ph.D.

Co-Supervisor: Assist. Prof. Tanja Švara, DVM, Ph.D.

Academic year 2021/22

## TABLE OF CONTENTS

|   |    |
|---|----|
| TABLE OF CONTENTS .....   | 4  |
| LIST OF ABBREVIATIONS .....   | 7  |
| LIST OF TABLES .....  | 10 |
| LIST OF FIGURES .....   | 11 |
| ABSTRACT .....  | 13 |
| 1 INTRODUCTION.....   | 14 |
| 2 LITERATURE REVIEW.....  | 16 |
| 2.1 NERVE ANATOMY .....   | 16 |
| 2.2 NERVE SHEATH TUMORS .....   | 17 |
| 2.2.1 Classification of nerve sheath tumors.....                                    | 17 |
| 2.2.2 Location of nerve sheath tumors .....   | 18 |
| 2.2.3 Genetic disorders and other factors associated with nerve sheath tumors ..... | 19 |
| 2.2.4 Nerve sheath tumors in other animal species .....                             | 19 |
| 2.2.5 Diagnosis of nerve sheath tumors.....   | 20 |
| 2.2.6 Morphological features of nerve sheath tumors .....                           | 20 |
| 2.2.6.1 Schwannoma .....  | 20 |
| 2.2.6.2 Neurofibroma .....  | 22 |
| 2.2.6.3 Perineurioma .....  | 23 |
| 2.2.6.4 Malignant nerve sheath tumor.....   | 24 |
| 2.2.6.4.1 Malignant nerve sheath tumor with divergent differentiation .....         | 25 |
| 2.2.6.4.2 Epithelioid malignant nerve sheath tumor .....                            | 26 |
| 2.2.6.4.3 Malignant perineurioma.....   | 26 |
| 2.2.7 Grading of malignant nerve sheath tumors .....                                | 26 |
| 2.2.8 Immunohistochemical features of nerve sheath tumors .....                     | 27 |

|         |  |    |
|---------|--|----|
| 2.2.8.1 | Sox10.....   | 29 |
| 2.2.8.2 | GFAP.....  | 29 |
| 2.2.8.3 | Claudin-1.....   | 30 |
| 2.2.8.4 | CNPase.....  | 30 |
| 2.2.8.5 | Ki-67.....   | 31 |
| 2.2.8.6 | H3K27me3.....  | 31 |
| 2.2.9   | Ultrastructural features of nerve sheath tumors.....       | 32 |
| 2.2.10  | Other tumors involving the nerve.....                      | 32 |
| 3       | MATERIALS AND METHODS.....                                 | 34 |
| 3.1     | SAMPLES.....   | 34 |
| 3.2     | HISTOPATHOLOGY.....  | 34 |
| 3.3     | IMMUNOHISTOCHEMISTRY.....                                  | 35 |
| 3.3.1   | Evaluation of immunohistochemical staining.....            | 40 |
| 3.4     | STATISTICAL ANALYSIS.....                                  | 46 |
| 4       | RESULTS.....   | 47 |
| 4.1     | SIGNALMENT AND CLINICAL FINDINGS.....                      | 47 |
| 4.2     | HISTOPATHOLOGY AND IMMUNOHISTOCHEMISTRY.....               | 53 |
| 4.2.1   | Benign nerve sheath tumors.....                            | 54 |
| 4.2.1.1 | Histopathological features of BNSTs.....                   | 54 |
| 4.2.1.2 | Immunohistochemical features of BNSTs.....                 | 55 |
| 4.2.2   | Malignant nerve sheath tumors.....                         | 61 |
| 4.2.2.1 | Histopathological features of MNSTs.....                   | 61 |
| 4.2.2.2 | Immunohistochemical features of MNSTs.....                 | 63 |
| 5       | DISCUSSION.....  | 81 |
| 5.1     | CLASSIFICATION AND GRADING OF CANINE NERVE SHEATH TUMORS.. | 81 |

|     |   |     |
|-----|---|-----|
| 5.2 | SOX-10, CLAUDIN-1, GFAP, CNPase, AND Ki-67 IN THE DIAGNOSIS OF<br>CANINE NERVE SHEATH TUMORS..... | 86  |
| 5.3 | LOSS OF H3K27me3 EXPRESSION IN CANINE NERVE SHEATH TUMORS ...                                     | 89  |
| 6   | CONCLUSIONS .....   | 93  |
| 7   | REFERENCES.....   | 94  |
| 8   | OTHER ACTIVITIES.....   | 113 |
| 9   | SUPPLEMENTARY MATERIAL .....  | 118 |
| 10  | ACKNOWLEDGMENTS .....   | 124 |

## LIST OF ABBREVIATIONS

|          |  |
|----------|--|
| BNST     | benign nerve sheath tumor  |
| CNS      | central nervous system   |
| CNPase   | 2',3'-Cyclic-nucleotide 3'-phosphodiesterase   |
| DNA      | deoxyribonucleic acid  |
| EED      | embryonic ectoderm development   |
| EMA      | epithelial membrane antigen  |
| EZH1     | enhancer of zeste homologue 1  |
| EZH2     | enhancer of zeste homologue 2  |
| FFPE     | formalin-fixed paraffin-embedded   |
| FNCLCC   | national federation of French comprehensive cancer centers<br>(French: <i>Fédération Nationale des Centres de lutte contre le cancer</i> ) |
| Glut1    | erythrocyte glucose transporter protein  |
| GFAP     | glial fibrillary acidic protein  |
| HE       | hematoxylin and eosin  |
| HPF      | high-power field   |
| H3K27me3 | trimethylation of lysine 27 on histone H3  |
| IHC      | immunohistochemistry/immunohistochemical   |
| IF       | intermediate filament  |
| LMN      | lower motor neuron   |
| MAG      | myelin-associated glycoprotein   |
| MBP      | myelin basic protein   |
| MNST     | malignant nerve sheath tumor   |

|       |                                      |
|-------|--------------------------------------|
| MUC1  | mucin 1                              |
| MW    | microwave oven                       |
| NA    | not applicable                       |
| ND    | no data                              |
| NSE   | neuron specific enolase              |
| NF1   | Neurofibromatosis type 1             |
| NF2   | Neurofibromatosis type 2             |
| NF200 | Neurofilament protein 200            |
| NGFR  | nerve growth factor receptor         |
| NST   | nerve sheath tumor                   |
| Olig2 | oligodendrocyte transcription factor |
| PNS   | peripheral nervous system            |
| PNST  | peripheral nerve sheath tumor        |
| PRC2  | Polycomb repressive complex          |
| PLP   | proteolipid protein                  |
| P0    | protein 0                            |
| P1    | protein 1                            |
| P2    | protein 2                            |
| P22   | peripheral membrane protein          |
| RBBP4 | retinoblastoma binding protein 4     |
| RBBP7 | retinoblastoma binding protein 7     |
| RTU   | ready to use                         |
| Sox10 | Sry-related HMg-Box gene 10          |

|       |                                  |
|-------|----------------------------------|
| STS   | soft tissue sarcoma              |
| SUZ12 | suppressor of zeste 12           |
| TEM   | transmission electron microscopy |
| UMN   | upper motor neuron               |
| WHO   | World Health Organization        |

## LIST OF TABLES

|  |    |
|--|----|
| <b>Table 1:</b> Grading system for STS modified for MNST. ....   | 35 |
| <b>Table 2:</b> Details of the primary antibodies and immunohistochemical protocols. ....  | 39 |
| <b>Table 3:</b> Signalment, clinical features, and tumor localization of the dogs included in the study.<br>.....  | 47 |
| <b>Table 4:</b> Tumor types and results of immunohistochemical stainings for each examined case.<br>.....  | 73 |
| <b>Table 5:</b> Results of immunohistochemical staining for Sox10, claudin-1, GFAP, and CNPase<br>in different subtypes and variants of canine NSTs. ....                      | 78 |
| <b>Table 6:</b> Results of immunohistochemical analysis for Sox10, Claudin-1, GFAP, CNPase, and<br>proliferation index Ki-67 in each subtype and variant of NSTs. ....         | 79 |
| <b>Table 7:</b> Immunohistochemical analysis of H3K27me3 expression in 68 canine NSTs divided<br>by type, subtype, and histological grade using the 4-tier scoring scale. .... | 80 |

## LIST OF FIGURES

|   |    |
|---|----|
| <b>Figure 1:</b> Diagram of the basic architecture of the nerve and schematics of the essential components of a nerve fascicle..... | 17 |
| <b>Figure 2:</b> Positive controls for immunohistochemical staining of Ki-67, CNPase, GFAP, and claudin-1 .....                     | 37 |
| <b>Figure 3:</b> Positive controls for immunohistochemical staining of Sox10 and H3K27me3 .....                                     | 38 |
| <b>Figure 4:</b> Evaluation of immunohistochemical expression of Sox10.....   | 41 |
| <b>Figure 5:</b> Evaluation of immunohistochemical expression of claudin-1 .....  | 42 |
| <b>Figure 6:</b> Evaluation of immunohistochemical expression of GFAP.....  | 43 |
| <b>Figure 7:</b> Evaluation of immunohistochemical expression of CNPase .....   | 44 |
| <b>Figure 8:</b> Variable proliferation activity detected by Ki-67 proliferation index .....  | 44 |
| <b>Figure 9:</b> Evaluation of immunohistochemical expression of H3K27me3 .....   | 45 |
| <b>Figure 10:</b> Excised tumor from the brachial plexus submitted for histopathologic examination .....                            | 53 |
| <b>Figure 11:</b> Histopathological and immunohistochemical characteristics of neurofibroma .....                                   | 57 |
| <b>Figure 12:</b> Histopathological and immunohistochemical characteristics of schwannoma.....                                      | 58 |
| <b>Figure 13:</b> Histopathological and immunohistochemical characteristics of hybrid benign nerve sheath tumor .....               | 59 |
| <b>Figure 14:</b> Histopathological and immunohistochemical characteristics of nerve sheath myxoma .....                            | 60 |
| <b>Figure 15:</b> Histopathological and immunohistochemical characteristics of conventional MNST .....                              | 65 |
| <b>Figure 16:</b> Histopathological and immunohistochemical characteristics of conventional MNST.....                               | 66 |
| <b>Figure 17:</b> Histopathological and immunohistochemical characteristics of conventional MNST.....                               | 67 |
| <b>Figure 18:</b> Histopathological and immunohistochemical characteristics of MNST with divergent differentiation .....            | 68 |
| <b>Figure 19:</b> Histopathological and immunohistochemical characteristics of MNST with perineurial differentiation.....           | 69 |

|   |    |
|---|----|
| <b>Figure 20:</b> Histopathological and immunohistochemical characteristics of epithelioid MNST .....   | 70 |
| <b>Figure 21:</b> Comparison of proliferation index Ki-67 between malignant nerve sheath tumors and benign nerve sheath tumors, and comparison of proliferation index Ki-67 between different grades of malignant nerve sheath tumors. .... | 71 |
| <b>Figure 22:</b> Correlation between proliferation index Ki-67 and mitotic count per 10 high power fields .....  | 71 |
| <b>Figure 23:</b> Comparison of the number of mitoses per ten high-power fields based on H3K27me3 expression .....  | 72 |
| <b>Figure 24:</b> Comparison of the Ki-67 proliferation index fields based on H3K27me3 expression .....   | 72 |

## ABSTRACT

**Keywords:** dog; nerve sheath tumor; histopathology; immunohistochemistry; Sox10; claudin-1; GFAP; CNPase; Ki-67; methylation; H3K37me3.

Nerve sheath tumors (NSTs) are a group of tumors that originate from Schwann cells, perineurial cells, and/or endoneurial or epineurial fibroblasts. In veterinary pathology, the terminology of NSTs remains inconsistent and sometimes confusing, and many pathologists are guided in practice by the human classification of such tumors. In particular, malignant NSTs often lack specific histopathological and immunohistochemical (IHC) features, making them difficult to distinguish from other neoplastic lesions. This study aimed to histopathologically reevaluate archival samples of canine NSTs and assess their reactivity for the IHC markers Sox10, claudin-1, GFAP, CNPase, Ki-67, and H3K27me3. Based on the results, we classified the tumors according to the latest human WHO classification and evaluated the potential diagnostic utility of the IHC markers tested. Of 79 NSTs, 12 cases were diagnosed as benign NSTs, including six neurofibromas, three nerve sheath myxomas, two hybrid NSTs (perineurioma/neurofibroma and perineurioma/schwannoma), and one schwannoma. Sixty-seven tumors were malignant NSTs, including 56 conventional, four perineural, one epithelioid NST, and six malignant NSTs with divergent differentiation. We identified Sox10, claudin-1, GFAP, and Ki-67 as useful IHC markers whereas CNPase was found to have no role in the diagnosis of canine NSTs. We found complete loss of H3K27me3 expression in 25% of NSTs (17/68), most of which were malignant, except for one benign NST – a neurofibroma. We believe that H3K27me3, in combination with other IHC markers, may also be useful for the diagnosis of NSTs. Considering our results and incorporating data from the literature, we believe that an updated classification of NSTs in dogs using the proposed IHC panel could largely follow the recent WHO classification of such tumors in humans although prospective studies monitoring the clinical course of the disease are needed to assess its prognostic value.

## 1 INTRODUCTION

Nerve sheath tumors (NSTs) are a group of tumors that arise from Schwann cells, perineurial cells, and/or endoneurial or epineurial fibroblasts. Depending on the cell type(s) from which they originate, there are four main subtypes of NST: schwannoma, perineurioma, and neurofibroma, which are benign, and malignant NST (MNST) (Higgins et al., 2016). In dogs, these are rare tumors that most commonly arise in the spinal nerve roots, particularly in the cervicothoracic spinal cord segment, and in the brachial plexus (Vandevelde et al., 2012; Higgins et al., 2016). The clear histopathological criteria for classifying NSTs in animals have not yet been established (Schöniger and Summers, 2009) and the current terminology for NSTs in veterinary texts is often inconsistent and confusing (Higgins et al., 2016). Because many similarities have been noted between NSTs in dogs and humans, many veterinary pathologists follow the human classification of such tumors in practice (Schöniger and Summers, 2009; Higgins et al., 2016). The latest version of the human WHO Classification of Tumors of the Central Nervous System, published in 2021, classifies tumors of the cranial and paraspinal nerves as follows: schwannoma, neurofibroma, perineurioma, hybrid NST, malignant melanotic NST, and paraganglioma (Louis et al., 2021).

Diagnosis of NSTs is often challenging, especially when distinguishing MNST from soft tissue sarcoma (STS) or other histopathologic mimics or when differentiating low-grade MNST that do not have obvious malignancy criteria from benign NST (BNST) (Rodriguez et al., 2012; Lanigan et al., 2021). The location of the tumor contributes significantly to the diagnosis of NSTs. In the absence of an anatomical relationship to the nerve, the diagnosis can be made based on its morphological, immunohistochemical (IHC), and ultrastructural features although these are often of limited diagnostic value (Rodriguez et al., 2012; Higgins et al., 2016; Lucas et al., 2020). IHC is an important tool in tumor diagnostics because it helps determine tumor origin and, among other things, is increasingly used to provide prognostic information and detect molecular alterations in tumors (Magaki et al., 2019). Unfortunately, there is still no optimal panel of IHC markers for the diagnosis of NSTs (Higgins et al., 2016). While many different markers have been tested and reported to be differentially expressed in NSTs, their sensitivity and specificity are limited because their expression is often lost in MNSTs or they are also expressed to varying degrees in other tumors (Higgins et al., 2016; Lucas et al., 2020; Lanigan et al., 2021).

This study aimed to histopathologically reevaluate archival specimens previously diagnosed as NSTs and to perform IHC for selected IHC markers to evaluate their potential utility for the diagnosis of NST in dogs. Samples were retrieved from the tissue archives of the Laboratory of Veterinary Neuropathology of the Department of Veterinary Sciences, University of Pisa (Italy), and the Institute of Pathology, Wild Animals, Fish and Bees of the Veterinary Faculty, University of Ljubljana (Slovenia). We thoroughly studied the existing literature on IHC features of NSTs from human and veterinary medicine and selected a panel of IHC markers based on the results of previous studies that indicated their potential role in the diagnosis of NST: Sry-related HMg-Box gene 10 (Sox10), claudin-1, glial fibrillary acidic protein (GFAP), 2',3'-Cyclic nucleotide 3'-phosphohydrolase (CNPase), proliferation index Ki-67, and trimethylation of lysine 27 on histone H3 (H3K27me3). Based on the results, we classified canine tumors according to the latest human WHO classification. We also graded MNSTs to evaluate the potential correlation of grading with histopathologic features and IHC results and to further investigate the potential applicability of the STS grading system in the diagnosis of NSTs.

## 2 LITERATURE REVIEW

### 2.1 NERVE ANATOMY

Nerves consist of bundles of neuronal processes – axons – encased in varying amounts of myelin produced by myelinating Schwann cells. Myelin consists of 70% lipids (cholesterol, galactosphingolipids) and 30% myelin-specific proteins (myelin basic protein (MBP), myelin-associated glycoprotein (MAG), protein 0, 1 and 2 (P0, P1, P2), peripheral membrane protein 22 (P22), and proteolipid protein (PLP)). The thickness of myelin depends on the diameter of the axon – larger axons have thicker myelin sheaths whereas small, unmyelinated axons are covered exclusively by a single layer of Schwann cell membrane. One Schwann cell envelops a single axon and forms an "internode" that covers on average about 1 to 1.5 mm of the length of an axon. Between two adjacent internodes are narrow gaps of the unmyelinated axon called nodes of Ranvier (Lanigan et al., 2021).

Each mature peripheral nerve is composed of multiple fascicles of axon-Schwann cell units surrounded by the endoneurium, a collagen-rich and vascularized connective tissue. The individual fascicles are ensheathed by the perineurium, which is part of a blood-nerve barrier that protects the interior of the nerves from unwanted cells, infections, and harmful molecules. Accordingly, the perineurial cells are covered by a basal lamina and are connected by desmosomes and tight junctions. The outer layer, which bundles all the nerve fascicles into a single nerve structure and separates them from the surrounding tissue, is the epineurium, composed mainly of collagen and adipocytes (**Figure 1**) (Kucenas, 2015; Higgins et al., 2016; Jessen and Mirsky, 2019).

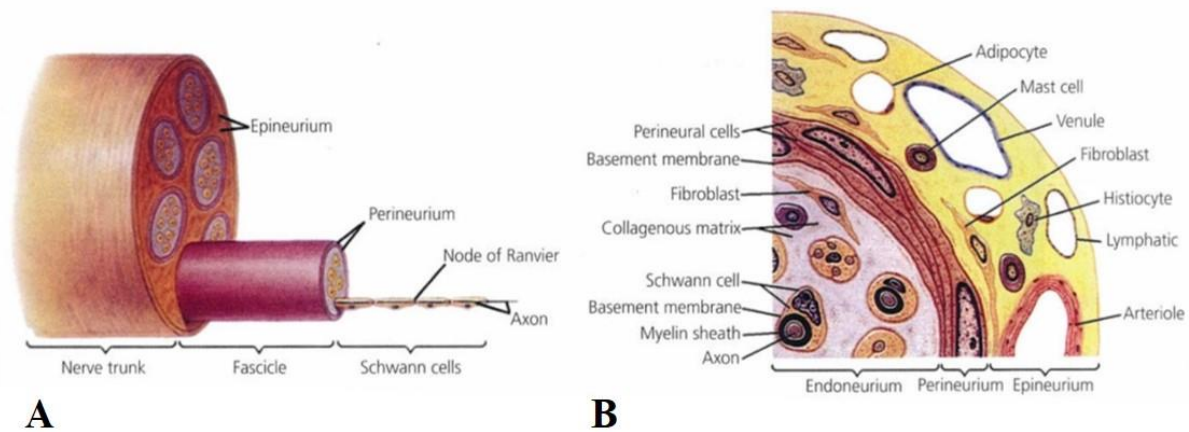


**Figure 1:** (A) Diagram of the basic architecture of the nerve. (B) Schematics of the essential components of a nerve fascicle (Higgins et al., 2016) (Reproduced from *Tumors in Domestic Animals*, 5th edn. John Wiley & Sons, Inc., pp 882, 2016 with copyright permission from Wiley Blackwell).

## 2.2 NERVE SHEATH TUMORS

Nerve sheath tumors (NSTs) are a group of tumors that originate from Schwann cells, perineurial cells, and/or epineurial or endoneurial fibroblasts. Accordingly, the four major subtypes of NSTs are schwannoma (benign tumor composed exclusively of neoplastic Schwann cells), perineurioma (benign tumor composed of neoplastic perineurial cells), neurofibroma (benign tumor composed of a mixture of neoplastic Schwann cells, perineurial cells, and fibroblasts), and malignant NST (MNST) (Higgins et al., 2016).

Although the most common and widely used term for this type of tumors is peripheral nerve sheath tumors (PNSTs), we decided to follow de Lahunta's suggestion to omit the "peripheral" with nerves because all nerves are part of the peripheral nervous system and therefore the word itself is redundant and unnecessary (de Lahunta, 2010).

### 2.2.1 Classification of nerve sheath tumors

The clear histopathological criteria for classifying NSTs in animals have not yet been established (Schöniger and Summers, 2009) and the current terminology associated with NSTs in the veterinary literature is often confusing, arbitrary, and inconsistent (Higgins et al., 2016). The last official classification of NSTs in veterinary medicine was published in 1999. In it, tumors were divided into benign and malignant PNSTs. Benign tumors were further subdivided

into schwannomas and neurofibromas while malignant tumors were malignant schwannomas and neurofibrosarcomas (Koestner, 1999).

Some authors refer to the term “nerve sheath tumor” in general in their publication, which is further subdivided into “benign NSTs” or “malignant NSTs”. In the case of benign NSTs (BNSTs), it seems that despite some histopathological and ultrastructural differences, most of them have similar clinical behavior and, thus, a similar prognosis (Schöniger and Summers, 2009).

Many of the NSTs observed in humans are also found in domestic animals, including their histological subtypes (Schöniger and Summers, 2009; Lanigan et al., 2021). Because of the marked gross and histologic similarities between such tumors in dogs and humans, many veterinary pathologists in practice follow the criteria and terminology of the human classification of NSTs (Higgins et al., 2016).

The latest, fifth edition and the sixth version of the human WHO Classification of Tumors of the Central Nervous System, published in 2021, divides tumors of the cranial and paraspinal nerves into the following major subtypes: schwannoma, neurofibroma, perineurioma, hybrid nerve sheath tumor, malignant melanotic nerve sheath tumor, malignant peripheral nerve sheath tumor, and paraganglioma (Louis et al., 2021).

### **2.2.2 Location of nerve sheath tumors**

Considering the distance of tumors from central nervous system components, NSTs may belong to the root group, which includes nerves adjacent to the brain, brainstem, or spinal cord, the plexus group, which includes the brachial plexus or lumbosacral plexus, and the peripheral group, which includes tumors occurring distal to the brachial plexus or lumbosacral plexus (Basa et al., 2020).

In dogs, NSTs arise most commonly at the roots of the spinal nerves, especially in the cervicothoracic segment of the spinal cord and in the brachial plexus. Less commonly, they originate from cranial nerves (Vandeveldt et al., 2012; Higgins et al., 2016). Occasionally, they arise in the skin (Gaitero et al., 2008; Higgins et al., 2016). Individual cases have also been reported in the testis (Rothwell et al., 1986), diaphragm (Anderson et al., 1999), eye (Sato et al., 2005), spleen (Bergmann et al., 2009), tongue, intestine (Schöniger and Summers, 2009),

liver (Park et al., 2011), heart (Thomason et al., 2015), eyelid (Vom Hagen et al., 2015), lung (Silva et al., 2017), adrenal gland (Ichikawa et al., 2018), and urinary bladder (Lee et al., 2020).

### **2.2.3 Genetic disorders and other factors associated with nerve sheath tumors**

In humans, many of the specific NSTs are associated with particular germline or somatic mutations and occur as part of familial tumor syndromes – Neurofibromatosis type 1 (NF1), Neurofibromatosis type 2 (NF2) and Schwannomatosis (Louis et al., 2016a). In veterinary medicine, we generally lack knowledge of genetic disorders associated with the occurrence of neoplasms although individual cases of different tumors in domestic animals caused by genetic mutations have been described (Lanigan et al., 2021). A hereditary predisposition to NSTs, similar to NF in humans, is suspected only in cattle so far (Osum et al., 2021).

About 10% of MNSTs in humans occur after radiation therapy (Yamanaka and Hayano, 2017). Ionizing radiation has a known carcinogenic potential (Dracham et al., 2018) which can cause DNA breaks in directly exposed tissue or indirectly lead to oxidative damage through the formation of free radicals (Khanna et al., 2021). In nerves, which are very sensitive to radiotherapy, it causes atypical proliferation of endothelial fibroblasts and Schwann cells. It can also cause lymphatic obstruction and perineural vascular fibrosis, which allows mutant Schwann cells to evade immune surveillance and proliferate (Yamanaka and Hayano, 2017). Some cases of radiation-induced bone tumors in dogs have been reported in the literature (Gillette et al., 1990; Hosoya et al., 2008) while to our knowledge no association between MNST and radiotherapy has been found in dogs or other animal species, excluding experimental animals.

### **2.2.4 Nerve sheath tumors in other animal species**

Besides dogs, NSTs are relatively common in cattle, the latter being the only species in which a hereditary predisposition is suspected (Osum et al., 2021). Occasional cases of NSTs have also been described in cats (Watrous et al., 1999; Schulman et al., 2009; Buza et al., 2012), horses (Sundberg et al., 1977; Schöniger and Summers, 2009; Schöniger et al., 2011), goats (Veazey et al., 1993; Ramírez et al., 2007), pigs (Resende et al., 2015; Stilwell and Rissi, 2019), chickens (Ochi et al., 2008; Schöniger and Summers, 2009), and fish (Armando et al., 2021;

Brocca et al., 2021). The literature also contains individual reports of NSTs in some other animal species, such as hamsters (Snyder et al., 2007) and snakes (Ramis et al., 1998).

### **2.2.5 Diagnosis of nerve sheath tumors**

Diagnosis of NSTs is often challenging. Different subtypes and variants can be morphologically very similar and are also difficult to distinguish from many other tumors that originate outside the peripheral nervous system (PNS) (Lanigan et al., 2021). The distinction between low-grade MNST and BNST can also be difficult; MNST may lack obvious criteria for malignancy, and BNST may sometimes have degenerative changes and mislead the pathologist to consider it as malignant neoplasm (Rodriguez et al., 2012; Lanigan et al., 2021). Sometimes, some non-neoplastic proliferative lesions of the PNS also mimic NSTs histologically (Lanigan et al., 2021). In particular, to distinguish MNSTs from other soft tissue sarcomas, tumor location contributes significantly to the diagnosis of MNST. Major nerve involvement without evidence of another specific line of differentiation or development of MNST in a previous BNST is two indicators of MNST. Without obvious relation to a nerve, the diagnosis may be made based on morphological, immunohistochemical (IHC), and ultrastructural features of the tumor cells although these are often nonspecific and of limited diagnostic value (Rodriguez et al., 2012; Higgins et al., 2016; Lucas et al., 2020).

### **2.2.6 Morphological features of nerve sheath tumors**

#### **2.2.6.1 Schwannoma**

Schwannomas are benign tumors arising exclusively from Schwann cells. They usually appear as nodular, well-circumscribed, and encapsulated masses (Higgins et al., 2016; Lanigan et al., 2021).

Several histologic variants have been identified in humans, including conventional schwannoma, cellular schwannoma, and plexiform schwannoma. Conventional schwannoma in humans typically consists of two basic architectural patterns: Antoni A and Antoni B patterns. The Antoni A pattern comprises areas of densely packed, spindle-shaped tumor cells arranged in a storiform pattern, with occasional nuclear palisading. When the latter is marked, the nuclear palisades are referred to as Verocay bodies. Antoni B areas are less cellular, and the tumor cells are loosely arranged and have indistinct processes. Cellular schwannoma consists

entirely or predominantly of Antoni A pattern without Verocay bodies, and its histologic features can sometimes lead to a misdiagnosis of malignancy while the clinical presentation resembles that of conventional schwannoma. Plexiform schwannoma grows in a multinodular or plexiform manner and may be either of conventional or cellular type. Another histologic variant of schwannoma that has been described in humans is ancient schwannoma, in which marked atypia, including nuclear pleomorphism with occasional bizarre forms and occasional mitoses, may raise a concern about malignant transformation but is only falsely suggestive of malignancy and should not be misinterpreted as such (Louis et al., 2016a).

In dogs, the most common histologic variant of schwannoma is cellular schwannoma. Nuclear palisading with Verocay bodies is extremely rare compared to its human counterparts (Higgins et al., 2016). Despite the high cellular density, the tumor lacks other features of malignancy, such as necrosis, nuclear pleomorphism, and mitotic figures (Lanigan et al., 2021). The tumor cells in canine schwannomas are usually uniform, ovoid, or elongated fusiform, with scant eosinophilic cytoplasm and poorly defined cytoplasmic borders. A collagen matrix of the variable amount and density is between the tumor cells. Less commonly, canine schwannomas are composed of areas of low cellularity and loose fibrous stroma consistent with the Antoni B pattern (Higgins et al., 2016). Another characteristic feature of schwannoma is occasionally hyalinized microvessels (Kawahara et al., 1988; Schöniger and Summers, 2009).

Another variant of schwannoma, which is rare in humans, is melanotic schwannoma. This entity represents pigmented tumor composed of cells with the ultrastructure and immunophenotype of Schwann cells but contains melanosomes and is reactive to melanocytic markers (Louis et al., 2016a). A few cases of this variant of NST have also been described in dogs (Patnaik et al., 1984; Warren et al., 2020). Due to its usually malignant course, this entity is renamed malignant melanotic nerve sheath tumor in the most recent human WHO classification (Louis et al., 2021).

Foci of presumed osseous or cartilaginous differentiation have also been described in schwannomas (Higgins et al., 2016). In humans, rare cases of glandular schwannomas characterized by benign glandular structures admixed with a spindle cell population have also been described in the literature (Yoshida and Toot, 1993; Kim et al., 2001; Holliday et al., 2017; Li et al., 2017; Saggini et al., 2019). To our knowledge, no cases of glandular schwannomas have been reported in dogs.

#### 2.2.6.2 Neurofibroma

Neurofibromas are benign nerve sheath tumors composed of a variable mixture of neoplastic Schwann cells, perineurial cells, and fibroblasts (Higgins et al., 2016). Based on data from the literature, the major component of neurofibroma is Schwann cell-derived (Schöniger and Summers, 2009).

Based on growth patterns in humans, they describe localized, plexiform, and diffuse neurofibromas. Plexiform neurofibromas are either multinodular nodules when multiple trunks of a plexus are involved, or rope-like lesions when multiple fascicles of a large, nonbranching nerve are involved (Louis et al., 2016a). A study on neurofibromas in dogs, horses, and a chicken also distinguished between localized, plexiform, and diffuse neurofibromas. Microscopic subtypes included classic, cellular, collagenous, myxoid, and pigmented neurofibromas. Study cases even included a hybrid neurofibroma/schwannoma (Schöniger and Summers, 2009).

Typically, neurofibromas are of less cellularity and consist of thin, elongated cells with indistinct cell borders. Usually, they have a single hyperchromatic, wavy, buckled, or tapering nucleus and scant eosinophilic cytoplasm. The cells show only mild atypia and the number of mitoses is low. There is a variable amount of collagenous to myxomatous stroma between the neoplastic cells (Schöniger and Summers, 2009). The stromal collagen component sometimes takes the form of dense, refractile bundles with a so-called shredded-carrot appearance (Louis et al., 2016a). In diffuse neurofibromas of dogs and humans, the neoplastic cells may form tactile-like structures called pseudo-Meissner (also pseudomeissnerian) corpuscles (Schöniger and Summers, 2009; Louis et al., 2016a).

In humans, ancient neurofibromas resemble ancient schwannomas and are characterized by nuclear atypia without additional features of malignancy. It is important to distinguish them from atypical neurofibromas, another variant defined by much more worrisome features, such as high cellularity, monomorphic cytology, scattered mitotic figures, and/or fascicular growth. The latter may have premalignant features based on their genetic characteristics and are difficult to distinguish from low-grade MNST (Louis et al., 2016a). Glandular neurofibromas in humans have also been reported in the literature although they are extremely rare (Woodruff and Christensen, 1993; Joshi et al., 2008). One case of a neurofibroma with pseudoglandular

structures has been described (Gómez-Mateo Mdel et al., 2015). Another rare variant of neurofibroma is lipomatous neurofibroma, which contains adipose tissue as a result of metaplasia or adipose differentiation from multipotent cells (Val-Bernal and González-Vela, 2005). No glandular or lipomatous neurofibromas have been described in dogs.

#### 2.2.6.3 Perineurioma

Perineuriomas are tumors composed entirely of neoplastic perineurial cells. Usually, they appear as solitary, small, and well-circumscribed tumors that form segmental, tubular enlargements of the affected nerve (Higgins et al., 2016). The characteristic histopathological feature of perineurioma is so-called pseudo-onion bulbs – concentric layers of neoplastic perineurial cells swirling around centrally located, thinly myelinated axons (Higgins et al., 2016; Louis et al., 2016a). Neoplastic cells are spindled and wavy, with thin cytoplasmic processes and elongated nuclei with inconspicuous nucleoli (Louis et al., 2016a). Mitotic figures are rare (Higgins et al., 2016).

Perineuriomas may be intraneural or extraneural if they arise in soft tissue (Louis et al., 2016a). Various morphological variants of extraneural perineurioma have occasionally been reported in humans (Rankine et al., 2004), including sclerosing perineurioma (Fetsch and Miettinen, 1997; Yamaguchi et al., 2003), reticular perineurioma (Graadt van Roggen et al., 2001), granular perineurioma (Al-Daraji, 2008), and lipomatous perineurioma (Zamecnik, 2003). In addition, ossification in the perineurioma has also been described (Rank and Rostad, 1998). Few cases of intraneural perineurioma in dogs are reported in the literature (Higgins et al., 2006; Martins et al., 2010; Cornelis et al., 2012; Jakab et al., 2012). One study of canine intraneural perineurioma describes Renault bodies at the periphery of the tumor (Cornelis et al., 2012). These are cylindrical hyaline structures composed of fibroblasts and perineurial cells with an amorphous extracellular matrix. Renault bodies are well-demarcated and connected to the interior of the perineurium. They are found mainly at sites where the nerve is compressed and may represent a secondary response to trauma. Nevertheless, their exact function remains unknown (Piña-Oviedo et al., 2009).

#### 2.2.6.4 Malignant nerve sheath tumor

MNSTs are malignant tumors that, like neurofibromas, are composed of a mixture of neoplastic Schwann cells, perineurial cells, and fibroblasts. They can vary greatly in appearance (Louis et al., 2016a). The majority of tumors are densely cellular and consist of pleomorphic spindle cells with eosinophilic cytoplasm and hyperchromatic, large nuclei that show distinct atypia. The tumor cells usually form interdigitating fascicles of storiform swirls (Higgins et al., 2016). Because most schwannomas in dogs are usually more cellular and therefore consist mainly of hypercellular Antoni A areas, cell density is a less reliable feature for distinguishing BNSTs from MNSTs. The mitotic index and necrosis in the tumor are two indicators of malignancy that can be used in the identification of MNSTs (Lanigan et al., 2021). In contrast to benign tumors, the mitotic rate in MNSTs is high, including atypical mitotic figures. The proliferation index may reach 15% (Higgins et al., 2016). In humans, MNSTs exceed 4 mitotic figures per 10 high-power fields, whereas in veterinary medicine there are no such established criteria to date (Lanigan et al., 2021). Necrosis is common and may be surrounded by a cellular pseudo-palisading pattern (Higgins et al., 2016). Another feature that helps to distinguish benign from MNST is cellular pleomorphism and atypia in the latter (Chijiwa et al., 2004). Specifically, in distinguishing atypical and cellular neurofibromas from low-grade MNSTs, the authors suggest that hypercellularity, nuclear enlargement, and hyperchromasia are morphologic criteria indicative of an MNST if the tumor would meet all three criteria (Rodriguez et al., 2012).

MNSTs may be localized or disseminated. They usually grow infiltratively and invade locally into adjacent tissues outside the epineurium, including bone and muscle (Higgins et al., 2016). They tend to recur locally and their long-term prognosis is considered poor (Poli et al., 2019). Occasionally, they can metastasize (Higgins et al., 2016). In humans, approximately 20-25% of patients develop metastases, which may spread by intraneural or hematogenous routes. The most common site for metastases is the lungs (Louis et al., 2016a). In dogs, only a few cases of metastatic NST have been described in the literature, with reports of metastases in the central nervous system, lungs, liver, kidneys, lymph nodes, spleen, and heart (Stoica et al., 2001; García et al., 2004; Kostov et al., 2008; Poli et al., 2019).

In humans, different histopathological variants of MNST have been identified, and their possibly different clinical course has been studied. Nevertheless, there are still insufficient data

to accurately predict their behavior. In addition to conventional MNST, there are three other histopathological variants defined in the human WHO classification: MNST with divergent differentiation, epithelioid MNST, and MNST with perineurial differentiation (malignant perineurioma) (Louis et al., 2016a). However, MNST with divergent differentiation represents a histopathological pattern rather than a variant. In contrast to variants, which have potential clinical utility, the different histopathological patterns, such as malignant triton tumor or glandular MNST, both of which belong to the group of MNST with divergent differentiation, usually have no clear clinicopathological significance (Louis et al., 2016b).

#### *2.2.6.4.1 Malignant nerve sheath tumor with divergent differentiation*

MNST with divergent differentiation is associated with poor prognosis (Patnaik et al., 2002). In humans, it is frequently associated with NF1 and correlates prognostically with conventional high-grade MNST. It may include areas of neoplastic cartilage, bone, skeletal muscle, smooth muscle, or angiosarcoma-like areas. MNST with rhabdomyosarcomatous differentiation is also called a malignant triton tumor. In addition to the mesenchymal component, it may also contain glandular or neuroendocrine epithelium, and rarely squamous epithelium (Louis et al., 2016a). Nevertheless, glandular epithelial structures do not necessarily imply malignancy – glandular schwannomas and neurofibromas are also occasionally described in the literature. Even in MNST, the degree of glandular atypia has less influence on tumor behavior, suggesting that the latter is more or exclusively related to the malignant spindle cell component (Saggini et al., 2019). Although up to 92% of glandular MNSTs consists of a malignant spindle cell component and a benign glandular component, rare cases of MNST with a malignant both glandular and spindle cell component have been described in the literature (Galatian et al., 2013).

Divergent differentiation has also been described in canine NSTs. Anderson et al. were among the first to describe a case of MNST with chondro-osseous differentiation, which originated from a diaphragm of a 1-year-old dog (Anderson et al., 1999). Only a few years later, Patnaik et al. described a case of MNST in a dog with osteosarcomatous and glandular differentiation (Patnaik et al., 2002), and Kim et al. reported MNST in a dog with osteosarcomatous, rhabdomyosarcomatous, and myxomatous differentiation (Kim et al., 2003). The study by Chijiwa et al. included two cases of MNST with cartilaginous and osseous metaplasia (Chijiwa et al., 2004).

#### 2.2.6.4.2 *Epithelioid malignant nerve sheath tumor*

Epithelioid MNST is a variant that can arise from the malignant transformation of a schwannoma. In humans, it shows no association with NF1, and the risk of recurrence, metastasis, and disease-related death appears to be lower compared to conventional MNST (Louis et al., 2016a). The main features of epithelioid MNST are a predominantly epithelioid cytomorphology and a frequently multilobular growth pattern. Foci of spindle-shaped neoplastic cells are observed only occasionally. Myxoid and/or fibrous stroma may be present among the tumor cells, and chondro-osseous differentiation sometimes occurs. Diffuse S100 positivity in MNST is a feature strongly suggestive of a diagnosis of epithelioid MNST (Jo and Fletcher, 2015).

In dogs, only a few cases of epithelioid MNST have been described in the literature (Pumarola et al., 1996; García et al., 2004). In one case, metastases were found in the liver, kidneys, lungs, and lymph nodes (García et al., 2004).

#### 2.2.6.4.3 *Malignant perineurioma*

MNSTs with perineurial differentiation appear to be less aggressive than conventional NSTs in humans although they have the potential to metastasize. They are rare tumors with histological, ultrastructural, and immunohistochemical features of perineurial cells. Similar to their benign counterparts, they are epithelial membrane antigen (EMA) positive and S100 negative. The main histological difference from benign perineurioma is hypercellularity, nuclear atypia, and increased mitotic activity (Louis et al., 2016a). Occasionally, these tumors are not EMA positive, which complicates the diagnosis. The reason for such a result might be related to the delicate cytoplasmic processes of neoplastic perineurial cells and the degree of differentiation. A higher antibody concentration, the use of a more sensitive method, or a longer incubation of the primary antibody could lead to an adequate result (Rosenberg et al., 2002).

Malignant perineurioma has not yet been described in dogs. There are some suspected cases in previous studies but they have not been confirmed (Chijiwa et al., 2004; Jakab et al., 2012).

### 2.2.7 **Grading of malignant nerve sheath tumors**

The grading of MNST in dogs is generally deficient because adequate histopathological grading criteria have not yet been established.

In grading MNST in humans, the French (Fédération Nationale des Centres de Lutte Contre le Cancer; FNCLCC) soft tissue sarcoma (STS) grading system is generally used. It is based on the study of a large number of tumors, is reproducible, and is useful in a wide variety of soft tissue tumors (Rodriguez et al., 2012). The French grading system includes three parameters that are incorporated into a composite score: tumor differentiation, mitotic index, and tumor necrosis (Coindre, 2006). The same grading system has been used to grade cutaneous and subcutaneous STSs in dogs (Dennis et al., 2011). Tumor differentiation score depends on the degree of differentiation ranging from well-differentiated tumors resembling mature counterparts. Mitotic count is based on the number of mitoses per 10 HPF or better 0.1734 mm<sup>2</sup>. Tumor necrosis includes an assessment of the extent of possible necrotic areas in the tumor. The histological grade corresponds to the sum of all three parameters assessed (Dennis et al., 2011; Rodriguez et al., 2012). Because the results regarding the prognostic significance of FNCLCC grading in human MNSTs are conflicting, the current recommendation of the College of American Pathologists is not to use this scheme in MNSTs. Some recent findings support its use as a clinically prognostic score that may contribute to clinical decision-making in the treatment of individuals with MNST (Lucas et al., 2020) although larger multi-institutional studies would be needed to confirm the association between grading and prognosis (Rodriguez et al., 2012).

According to Rodriguez et al., another practical approach to grading MNSTs is to divide tumors into low-grade and high-grade MNSTs. Taking into account cytological atypia, mitotic activity (> 5/10 HPF) and hypercellularity with or without necrosis, most MNSTs (about 85%) fall into the "high-grade" category (Rodriguez et al., 2012). On the other hand, Lucas et al. mention the possible use of the modified 2-tier system that groups FNCLCC grade I and II MNSTs into low-grade MNSTs and grade III into high-grade MNSTs (Lucas et al., 2020).

### **2.2.8 Immunohistochemical features of nerve sheath tumors**

IHC is an important tool in tumor diagnostics. It is based on the specific binding between a specific antibody and an antigen and is used to detect specific antigens in cells and tissues, usually under a light microscope. It helps determine tumor origin in poorly differentiated tumors or cases with nonspecific phenotypes and detect small tumor foci not visible on routine HE

examination. It facilitates tumor classification. It is also increasingly used to provide prognostic information and detect molecular alterations in tumors (Magaki et al., 2019).

Although the identification of specific tumor cell types can be based to some extent on immunophenotyping and also electron microscopy, accurate data on the optimal IHC panel in the diagnosis of NSTs are still lacking (Higgins et al., 2016). While some IHC markers are more useful in the diagnosis of NSTs (Higgins et al., 2016; Lanigan et al., 2021), their sensitivity and specificity often reach their limits because their expression is lost in MNSTs or they are variably expressed in other tumors that are differentials for NSTs. Therefore, the diagnosis of MNST is often based on the exclusion of other differential diagnoses using a comprehensive IHC panel (Lucas et al., 2020), which must be evaluated in conjunction with relevant clinicopathologic data (Lanigan et al., 2021).

Below, we have provided a brief summary of some of the most commonly used markers in the literature that are expressed to some extent in NSTs and may contribute to the final diagnosis. The panel of IHC markers tested in our study – Sox10, claudin-1, GFAP, CNPase, Ki-67, and H3K27me3 – are further described in more detail.

All NSTs usually express vimentin, which confirms a mesenchymal origin of tumor cells and is commonly used to distinguish between epithelial and mesenchymal neoplasms (Gaitero et al., 2008; Ramos-Vara and Borst, 2016). Laminin and collagen IV are useful for identifying Schwann cells, which have a basement membrane containing several proteins, including the two mentioned (Gaitero et al., 2008; Lanigan et al., 2021). Their use is necessary to distinguish melanocytic schwannomas from melanomas or melanocytomas (Lanigan et al., 2021). S-100 also labels neoplastic Schwann cells (Schöniger and Summers, 2009). It was originally thought to be a specific marker of neural crest origin but was later shown to be expressed in various tissues and cell types (Kuberappa et al., 2016). Compared to human NSTs, its immunoreactivity is more variable in animals but may still be useful in distinguishing NSTs from some other differential diagnoses (Lanigan et al., 2021). In humans, the IHC marker EMA (also known as mucin 1 (MUC1) or CA15-3), expressed in neoplastic or non-neoplastic perineural cells, appears to be useful for the diagnosis of perineurioma. In dogs, commercially available human antibodies against EMA were not shown to react to formalin-fixed paraffin-embedded (FFPE) tissue from dogs until recently when reactivity was reported in some canine mammary tumors and in canine meningiomas (Higgins et al., 2006; de Oliveira et al., 2009; Campos et al., 2015;

Mandara et al., 2021). Neurofilament protein (NF-200) and periaxin (PRX) are markers that reveal entrapped myelinated axons and can help identify the nerve origin of the tumor (Suzuki et al., 2014; Ramos-Vara and Borst, 2016). In addition, many other markers have been tested that are expressed to varying degrees in human and/or canine NSTs, such as nestin (Shimada et al., 2007; Suzuki et al., 2014), nerve growth factor receptor (NGFR) (Chijiwa et al., 2004; Suzuki et al., 2014; Ramos-Vara and Borst, 2016), oligodendrocyte transcription factor (Olig2) (Suzuki et al., 2014), CD57 (Leu-7) (Hirose et al., 1992; Suzuki et al., 2014; Ramos-Vara and Borst, 2016), myoglobin (Chijiwa et al., 2004), Sox-2 (Ersen et al., 2017), P75NTR (Pekmezci et al., 2015; Ersen et al., 2017), calretinin (Fine et al., 2004), PGP 9.5 (Gaitero et al., 2008), neuron specific enolase (NSE) (Gaitero et al., 2008), erythrocyte glucose transporter protein (Glut1) (Hirose et al., 2003), CD34 (Hirose et al., 2003; Naber et al., 2011), podoplanin (Jokinen et al., 2008; Naber et al., 2011), and neurofibromin (Pekmezci et al., 2015; Röhrich et al., 2016).

#### 2.2.8.1 Sox10

The transcription factor Sox10 plays an important role in the specification, maturation, and maintenance of Schwann cells and melanocytes (Kelsh, 2006; Nonaka et al., 2008). Therefore, this neuroectodermal stem cell/progenitor marker is expressed in the glia of peripheral ganglia and nerves as well as in differentiating melanocytes, whereas it is absent in neurons and other non-neural derivatives of the neural crest (Woodhoo and Sommer, 2008; Ersen et al., 2017). It is not entirely specific, as it has also been expressed in acinar and myoepithelial cells of salivary gland tissue and myoepithelial cells of mammary tissue (Karamchandani et al., 2012). Many studies in human medicine claim its usefulness for diagnostic purposes in NSTs, along with the use of some other immunohistochemical markers (Karamchandani et al., 2012; Thway and Fisher, 2014; Miettinen et al., 2015; Pekmezci et al., 2015; Ersen et al., 2017). Consistent with this, the literature in veterinary medicine also suggests that Sox10 confirms the derivation of tumor cells from the neural crest and is therefore useful for the diagnosis of NSTs in animals (Higgins et al., 2016; Stilwell and Rissi, 2019; Lanigan et al., 2021).

#### 2.2.8.2 GFAP

GFAP (also known as GFA protein or plaque protein) belongs to the cytoskeletal protein family. It is the major intermediate filament (IF) in mature astrocytes and is involved in regulating their

shape and motility by providing structural stability to the extensions of astrocytic processes (Eng et al., 2000). It also supports neighboring neurons and the blood-brain barrier. In addition, it is found in non-myelinating Schwann cells in the PNS and enteric glial cells (Yang and Wang, 2015). It is absent in neoplasms of mesenchymal origin (Tascos et al., 1982). The first mention of GFAP expression in NST was in 1982 when Tascos et al. detected it in one schwannoma (Tascos et al., 1982). Its expression in NSTs varies according to the human and veterinary literature (Tascos et al., 1982; Memoli et al., 1984; Kawahara et al., 1988; Gray et al., 1989; Chijiwa et al., 2004; Gaitero et al., 2008).

#### 2.2.8.3 Claudin-1

Claudin-1 belongs to the group of claudins, a family of at least 24 different integral membrane proteins involved in the formation of tight junctions of endothelial and epithelial cells (Piña-Oviedo and Ortiz-Hidalgo, 2008). Tight junctions are the most apical type of intercellular contact in the lateral membrane between polarized cells. They exhibit a wide variability of tightness in different organs, ranging from almost complete sealing of the paracellular cleft to the formation of pores for the passage of certain atoms and molecules. Transmission electron microscopy (TEM) shows that tight junctions are the fusion of plasma membranes of opposing cells (Krause et al., 2008). According to tissue-specific barrier properties, claudin family members are differentially expressed in different tissues (Folpe et al., 2002; Krause et al., 2008). Claudin-1 is widely expressed in epithelia in general and has also been found in normal and neoplastic perineurial cells, which are known to form tight junctions, consistent with their role in the blood-nerve barrier (Folpe et al., 2002; Kucenas, 2015). According to the human medical literature, it appears to be a highly sensitive and relatively specific marker for perineuriomas (Folpe et al., 2002).

#### 2.2.8.4 CNPase

2',3'-Cyclic nucleotide 3'-phosphohydrolase (CNPase) is the first known enzyme of the myelin membrane (Vogel and Thompson, 1988) localized mainly in the two cell types responsible for myelin sheath formation – oligodendrocytes and Schwann cells (Reynolds et al., 1989; Sprinkle, 1989). Literature indicates that the amount of CNPase is lower in PNS myelin compared to CNS myelin. Its activity increases during brain development, consistent with increasing myelination (Reddy et al., 1982). It is apparently present not only in myelin-rich

cells but has also been found in myelin-free cultured human Schwann cells, suggesting that such Schwann cells may be enzymatically primed to begin myelin production upon receipt of the final stimulus (Reddy et al., 1982). In addition, it is also present at lower levels in some other cell types, such as the liver, thymus, spleen, adrenal glands, kidney, heart, and skeletal muscle. In humans, low CNPase activity has been found in some nervous system tumors, such as astrocytoma, neurinoma, oligodendroglioma, glioblastoma multiforme, undifferentiated glioma, medulloblastoma, and meningioma but its role remains unknown (Olga et al., 2020). Nielsen et al. have shown that it is a sensitive marker for bovine NSTs (Nielsen et al., 2011), and Armando et al. used it in the diagnosis of NSTs in goldfish (Armando et al., 2021), whereas to our knowledge it has not yet been tested in NSTs of other animal species or humans.

#### 2.2.8.5 Ki-67

Ki-67 is a protein closely associated with cell proliferation. It is present in all active phases of the cell cycle (G1, S, G2, and M) and absent in quiescent cells (G0) (Scholzen and Gerdes, 2000). The expression of Ki-67 is therefore related to the proliferation activity of intrinsic cell populations in malignant tumors. Its prognostic value has been investigated in numerous studies on cancers of various origins (Li et al., 2015), including MNST. In the case of the latter, it has been described as an important prognostic indicator in humans, with an increased index indicating a poorer prognosis (Watanabe et al., 2001; Lucas et al., 2020; Martin et al., 2020).

#### 2.2.8.6 H3K27me3

The trimethylation of lysine 27 on histone H3 (H3K27me3) is a repressive histone modification associated with gene silencing (Mito et al., 2017) and is abundant in genomic regions known as facultative heterochromatin (Piunti and Shilatifard, 2021). Facultative heterochromatin refers to genomic regions in the nucleus of a eukaryotic cell that has the ability to adopt open or compact conformations within a temporal and spatial context (Trojer and Reinberg, 2007). Responsible for H3K27me3 is a methyltransferase called Polycomb repressive complex 2 (PRC2). PRC2 is one of the two distinct multiprotein complexes with catalytic activity. Its four core subunits are embryonic ectoderm development (EED), suppressor of zeste 12 (SUZ12), enhancer of zeste homologue 2 (EZH2) or its paralogue EZH1, and retinoblastoma binding protein 4 (RBBP4) or RBBP7. The core subunits can then form various complexes with other proteins (Piunti and Shilatifard, 2021). Genetic alterations of EED and SUZ12 lead to the loss

of function of PRC2 and consequently loss of H3K27me3 (Lee et al., 2014). In recent years, loss of H3K27me3 has been considered a useful tool in the diagnosis of human NSTs because it is rare in other high-grade sarcomas and, according to some studies, is also useful for distinguishing benign and low-grade MNSTs from high-grade MNSTs (Cleven et al., 2016; Prieto-Granada et al., 2016; Asano et al., 2017; Le Guellec et al., 2017; Lyskjaer et al., 2020; Sugita et al., 2021). To date, only one study of H3K27me3 expression has been performed on a small number of MNSTs in dogs, which found epigenetic subtypes similar to MNSTs in humans (Kochat et al., 2021).

### **2.2.9 Ultrastructural features of nerve sheath tumors**

TEM is a useful technique for detecting the basal lamina in Schwann cells or neoplastic cells derived from Schwann cells. The basal lamina is absent in neoplastic cells originating from endoneurial or epineurial fibroblasts that are part of MNST or neurofibromas. Epineurial cells have characteristic long, thin processes, interrupted basal membranes, and pinocytotic vesicles (Higgins et al., 2016). Perineurial cells have long, thin, bipolar cell processes, pinocytotic invaginations of the plasmalemma, and tight junctions that often connect the terminal cell processes of adjacent cells (Erlandson and Woodruff, 1982). In MNSTs, there are no clear specific ultrastructural features. Sometimes TEM is used to exclude other specific features from other STSs (Higgins et al., 2016).

### **2.2.10 Other tumors involving the nerve**

In rare cases, lymphoma involving the nerves (neurolymphomatosis) has been reported in dogs (Pfaff et al., 2000; Schaffer et al., 2012; Ueno et al., 2014). A slightly larger number of cases of neurolymphomatosis, although still rare, have been reported in humans (Foo et al., 2017; Bourque et al., 2019; Sato et al., 2019) and cats (Higgins et al., 2008; Mandrioli et al., 2012; Sakurai et al., 2016; Hsueh et al., 2019). In chickens, neurolymphomatosis is induced by the herpesvirus that causes Marek's disease (Denesvre, 2013).

The literature from human medicine contains some reports of intraneural lipomas (Marek et al., 2018; DeSano et al., 2021), intraneural hemangiomas (Kwong et al., 2018; Bacigaluppi et al., 2020; Guo et al., 2021; Ravanbod et al., 2021), a mixed intraneural lymphangioma and hemangioma (Prater and Janz, 2017), and rare cases of intraneural glomus tumors (Muthiah et

al., 2018). Intra-neural angiosarcoma has also been described (Mentzel and Katenkamp, 1999).  
To our knowledge, no such intra-neural tumors have been described in veterinary medicine.

## **3 MATERIALS AND METHODS**

### **3.1 SAMPLES**

In our study, we included 79 samples of canine tumors that were previously diagnosed as NSTs based on the location and histopathological features of the tumors. Seventy-eight samples, collected between 2000 and 2022 were from the tissue archive of the Laboratory of Veterinary Neuropathology of the Department of Veterinary Science, University of Pisa (Italy) while one sample from 2021 was from the archive of the Institute of Pathology, Wild Animals, Fish and Bees of the Veterinary Faculty, University of Ljubljana (Slovenia). The tumors were topographically classified based on their localization in the following groups: cranial nerve; cervical, cervicothoracic, thoracolumbar, or lumbosacral spinal cord segments; brachial or lumbosacral plexus; and appendicular nerve.

Although a total of 96 nerve sheath tumors were initially obtained from the tissue archives, 17 cases were excluded from the study because they contained insufficient clinical information, the biopsy specimens were too small, or the tissue material was not adequately preserved for further procedures.

### **3.2 HISTOPATHOLOGY**

All tumor specimens were submitted to laboratories fixed in 10% formalin, were further trimmed by pathologists, and routinely embedded in paraffin. Formalin-fixed paraffin-embedded (FFPE) tissue blocks were archived in the tissue archives. After retrieving the samples from the archives, we prepared 4  $\mu\text{m}$  thick paraffin sections and stained them with hematoxylin and eosin (HE). We examined the HE slides under a light microscope and evaluated the tissue and cellular characteristics of the tumors. Tissue criteria included evaluation of tumor shape, demarcation, encapsulation, growth type, cellularity, growth pattern, amount and type of stroma, the extent of necrosis, the extent of hemorrhage, invasion of blood and lymphatic vessels, herniation into vessels, inflammatory infiltrates, hyalinization, and bony and cartilaginous components. Cellular criteria included evaluation of cell morphology, anisocytosis, anisokaryosis, cell margins, nuclear/cytoplasmic ratio, nuclear pleomorphism, nucleoli, number of mitoses per 10 HPF (400 $\times$  magnification – 0.196  $\text{mm}^2$ ), and presence of multinucleated cells. For evaluation of the listed criteria, we have prepared a detailed form for

histopathologic evaluation of specimens that allowed accurate and consistent assessment of the tissue and cellular criteria of tumors. The form is included in the supplementary material (**Supplementary Table 1**).

Tumors histopathologically diagnosed as MNSTs were classified into three histopathologic grades according to the STS grading system used in human pathology, which has also been used to grade cutaneous and subcutaneous STSs in dogs (Coindre, 2006; Dennis et al., 2011). We used the grading system suggested for human NSTs by Rodriguez et al. (Rodriguez et al., 2012), as shown in Table 1.

**Table 1:** Grading system for STS modified for MNST.

---

|                              |   |
|------------------------------|---|
| <i>Differentiation score</i> |   |
| 1                            | Well-differentiated MNST arising in transition from neurofibroma          |
| 2                            | Conventional, monomorphous spindle cell MNST                              |
| 3                            | Highly pleomorphic MNSTs, as well as MNSTs with divergent differentiation |

---

|                      |                      |
|----------------------|----------------------|
| <i>Mitotic count</i> |                      |
| 1                    | 0–9 mitoses/10 HPF   |
| 2                    | 10–19 mitoses/10 HPF |
| 3                    | >19 mitoses/10 HPF   |

---

|                       |               |
|-----------------------|---------------|
| <i>Tumor necrosis</i> |               |
| 0                     | No necrosis   |
| 1                     | ≤50% necrosis |
| 2                     | >50% necrosis |

---

|                             |     |
|-----------------------------|-----|
| <i>HISTOLOGICAL GRADE *</i> |     |
| I                           | ≤3  |
| II                          | 4–5 |
| III                         | ≥6  |

---

STS: soft tissue sarcoma. MNST: malignant nerve sheath tumor. HPF: high power fields. \* Histological grade corresponds to the sum of all three parameters assessed – differentiation score, mitotic count, and tumor necrosis.

### 3.3 IMMUNOHISTOCHEMISTRY

IHC staining for claudin-1, GFAP, Ki-67, and H3K27me3 was performed using an automated IHC stainer, whereas IHC staining for Sox10 and CNPase was performed manually. Paraffin sections of 4 μm thickness were prepared on positively charged slides. Sections were deparaffinized and rehydrated before performing IHC staining protocols. Appropriate positive

and negative tissue controls were used in the staining procedures: canine lymph node as a positive control for Ki-67 (**Figure 2A**), canine brain for CNPase (**Figure 2B**) and GFAP (**Figure 2C**), canine skin for claudin-1 (**Figure 2D**), and canine amelanotic melanoma for Sox10 (**Figure 3A**). Canine lymph node and human tonsil served as positive tissue controls (**Figures 3B and 3C**), and a human diffuse midline glioma with a histone H3 K27M mutation and known H3K27me3 loss served as a negative tissue control for H3K27me3 (**Figure 3D**). The same tissues incubated with antibody diluent without primary antibody served as negative reagent controls. Sections were counterstained with Mayer's hematoxylin and mounted.

Vascular endothelial cells and lymphocytes served as internal positive controls for H3K27me3, and in some specimens, portions of surrounding nervous tissue or remnants of affected nerves served as internal positive controls for Sox10, CNPase, GFAP, and claudin-1. In the absence of immunopositivity in the internal positive control, staining was repeated, and samples that remained negative were evaluated as unreliable.

Details of the primary antibodies and IHC protocols used are given in Table 2.

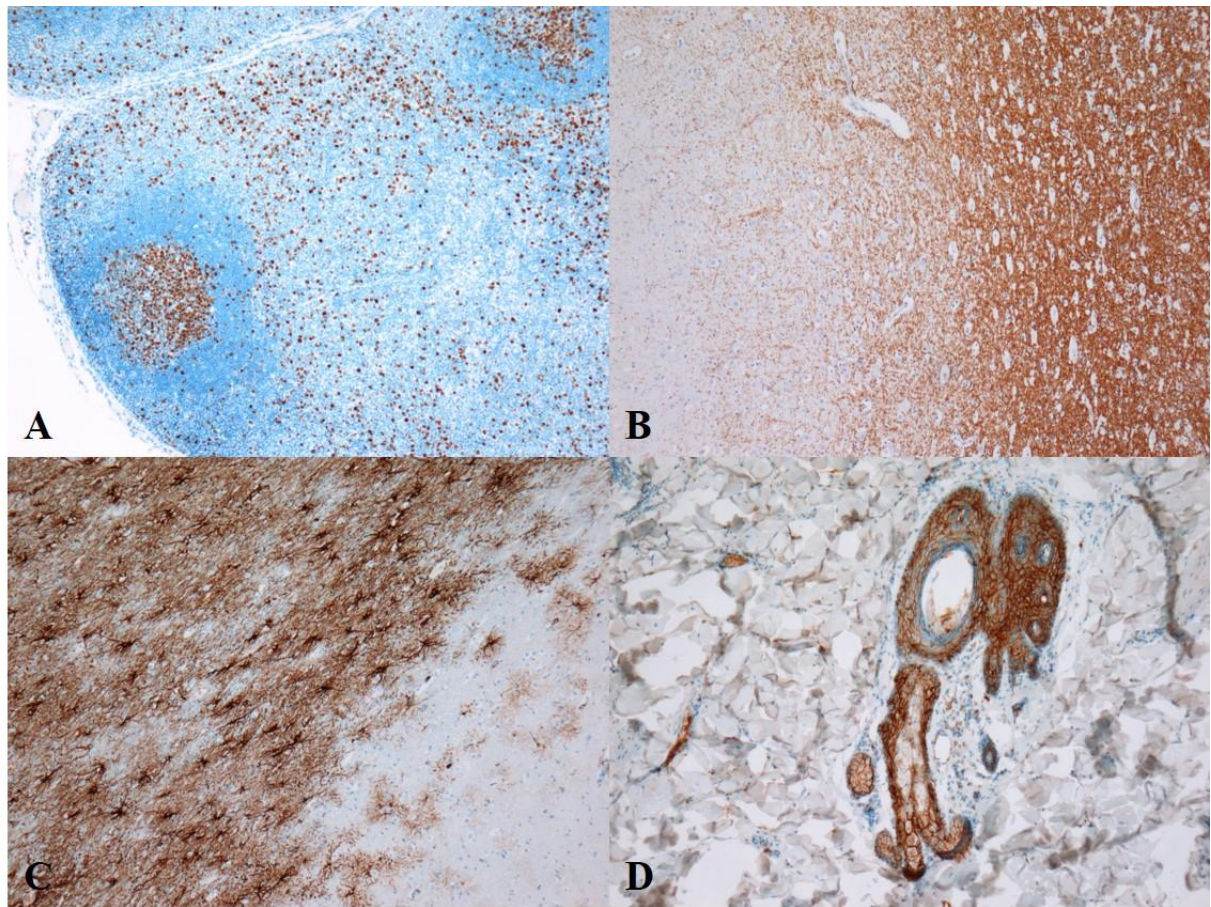


**Figure 2:** Positive controls for immunohistochemical staining of Ki-67, CNPase, GFAP, and claudin-1. (A) Canine lymph node. The highest proliferative activity is in the germinal centers of the follicles in the cortex. Ki-67, 100x. (B) Canine brain. CNPase is diffusely expressed in white matter. CNPase, 100x. (C) Canine brain. GFAP is diffusely expressed in astrocytes. GFAP, 100x. (D) Skin. Claudin-1 labels the tight junction between hair follicle epithelial cells. Claudin-1, 100x.

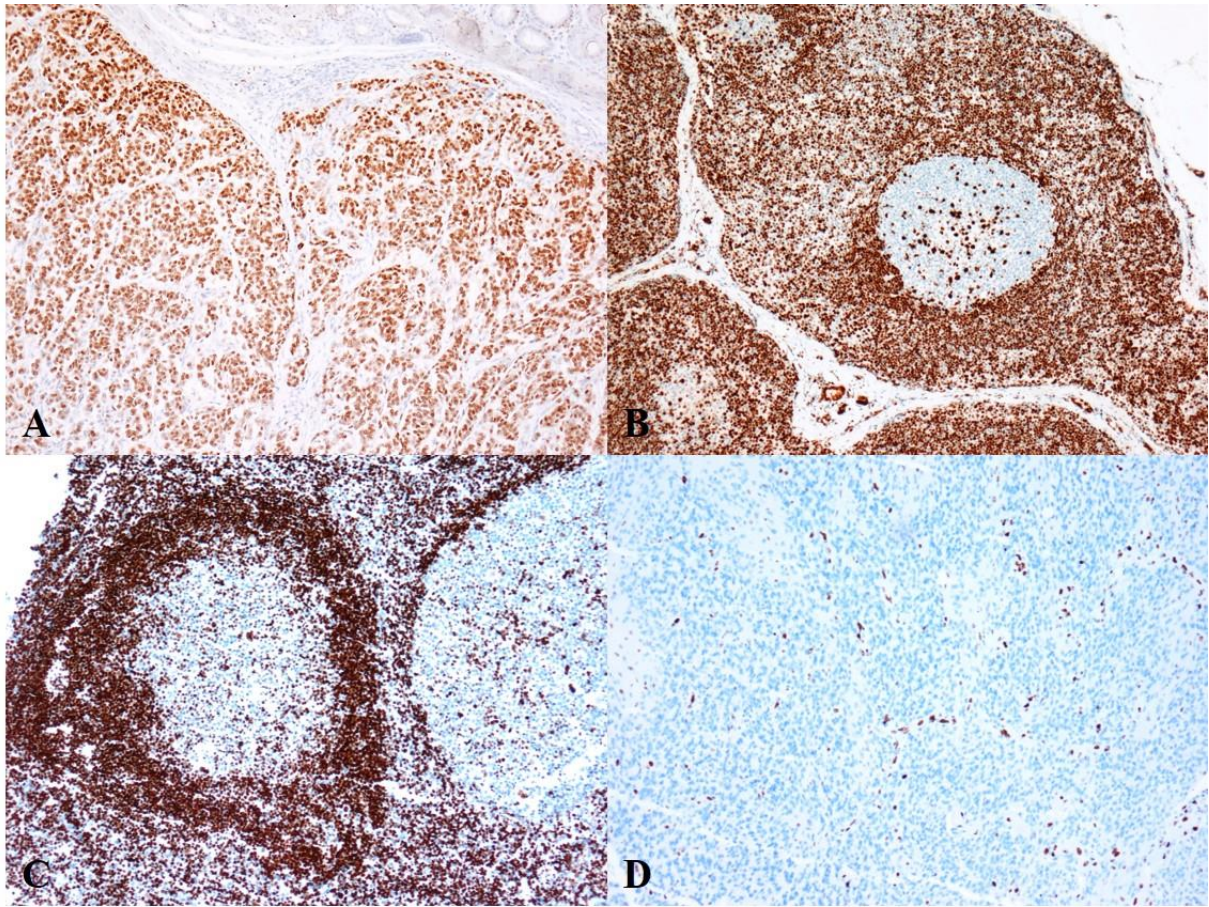


**Figure 3:** Positive controls for immunohistochemical staining of Sox10 and H3K27me3. (A) Canine amelanotic melanoma with tumor cells showing a strong nuclear reaction for Sox10. Sox10, 100x. (B) Canine lymph node and (C) human tonsil showing the strong nuclear reaction of small lymphocytes and endothelial cells to H3K27me3. H3K27me3, 100x. (D) Human diffuse midline glioma with a histone H3 K27M mutation with immunohistochemical loss of H3K27me3 expression. The positive reaction is expressed in the endothelial cells and scattered lymphocytes. H3K27me3, 100x.

**Table 2:** Details of the primary antibodies and immunohistochemical protocols.

| <b>Primary Antibody,<br/>Clone, and Catalogue<br/>Number</b> | <b>Manufacturer</b>    | <b>Antigen Retrieval</b>                             | <b>Antibody<br/>Dilution</b> | <b>Time and Temperature<br/>of Incubation of the<br/>Primary Antibody</b> | <b>Detection system</b>  | <b>IHC Automated<br/>Stainer</b> |
|--|------------------------|--|------------------------------|---|--|----------------------------------|
| <b>Ki67,<br/>MIB-1,<br/>(M7240)</b>                          | Dako, Denmark          | CC1, pH 8.5,<br>60 min, 25 °C                        | 1/50                         | 32 min, 37 °C   | UltraView Universal DAB<br>Detection Kit (Ventana<br>Medical Systems Inc., Tucson,<br>AZ, USA) | Ventana Benchmark XT<br>(USA)    |
| <b>CNPase,<br/>11-5B,<br/>(ab6319)</b>                       | Abcam, UK              | Citrate buffer, pH<br>6.0, MW<br>(1100 W),<br>20 min | 1/750                        | 60 min, 23 °C   | DAKO REAL™ EnVision<br>Detection System<br>Peroxidase/DAB+,<br>Rabbit/Mouse<br>(Dako, Denmark) | /                                |
| <b>Claudin-1,<br/>(ab15098)</b>                              | Abcam, UK              | ULTRA CC1,<br>pH 8.45-8.65,<br>56 min, 25 °C         | 1/50                         | 20 min, 37 °C   | OptiView DAB Detection Kit<br>(Ventana Medical Systems<br>Inc., Tucson, AZ, USA)               | Ventana Benchmark<br>ULTRA (USA) |
| <b>GFAPmo,<br/>EP672Y,<br/>(05269784001)</b>                 | Ventana, USA           | ULTRA CC1,<br>pH 8.45-8.65,<br>56 min, 25 °C         | RTU *                        | 16 min, 37 °C   | OptiView DAB Detection Kit<br>(Ventana Medical Systems<br>Inc., Tucson, AZ, USA)               | Ventana Benchmark<br>ULTRA (USA) |
| <b>Sox10,<br/>EP268,<br/>(383R-15)</b>                       | Cell Marque, USA       | Citrate buffer, pH<br>6.0, MW<br>(1100 W),<br>20 min | 1/100                        | 60 min, 23 °C   | DAKO REAL™ EnVision<br>Detection System<br>Peroxidase/DAB+,<br>Rabbit/Mouse<br>(Dako, Denmark) | /                                |
| <b>H3K27me3,<br/>C36B11,<br/>(9733)</b>                      | Cell Signaling,<br>USA | CC1, pH 8.5,<br>64 min, 25 °C                        | 1/400                        | 44 min, 37 °C   | OptiView DAB Detection Kit<br>(Ventana Medical Systems<br>Inc., Tucson, AZ, USA)               | Ventana Benchmark XT<br>(USA)    |

\* RTU: ready to use; IHC: immunohistochemistry; MW: microwave oven.

### 3.3.1 Evaluation of immunohistochemical staining

To evaluate the expression of Sox10, GFAP, claudin-1, and CNPase, we used the four-point system of Adams et al. as follows (Adams et al., 1999; Kang et al., 2014):

- Strong (+++): dark staining that is clearly visible at low magnification and encompasses >50% of cells.
- Moderate (++) : focal darkly stained areas encompassing <50% of cells or moderate staining of >50% of cells.
- Weak (+): focal moderate staining in <50% of cells or pale staining in any proportion of cells that is not readily visible at low magnification.
- Negative (-): none of the above.

The expression scales for Sox10, GFAP, claudin-1, and CNPase are shown separately for each marker in **Figures 4, 5, 6, and 7**, respectively.

The Ki-67 proliferation index was defined as the percentage of positive tumor cell nuclei per 1000 nuclei counted in selected fields at 400× magnification. The proliferation index was determined in the areas subjectively identified as having the highest proportion of immunoreactive tumor cells. Examples of different proliferation activity detected by Ki-67 IHC staining are shown in **Figure 8**.

Loss of H3K27me3 expression was evaluated according to three different scoring scales previously described in human pathology, and statistical analysis was performed separately for each of the three scoring scales:

- 1) The 4-tier scoring scale (Pekmezci et al., 2017):
  - +++: retained expression in  $\geq 95\%$  of tumor cells (diffuse staining),
  - ++: retained expression in 50–94% of tumor cells (loss in the minority),
  - +: retained expression in 5–49% of tumor cells (loss in the majority) or
  - -: retained expression in <5% of tumor cells (complete loss).
- 2) The 3-tier scoring scale (Asano et al., 2017):
  - complete loss (-),
  - partial loss (+ or ++)
  - complete retention (+++).

3) The 2-tier scoring scale (Pekmezci et al., 2017):

- complete loss (-) or
- retention (+, ++ or +++).

Partial loss, in which H3K27me3 expression was retained in 5–94% of tumor cells (+ or ++), was also referred to as mosaic loss and was determined when immunopositive and immunonegative tumor cells were intermingled. When loss of H3K27me3 expression occurred in a well-defined area on a background of preserved expression, this was termed geographic loss, a variant of complete loss of expression, regardless of the percentage of tumor cells that retained expression (Asano et al., 2017).

The different ranges of H3K27me3 expression are shown in **Figure 9**.

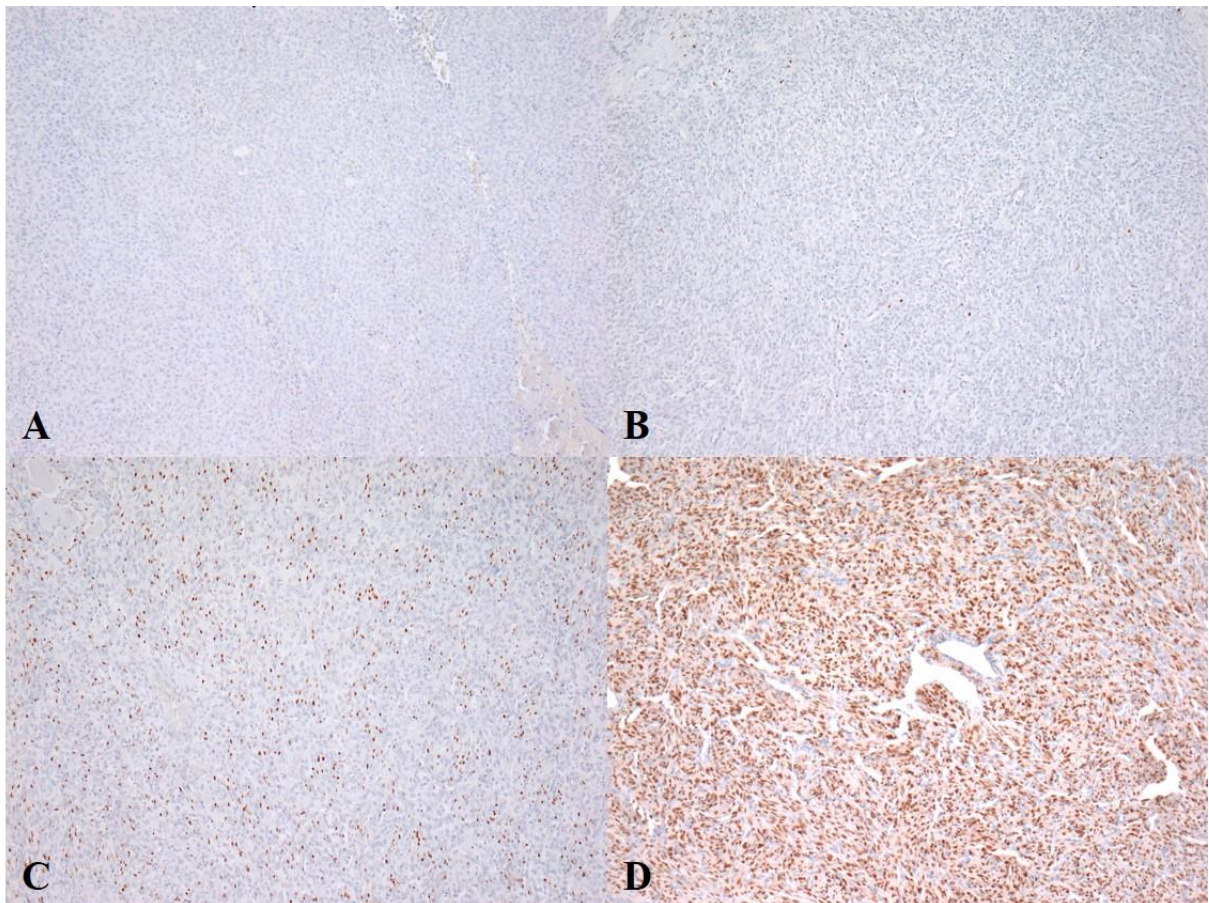


**Figure 4:** Evaluation of immunohistochemical expression of Sox10. Sox10, 100x. (A) Negative staining (-), case no. 74. (B) Weak staining (+), barely visible at low magnification, case no. 2. (C) Moderate staining (++) with strong nuclear reaction in < 50% of tumor cells, case no. 8. (D) Strong staining (+++) in the majority of tumor cells, case no. 20.

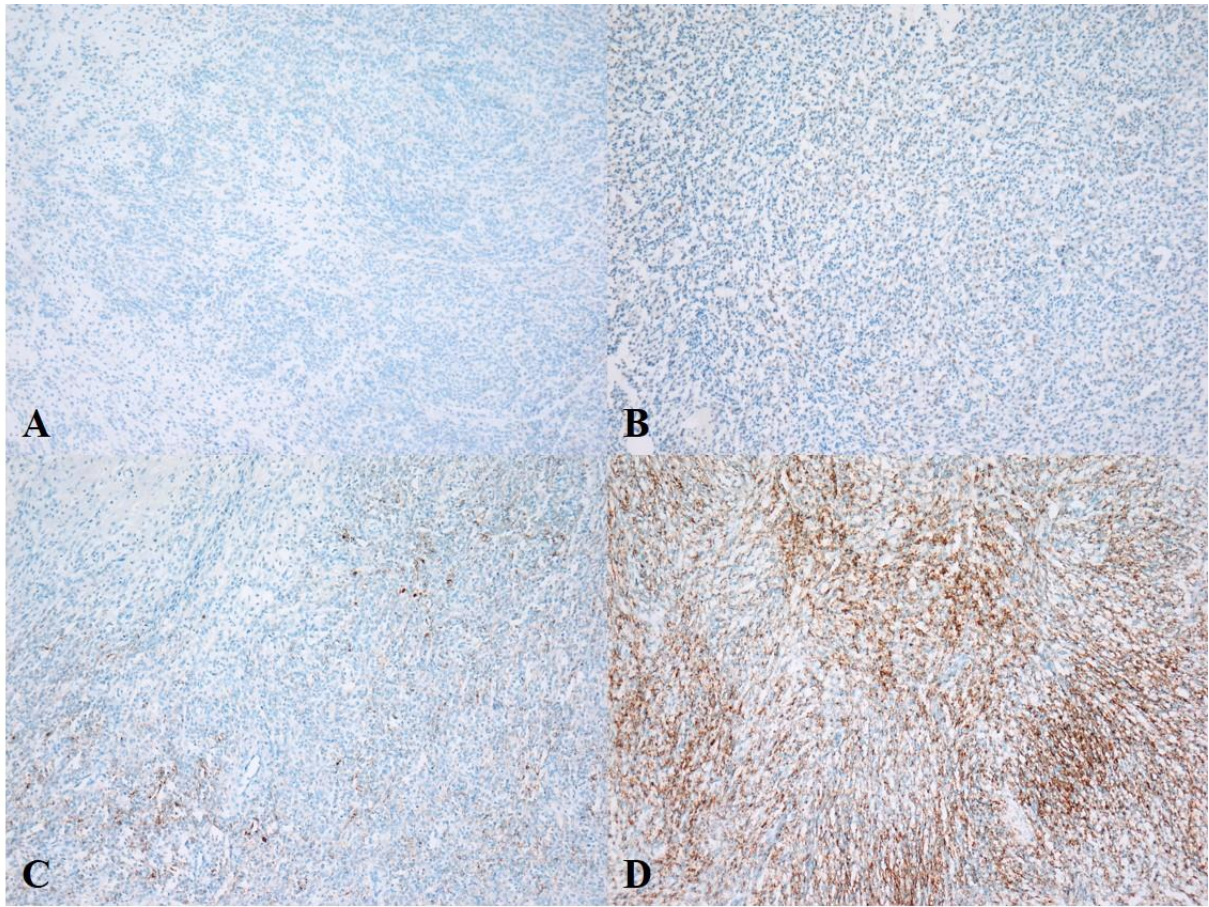


**Figure 5:** Evaluation of immunohistochemical expression of claudin-1. Claudin-1, 100x. **(A)** Negative staining (-), case no. 75. **(B)** Weak staining (+), barely visible at low magnification, case no. 40. **(C)** Moderate staining (++) with strong membranous reaction in <50% of tumor cells, case no. 2. **(D)** Strong staining (+++) in >50% of tumor cells, case no. 9.

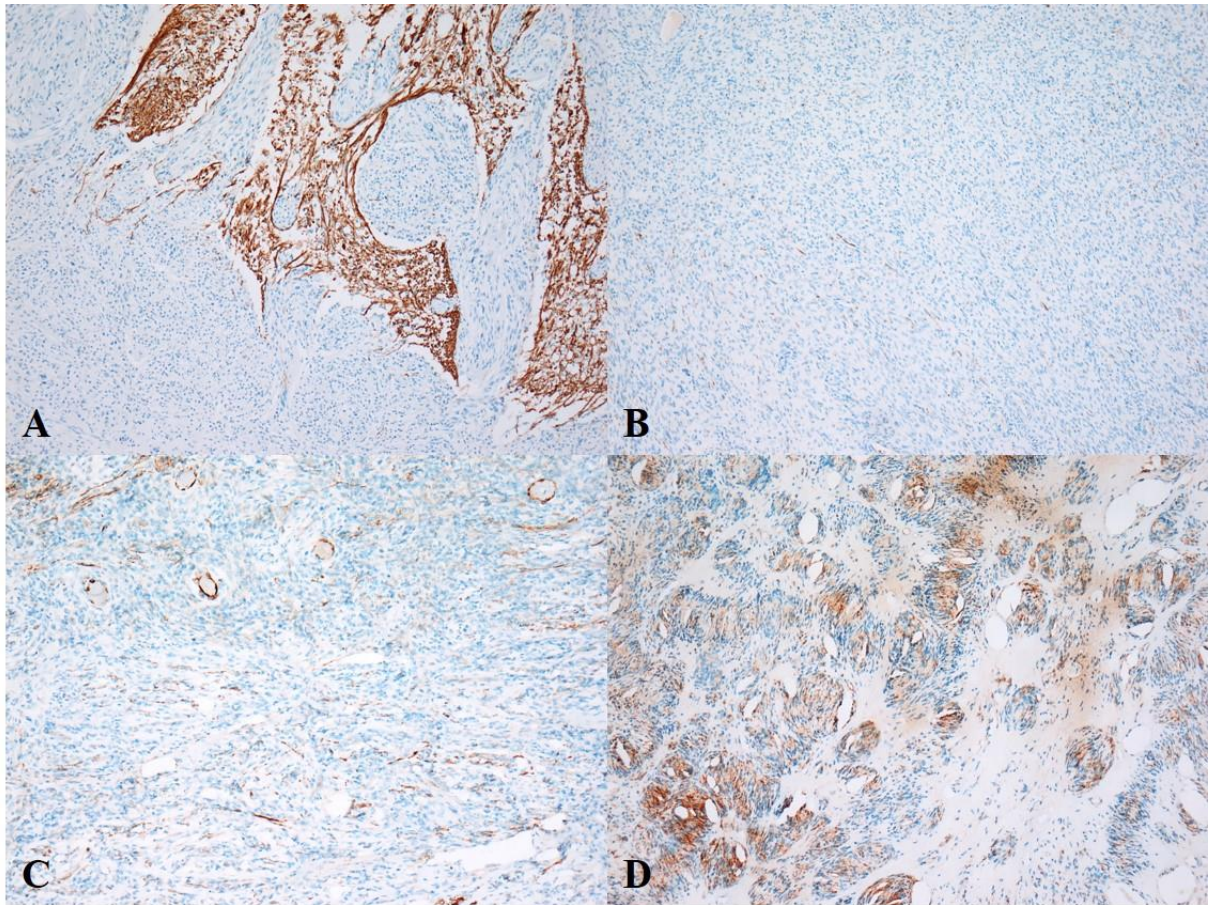


**Figure 6:** Evaluation of immunohistochemical expression of GFAP. GFAP, 100x. **(A)** Positive reaction in brain tissue remnants, whereas tumor is negative (-), case no. 7. **(B)** Weak staining (+), barely visible at low magnification, case no. 3. **(C)** Moderate staining (++) with strong cytoplasmic reaction in <50% of tumor cells, case no. 67. **(D)** Area of strong staining (+++) in >50% of tumor cells, case no. 38. Although the overall assessment of IHC response in this tumor showed moderate staining, as <50% of tumor cells expressed the marker. No tumor in the study showed a strong reaction to GFAP in >50% of tumor cells.

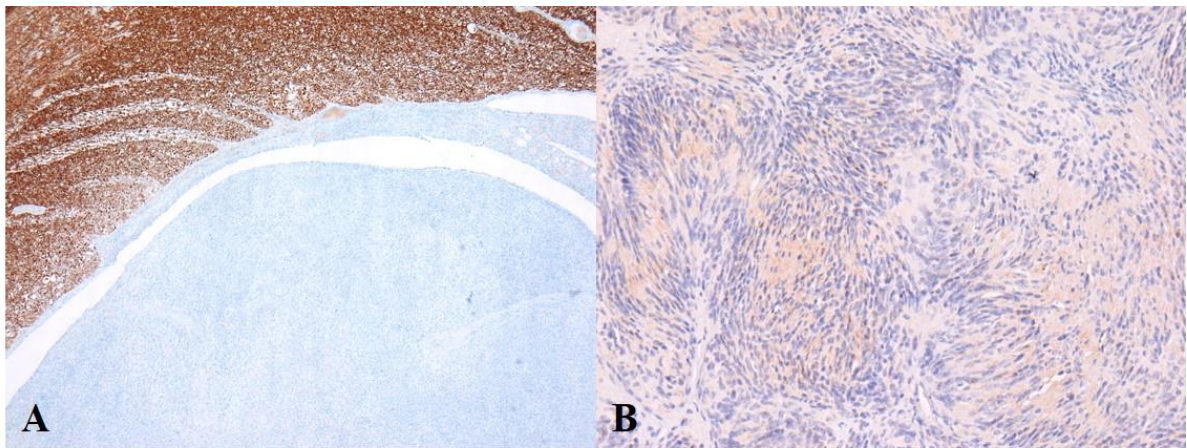


**Figure 7:** Evaluation of immunohistochemical expression of CNPase. CNPase, 100x. **(A)** Strong positive reaction in brain tissue adjacent to the tumor, whereas the tumor stains negatively (-), case no. 3. **(B)** Weak staining (+), barely visible at low magnification, case no. 38. No tumor in the study showed a moderate or strong reaction to CNPase.

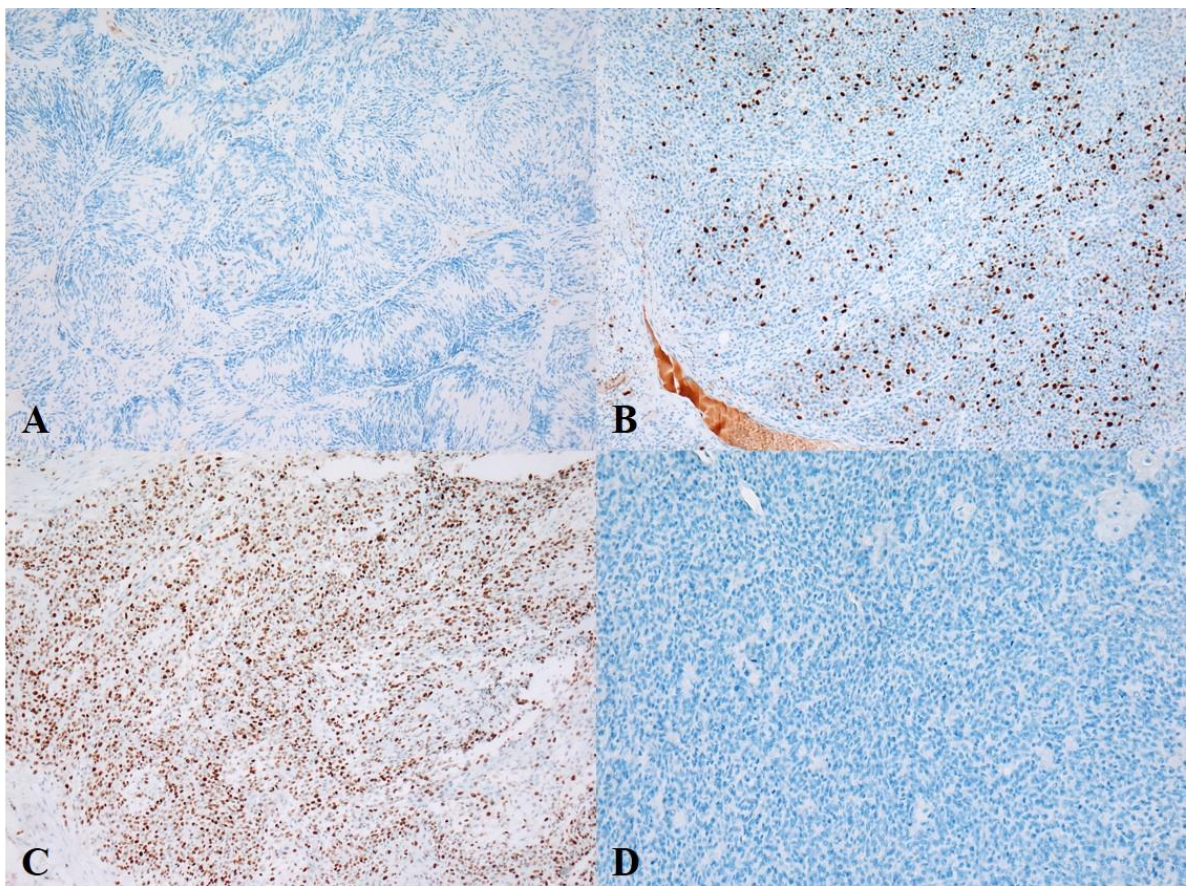


**Figure 8:** Variable proliferation activity detected by Ki-67 proliferation index. Ki-67, 100x. **(A)** Ki-67 proliferation index = 1.5%. Case no. 38. **(B)** Ki-67 proliferation index = 20.4%. Case no. 64. **(C)** Ki-67 proliferation index = 71.4%. Case no. 60. **(D)** No positive reaction is seen; staining for Ki-67 was considered unreliable in this case. Case no. 5.

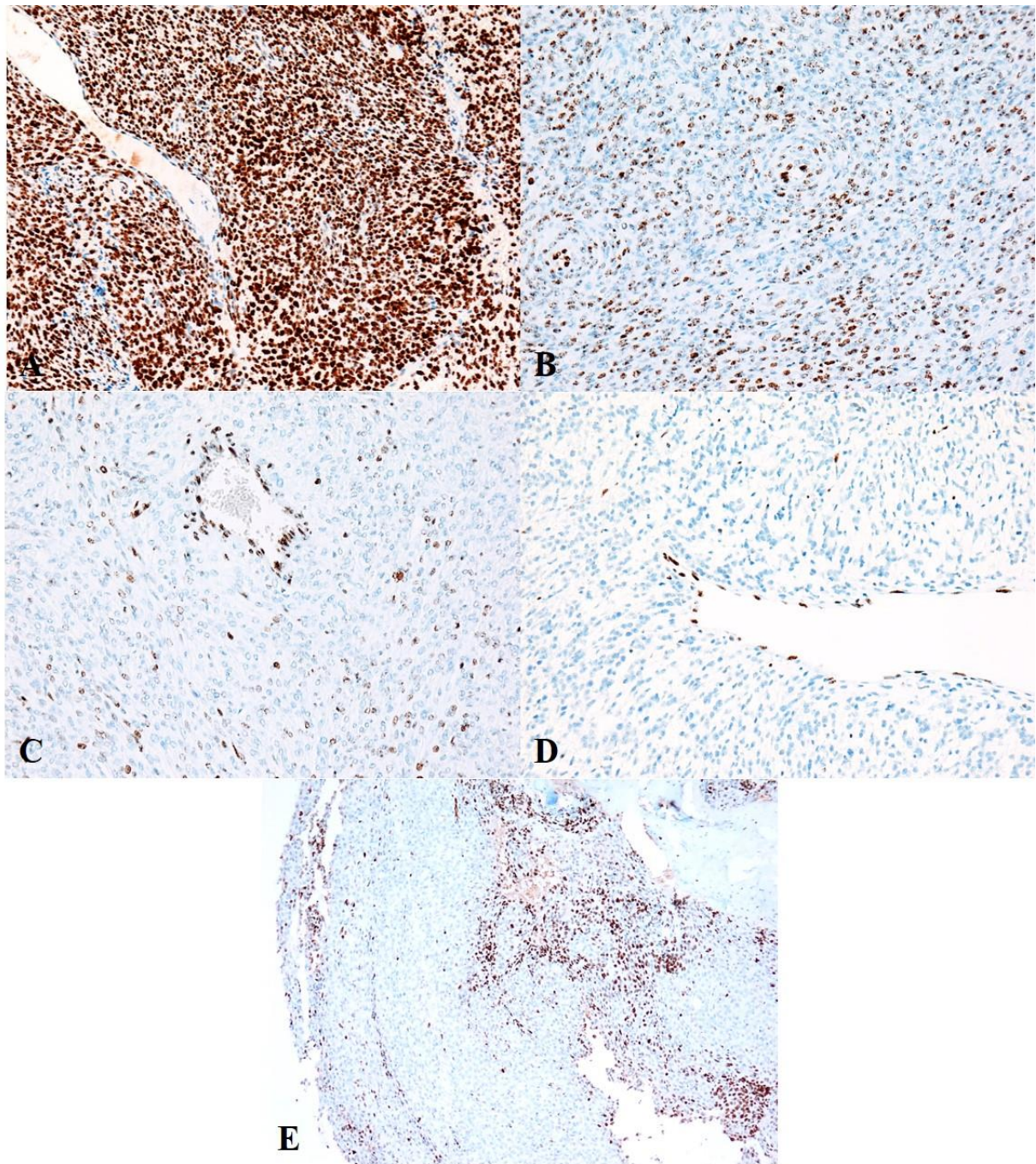


**Figure 9:** Evaluation of immunohistochemical expression of H3K27me3. (A) Retained expression in  $\geq 95\%$  of tumor cells (+++). Case no. 21, H3K27me3, 200x. (B) Mosaic loss of expression with retained expression in 50–94% of tumor cells (++). Case no. 56, H3K27me3, 200x. (C) Mosaic loss of expression with retained expression in 5–49% of tumor cells (+). Case no. 33, H3K27me3, 200x. (D) Complete loss of expression (-). The reaction is visible only in endothelial cells, which served as an internal positive control. Case no. 37, H3K27me3, 200x. (E) Geographic loss, a variant of complete loss of expression. Case no. 74, H3K27me3, 100x.

### 3.4 STATISTICAL ANALYSIS

Statistical analysis was performed using R statistical software, version 4.1.2 (R Core Team, 2021). The difference in dog age, number of mitoses, and Ki-67 percentage between the different groups according to tumor type, grading system, and tiers of H3K27me3 expression for all three scoring scales described above was calculated using the Wilcoxon rank sum test or the Kruskal-Wallis rank sum test, depending on the number of groups. The same tests were used to compare the proportion of Ki-67 by the IHC markers Sox10, claudin-1, GFAP, and CNPase separately. Non-parametric tests were used because the variables were not normally distributed, which was tested with the Shapiro-Wilk normality test. For the comparison of proportions between tumor type and grading system, Pearson's chi-squared test or Fisher's exact test were used if the assumptions for Pearson's chi-squared test were violated. Fisher's exact test was also used to evaluate the association between H3K27me3 expression and other factor variables, such as histopathological features (tissue and cellular characteristics of the tumors), the grade of MNSTs, and immunohistochemical staining results for Sox10, claudin-1, and GFAP. Because there were multiple comparisons with the same data set, p-values were adjusted with a Benjamini-Hochberg correction. Correlations between dog age, number of mitoses, and Ki-67 percentage were calculated using Spearman's rank correlation coefficient, and p-values were adjusted using Holm's method. For all statistical tests, a  $p$ -value  $<0.05$  was considered statistically significant while a  $p$ -value  $<0.1$  was interpreted as marginally statistically significant.

## 4 RESULTS

The results obtained in the context of this Ph.D. study have already been presented in two articles published in peer-reviewed journals (Tekavec et al., 2022a; Tekavec et al., 2022b).

### 4.1 SIGNALMENT AND CLINICAL FINDINGS

The breed, sex, and age of the dogs, reported clinical signs, and the location of the primary tumor are listed in **Table 3**.

**Table 3:** Signalment, clinical features, and tumor localization of the dogs included in the study.

| No. | Breed           | Age (years) | Sex | Clinical presentation  | Location  | Group |
|-----|-----------------|-------------|-----|--|---|-------|
| 1   | Mixed breed     | 8           | M   | Lameness/paresis of the thoracic limbs (LMN and UMN type).   | Below the spine at the level of C6-T1, extending upward through the foramina and infiltrating the epidural space. | C     |
| 2   | Fox Terrier     | 10          | F   | Vestibular syndrome, facial paralysis, bilateral progressive paraparesis (LMN type), and paralysis of the urinary bladder. | Nerve roots at the level of L3-L5.  | D, E  |
| 3   | Mixed breed     | 7.5         | F   | Atrophy of the right shoulder. Right pleurothotonus  | Extra- and intradural lesions at the level of C6-C7   | C     |
| 4   | Cocker Spaniel  | 13          | M   | Central vestibular syndrome.<br>Compulsive gait.   | Left V. and VII. cranial nerve.   | A     |
| 5   | German Shepherd | 11          | F   | Acute paraparesis-paraplegia.  | Tumor at the level of T8-T9 with involvement of the left nerve root.  | D     |
| 6   | Mixed breed     | 8           | M   | Paraplegia (LMN type) and absence of deep pain perception.   | Lumbosacral extra- and intradural lesion  | E     |
| 7   | Mixed breed     | 6           | M   | NR   | Right brachial plexus (C6-C7)   | F     |
| 8   | English Setter  | 7           | M   | The postural deficit, and hyporeflexia of the right forelimb.  | Nerve root involvement at the level of the cervicothoracic spine.   | C     |

|    |                           |     |   |   |   |   |
|----|---------------------------|-----|---|---|---|---|
| 9  | Beagle                    | 8   | M | NR  | Brachial plexus.  | F |
| 10 | Mixed breed               | 8   | M | NR  | Nerve roots at the level of C7-T1   | C |
| 11 | Dalmatian                 | 11  | M | Lameness of the left forelimb with muscular atrophy.<br>Reduced forelimbs proprioception.<br>Neck pain. | Nerve roots at the level of the C6-T1.  | C |
| 12 | German Wirehaired Pointer | 8   | M | Left forelimb paresis.<br>Absence of spinal reflexes.<br>Pain on palpation of the axilla.               | Extramedullary centripetal lesion at the root of the left radial nerve.   | F |
| 13 | Shih-Tzu                  | 4   | F | Pulmonary and brain metastases.   | Brachial plexus.  | F |
| 14 | Newfoundland dog          | 1.5 | M | Lameness of the left hindlimb with impaired proprioception.   | Tumor is located ventral to the left transverse process of L7, adjacent to the nerve root L6. The tumor is encapsulated proximally and continues distally within the nerve. | E |
| 15 | Yorkshire Terrier         | 7   | M | NR  | Intradural extramedullary lesion at the level of C7-T1.   | C |
| 16 | Labrador Retriever        | 10  | M | NR  | Extradural mass at the level of L1-L2 – lateralized on the left.  | D |
| 17 | Mixed breed               | 11  | M | Chronic lameness and paresis of the left forelimb. EMG: denervation atrophy.                            | Nerve roots – T1.   | C |
| 18 | Labrador Retriever        | 7   | F | Lameness and muscle atrophy of the right pelvic limb  | Right femoral nerve.  | H |
| 19 | Labrador Retriever        | 6   | M | Head tilt to the left.  | Left V. nerve.  | A |
| 20 | Mixed breed               | 8   | M | Neck pain and lameness of the right forelimb.   | Intradural extramedullary neoplasia of the roots C6-C7.   | C |
| 21 | German Shepherd           | 12  | M | NR  | Nerve root C8.  | C |

|    |                             |    |   |  |   |   |
|----|-----------------------------|----|---|--|---|---|
| 22 | Mixed breed                 | 13 | M | NR   | Extradural mass of the right cervical spinal cord segment (C1-C6).          | B |
| 23 | German Shepherd             | 12 | M | Progressive left hemiparesis, progressing to recumbency.         | Extra- and intravertebral neoplasm at the level of the left foramina C5-C6. | C |
| 24 | German Shepherd             | 6  | M | NR   | Left axillary region – the T2 root.   | C |
| 25 | French Bulldog              | 6  | M | NR   | Lateral mass on the left <i>medulla oblongata</i> and <i>pons</i> .         | A |
| 26 | Labrador Retriever          | 6  | M | NR   | Right brachial plexus.  | F |
| 27 | Maltese                     | 6  | F | NR   | Involvement of the nerve roots C7-T1.                                       | C |
| 28 | Yorkshire Terrier           | 12 | F | NR   | Intramedullary lesions at the level of C2 and C6.                           | B |
| 29 | Mixed breed                 | 12 | M | Lameness of the right forelimb is associated with hypomyotrophy. | Tumor of the nerve roots at the cervicothoracic spinal cord.                | C |
| 30 | Labrador Retriever          | 5  | M | NR   | Left sciatic nerve.   | H |
| 31 | Mixed breed                 | 6  | F | Atrophy of the muscles of the shoulder and left forelimb.        | Tumor of the nerve roots at the cervicothoracic spinal cord.                | C |
| 32 | Mixed breed                 | 6  | M | NR   | Left brachial plexus.   | F |
| 33 | English Setter              | 11 | M | NR   | Neoplasia of the left brachial plexus (C7-T1).                              | F |
| 34 | Czechoslovakian Wolfdog     | 11 | M | NR   | Nerve root C8.  | C |
| 35 | Boston Terrier              | 8  | M | NR   | Brachial plexus.  | F |
| 36 | Labrador Retriever          | 4  | M | NR   | Lardaceous extradural neoplasia C1-C2.                                      | B |
| 37 | Mixed breed                 | 9  | M | NR   | Brachial plexus.  | F |
| 38 | Rottweiler                  | 9  | F | NR   | Tumor of the right C1-C2.   | B |
| 39 | German Shepherd             | 12 | M | NR   | Left radial nerve.  | H |
| 40 | German Shepherd             | 4  | M | NR   | Medullary lesion of the cervical spine.                                     | B |
| 41 | Mixed breed                 | 11 | M | NR   | Nerve root of the left C7.  | C |
| 42 | West Highland White Terrier | 10 | M | NR   | Lumbosacral plexus.   | G |

|    |                             |    |   |  |   |      |
|----|-----------------------------|----|---|--|---|------|
| 43 | German Shepherd             | 8  | M | NR   | Brachial plexus.  | F    |
| 44 | Golden Retriever            | 10 | M | NR   | Right pontomesencephalic extra-axial neoplasia.   | A    |
| 45 | Beagle                      | 8  | M | NR   | Intradural extramedullary neoplasia C4-C5.  | B    |
| 46 | Mixed breed                 | 7  | M | NR   | Tumor of the nerve roots at the cervicothoracic spinal cord.  | C    |
| 47 | Mixed breed                 | 13 | F | NR   | T13 and L5 nerve roots.   | D, E |
| 48 | Mixed breed                 | 11 | M | NR   | Right brachial plexus.  | F    |
| 49 | Labrador Retriever          | 7  | M | NR   | Endocanal, extramedullary C6 lesion.  | C    |
| 50 | West Highland White Terrier | 12 | M | Progressive hemiparesis for 15 days.   | Intradural extramedullary mass involving the nerve roots at the level of the cervicothoracic spinal cord. | C    |
| 51 | Mixed breed                 | 7  | M | Paralysis of the right VII., IX., and X. cranial nerves.                                   | Right VII., IX., and X. cranial nerves.   | A    |
| 52 | Mixed breed                 | 11 | M | Progressive lameness of left forelimb.   | A mass in the left shoulder region – involving the brachial plexus and cervicothoracic spinal cord C4-T7. | F    |
| 53 | Cane Corso                  | 8  | M | Bilateral flexor hyporeflexia and proprioceptive deficit of the right forelimb. Neck pain. | Neoplasia of the right C4 with medullary infiltration.  | B    |
| 54 | Mixed breed                 | 12 | F | NR   | Left trigeminal nerve.  | A    |
| 55 | Mixed breed                 | 9  | M | NR   | Nerve root involvement at the level of the lumbosacral spinal cord.                                       | E    |
| 56 | Mixed breed                 | 11 | M | NR   | Left brachial plexus.   | F    |
| 57 | Mixed breed                 | 8  | M | Left hemiparesis.  | Intradural extramedullary mass on the left C2-C3.   | B    |
| 58 | Mixed breed                 | 4  | M | Paraparesis with the proprioceptive deficit, urinary, and fecal incontinence.              | Intradural, intramedullary mass L4-L7.  | E    |
| 59 | Dogo Argentino              | 5  | F | NR   | Tumor of the right C6.  | C    |

|    |                               |    |   |  |  |   |
|----|-------------------------------|----|---|--|--|---|
| 60 | Mixed breed                   | 11 | F | Right forelimb lameness, decreased proprioception, and pain. Right Horner syndrome. Absence of panniculus reflex cranial to right T11. | Right axillary mass extending to the spinal cord by multiple nerve roots.            | C |
| 61 | Bernese Mountain dog          | 12 | M | NR   | Brachial nerve.  | H |
| 62 | Labrador Retriever            | 3  | M | NR   | Lesion of the T9-T10.  | D |
| 63 | German Shepherd               | 10 | F | Right forelimb lameness, flexor areflexia, and muscular atrophy.   | Right C8 nerve.  | C |
| 64 | Boxer                         | 6  | M | Chronic lameness and pain of the left forelimb.  | Left ulnar nerve.  | H |
| 65 | French Bulldog                | 8  | F | NR   | Neoplasia of C2 with compression of the spinal cord.                                 | B |
| 66 | German Shepherd               | 7  | F | Left forelimb paresis and hyporeflexia.  | Left C8 nerve root.  | C |
| 67 | Papillon                      | 7  | M | Progressive pain of the right forelimb (radicular syndrome) and neck pain.   | Right brachial plexus tumor (C1-T2).   | F |
| 68 | Mixed breed                   | 11 | M | Right paraparesis, ataxia, and proprioceptive deficit.   | Nerve root T13.  | D |
| 69 | Bernese Mountain dog          | 7  | M | Ataxia of the four limbs and neck pain.  | NR   | C |
| 70 | Mixed breed                   | 9  | M | NR   | Lumbar plexus (L6-L7).   | G |
| 71 | Mixed breed                   | 10 | M | NR   | Neoplasia of the left root L3. Invasion of the spinal canal – intramedullary growth. | D |
| 72 | Mixed breed                   | 8  | F | Chronic paresis of the left forelimb.  | Left brachial plexus.  | F |
| 73 | Cavalier King Charles Spaniel | 12 | M | NR   | Lumbar paravertebral lesion on the left side.  | E |
| 74 | Golden Retriever              | 4  | M | Progressive tetraparesis.  | Epidural lesion C2-C4.   | B |

|    |                       |      |   |   |  |   |
|----|-----------------------|------|---|---|--|---|
| 75 | Staffordshire Terrier | 8    | F | Right hindlimb paresis.   | Extramedullary mass at the level of the L4-L5 nerve roots.                           | E |
| 76 | Staffordshire Terrier | 9    | M | NR  | Neoplasia of the right C2 root with endocanal extension and spinal cord compression. | B |
| 77 | French Bulldog        | 10.5 | F | NR  | Neoplasia of the right C7 root.  | C |
| 78 | Mixed breed           | 6    | F | Progressive ataxia with severe proprioceptive deficits and cervical pain. | Intradural, extramedullary mass at the level of right C2.                            | B |
| 79 | Jack Russel Terrier   | 6.5  | M | Chronic lameness of the right forelimb.                                   | Neoplasia of the right brachial plexus extending to the C6-T1 nerve roots.           | F |

M: male; F: female; LMN: lower motor neuron; UMN: upper motor neuron; EMG: electromyography; NR: not reported. The letter in the last column is referred to the group: A: cranial nerve; B: cervical spinal cord segment; C: cervicothoracic spinal cord segment; D: thoracolumbar spinal cord segment; E: lumbosacral spinal cord segment; F: brachial plexus; G: lumbosacral plexus; H: appendicular nerve.

The majority of dogs included in the study were a mixed breed (29/79, 36.7%). There were also 26 different purebred dog breeds represented, with the German Shepherd being the most representative breed (9/79, 11.4%), followed by the Labrador Retriever (8/79, 10.1%).

Fifty-nine dogs were male (74.7%) and 20 were female (25.3%); their ages ranged from 1.5 to 13 years, with a median age of 8 years. The median age at diagnosis was 7.5 years (range 1.5–12) for BNSTs and 8 years (range 4–13) for MNSTs.

The most frequent localization of tumors was the roots of spinal nerves (50/79, 63.3%), especially at the level of the cervicothoracic spinal cord segment (group C, 25/50, 50.0%) and at the brachial plexus (group F, 16/79, 20.3%) (**Figure 10**). A small number of tumors occurred in cranial nerves (group A, 6/79, 7.6%), appendicular nerves (group H, 5/79, 6.3%), and the lumbosacral plexus (group G, 2/79, 2.5%). All BNSTs in our study were located at the nerve roots of different spinal cord segments.

According to the available clinical information, the clinical signs depended on the location of the tumor. Usually, they manifested as motor and/or sensory deficits as a result of compression or injury of the nerves. Involvement of the cranial nerves resulted in a cranial deficit and

brainstem syndrome; involvement of the brachial/lumbosacral plexus or appendicular nerves corresponded to a lower motor neuron (LMN) syndrome; whereas extradural or intradural tumor extension and spinal cord compression were often reflected in symptoms of both LMN and upper motor neuron (UMN). One case (no. 13) was presented with metastatic disease in which the brachial plexus tumor had metastasized to the lung and brain.



**Figure 10:** Excised tumor from the brachial plexus submitted for histopathologic examination (case no. 79). The letters T1-C6 refer to the spinal nerves. (Photo courtesy of: Dr. Cristian Falzone, Clinica Veterinaria Pedrani).

#### 4.2 HISTOPATHOLOGY AND IMMUNOHISTOCHEMISTRY

Based on their histopathological features in conjunction with the results of IHC staining for Sox10, claudin-1, GFAP, CNPase, and Ki-67, 12 cases (15.2%) were diagnosed as BNSTs and 67 cases (84.8%) were diagnosed as MNSTs. In the following, we describe the main histopathological and IHC features of the different subtypes and their variants. The exact diagnoses and expressions of the IHC markers used in this study are listed in **Table 4** for each case. IHC staining for Ki-67 was weak or without reaction and was considered unreliable for samples nos. 1–24 submitted for histopathological examination between the years 2000 and 2008. Due to a lack of immunohistochemical reaction in the internal positive controls, staining for H3K27me3 was considered unreliable for samples nos. 2, 4, 5, 7, 11, 22, 24, 29, 44, 51, and

57; staining for Sox10 was unreliable for samples no. 11 and 58; staining for GFAP was unreliable for sample no. 11.

A summary of the expression of Sox10, claudin-1, GFAP, and CNPase in the different subtypes and variants of NST is provided in **Table 5**, and a detailed IHC analysis of the cases is provided in **Table 6**. Analysis of H3K27me3 expression is presented separately in **Table 7** for 68 successfully stained NSTs, representing the results of a 4-tier scoring scale from which 2- and 3-tier scales can be calculated.

#### **4.2.1 Benign nerve sheath tumors**

Of 12 BNSTs, we diagnosed six neurofibromas (nos. 29, 62, 63, 69, 76, 78) (**Figure 11**), one schwannoma (no. 38) (**Figure 12**), and two hybrid NSTs – a perineurioma/neurofibroma (no. 11) and a perineurioma/schwannoma (no. 24) (**Figure 13**). We designated three cases as nerve sheath myxomas (nos. 14, 45, 59) (**Figure 14**).

##### 4.2.1.1 Histopathological features of BNSTs

Of 12 BNSTs, eleven presented as localized nodular masses; while one was a plexiform neurofibroma that involved multiple nerves (no. 63). Five BNST specimens were submitted to the laboratory as incisional biopsies or were incompletely excised, assessing their demarcation, encapsulation, and growth pattern impossible. The remaining six BNSTs were mostly well-demarcated, encapsulated, or partially encapsulated masses confined to the epineurium, with occasional mild infiltrative growth longitudinally along the nerve.

None of the BNSTs had atypical histologic features that would raise concern for malignancy, vascular invasion, or herniation of tumor cells into vessels. Occasionally, hyalinization of blood vessels was observed (3/12).

Small necrotic areas were noted in three BNSTs and hemorrhage in four BNSTs, the latter most likely caused by sampling.

Multifocal inflammatory infiltrates were present in 50% of BNSTs and consisted mostly of lymphocytes and occasionally plasma cells.

Tumor cells exhibited mild or no atypia, were mostly spindle- to stellate, sometimes elongated, with a small to moderate amount of eosinophilic cytoplasm, indistinct cell borders, and a single

oval to round or wavy hyperchromatic nucleus and only occasionally a small nucleolus. The mitotic count per 10 HPF was zero in seven BNSTs and at most three in five other BNSTs. There was a moderate to a large amount of collagenous or myxoid stroma between tumor cells. Occasionally, the stromal collagen component in neurofibromas showed the so-called "shredded carrot" appearance (no. 76).

Four BNSTs contained metaplastic elements that lacked atypia; osseous metaplasia was noted in a hybrid perineurioma/neurofibroma (no. 11) and cartilaginous metaplasia in a hybrid perineurioma/schwannoma (no. 24) and one nerve sheath myxoma (no. 14), whereas both osseous and cartilaginous metaplasias were observed in another nerve sheath myxoma (no. 59).

In one case (no. 38), pronounced nuclear palisading (Verocay bodies) was noted, leading to the diagnosis of classic schwannoma. Characteristics of perineurioma were neoplastic perineurial cells arranged concentrically in multiple layers around centrally located axons, forming so-called pseudobulbs. Perineurioma regions were detected in both hybrid NSTs, whereas no BNST was diagnosed exclusively as perineurioma. Nerve sheath myxomas were characterized by a predominant myxoid stroma separating stellate and spindle-shaped tumor cells without atypia (nos. 14, 45, 59). Multinucleated cells were occasionally noted in one nerve sheath myxoma (no. 14). The myxoid lobules in nerve sheath myxomas were separated by collagenous septa and were particularly prominent in one case (no. 59).

#### 4.2.1.2 Immunohistochemical features of BNSTs

More than 90% of BNSTs expressed Sox10, claudin-1, and GFAP to varying degrees. In the majority of tumors, expression of these IHC markers was moderate (++) . CNPase, on the other hand, was weakly expressed only in classical schwannoma (no. 38). Classical schwannoma was the only BNST that was negative for claudin-1, strongly positive for Sox10 (+++), and moderately positive for GFAP (++) . One neurofibroma was negative for Sox10 but the specimen did not contain an internal positive control to prove that IHC staining was adequate. Perineurioma regions in both hybrid BNSTs (nos. 11 and 24) were moderately to strongly positive for claudin-1 (++)/+++ and negative for Sox10 and GFAP. Tumor cells in the schwannoma region of hybrid perineurioma/schwannoma expressed Sox10 (++) and GFAP (+) and were negative for claudin-1. As mentioned previously, staining for GFAP and Sox10 in

hybrid neurofibroma/perineurioma (no. 11) proved unreliable because the positive control (non-neoplastic Schwann cells) was negative.

The Ki-67 proliferation index in BNSTs ranged from 0.8% to 11.0% (mean  $4.89 \pm 4.06\%$ ).

Immunohistochemical expression of H3K27me3 was examined in nine BNSTs (nos. 14, 38, 45, 59, 62, 63, 69, 76, and 78), and complete loss was observed in one neurofibroma (no. 69). Fifty-six percent of BNSTs showed complete retention of staining in  $\geq 95\%$  of tumor cells, whereas the remaining 33% (3/9) showed mosaic loss with retained expression in 50–94% of tumor cells (++) .

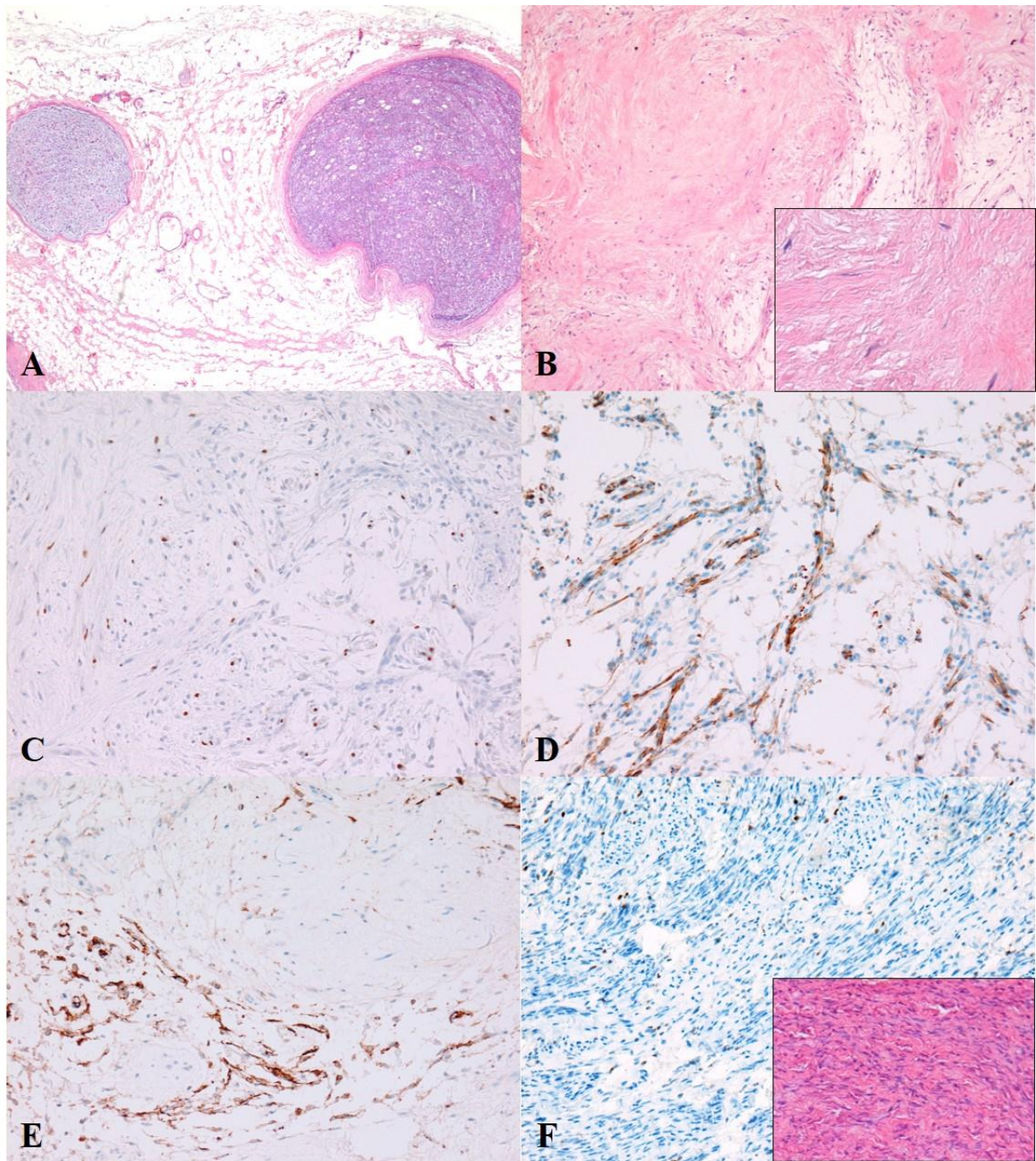


**Figure 11:** Histopathological and immunohistochemical characteristics of neurofibroma. (A) Plexiform neurofibroma (case no. 63). HE, 40x. (B) Neurofibroma with abundant collagenous stroma that has the so-called shredded-carrot appearance (case no. 76). HE, 100x. Insert image: HE, 400x. (C) Moderate expression of Sox10 (++) (case no. 76). Sox10, 200x. (D) Moderate expression of GFAP (++) (case no. 76). GFAP, 200x. (E) Strong expression of claudin-1 (+++) (case no. 76). Claudin-1, 200x (F) Neurofibroma with loss of H3K27me3 (case no. 69). H3K27me3, 200x. Insert image: histopathological features indicate the benignity of the tumor. HE, 200x.

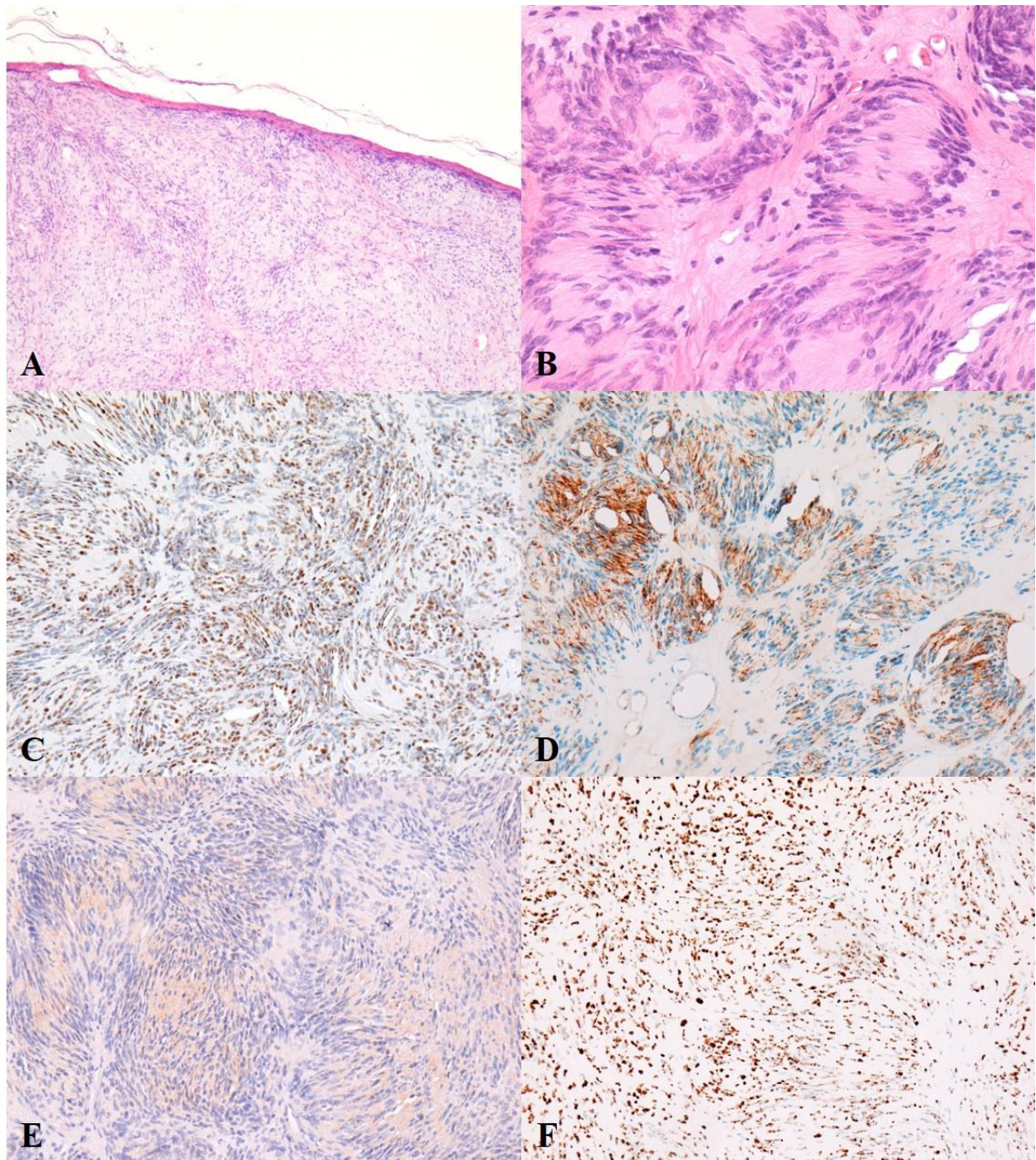


**Figure 12:** Histopathological and immunohistochemical characteristics of schwannoma (case no. 38). (A) Well-demarcated tumor surrounded by a capsule. HE, 100x. (B) Distinct nuclear palisading (Verocay bodies) is characteristic of classic schwannoma, HE, 400x. (C) Diffuse strong nuclear immunoreactivity (+++) for Sox10. Sox10, 200x. (D) Multifocally (<50% of tumor), the neoplastic cells moderately to strongly express GFAP (++). GFAP, 200x. (E) Multifocally, the cytoplasm of neoplastic cells shows mild immunoreactivity (+) for CNPase. CNPase, 200x. (F) This case of schwannoma shows complete retention (+++) of H3K27me3 expression.

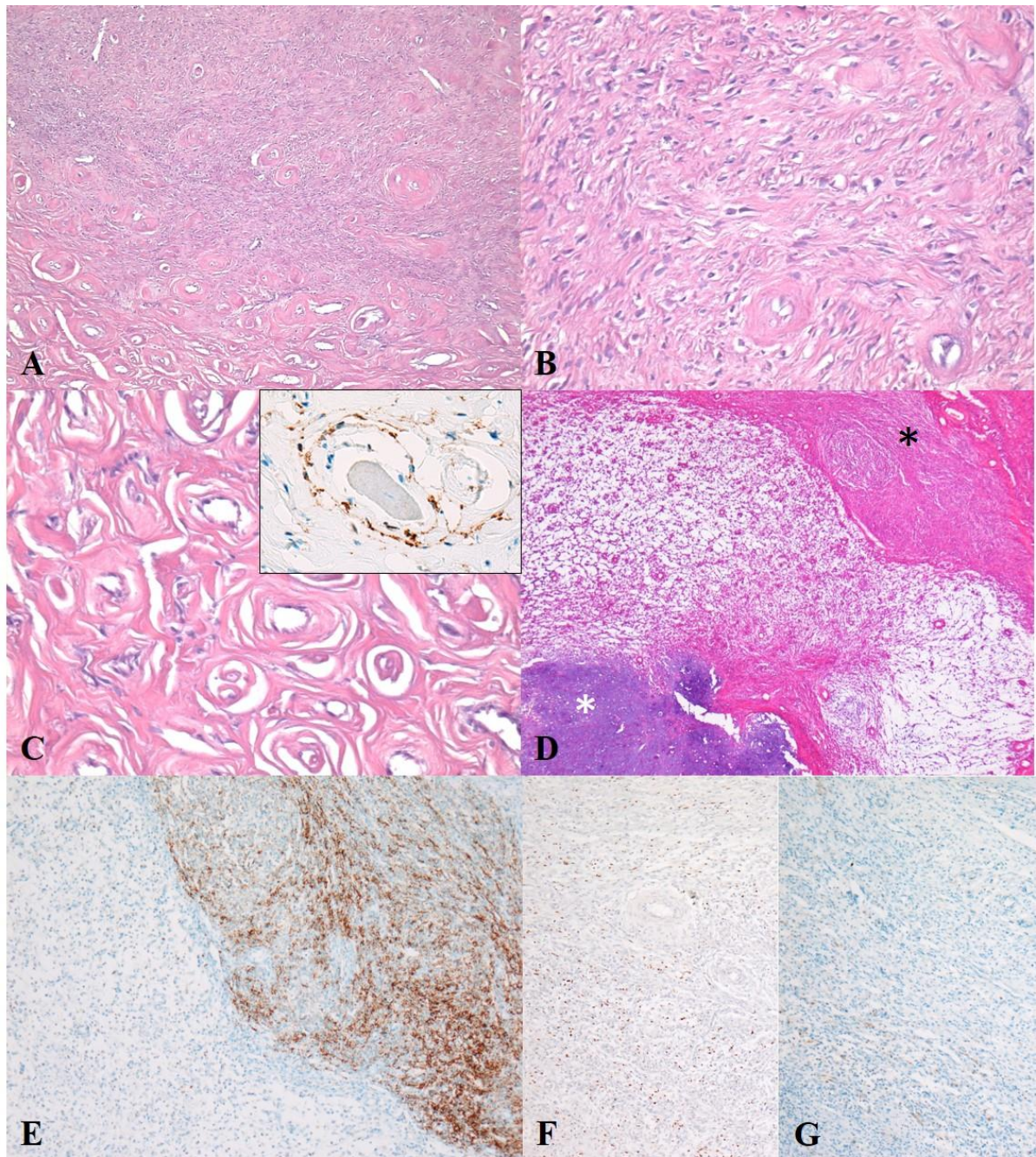


**Figure 13:** Histopathological and immunohistochemical characteristics of hybrid benign nerve sheath tumor. (A, B, C) Hybrid perineurioma/neurofibroma (case no. 11). (A) The upper part of the image represents a neurofibroma and the lower part a perineurioma. HE, 40x. (B) Neurofibroma part. HE, 400x. (C) The Perineurioma part is characterized by a concentric arrangement of neoplastic perineurial cells forming the so-called pseudo-onion bulbs. HE, 400x. Insert image: membranous claudin-1 immunoreactivity of neoplastic perineurial cells. Claudin-1, 400x. (D, E, F, G) Hybrid perineurioma/schwannoma (case no. 24). (D) HE, 40x. The perineurioma part is more densely cellular (black asterisk), whereas the schwannoma regions below are looser. In this case, cartilaginous metaplasia was observed (white asterisk). (E) Perineurioma regions show diffuse strong positivity (+++) for claudin-1. Claudin-1, 100x. (F) Schwannoma regions show moderate positivity for Sox10 (++) Sox10, 100x, and (G) mild positivity (+) for GFAP, GFAP, 100x.

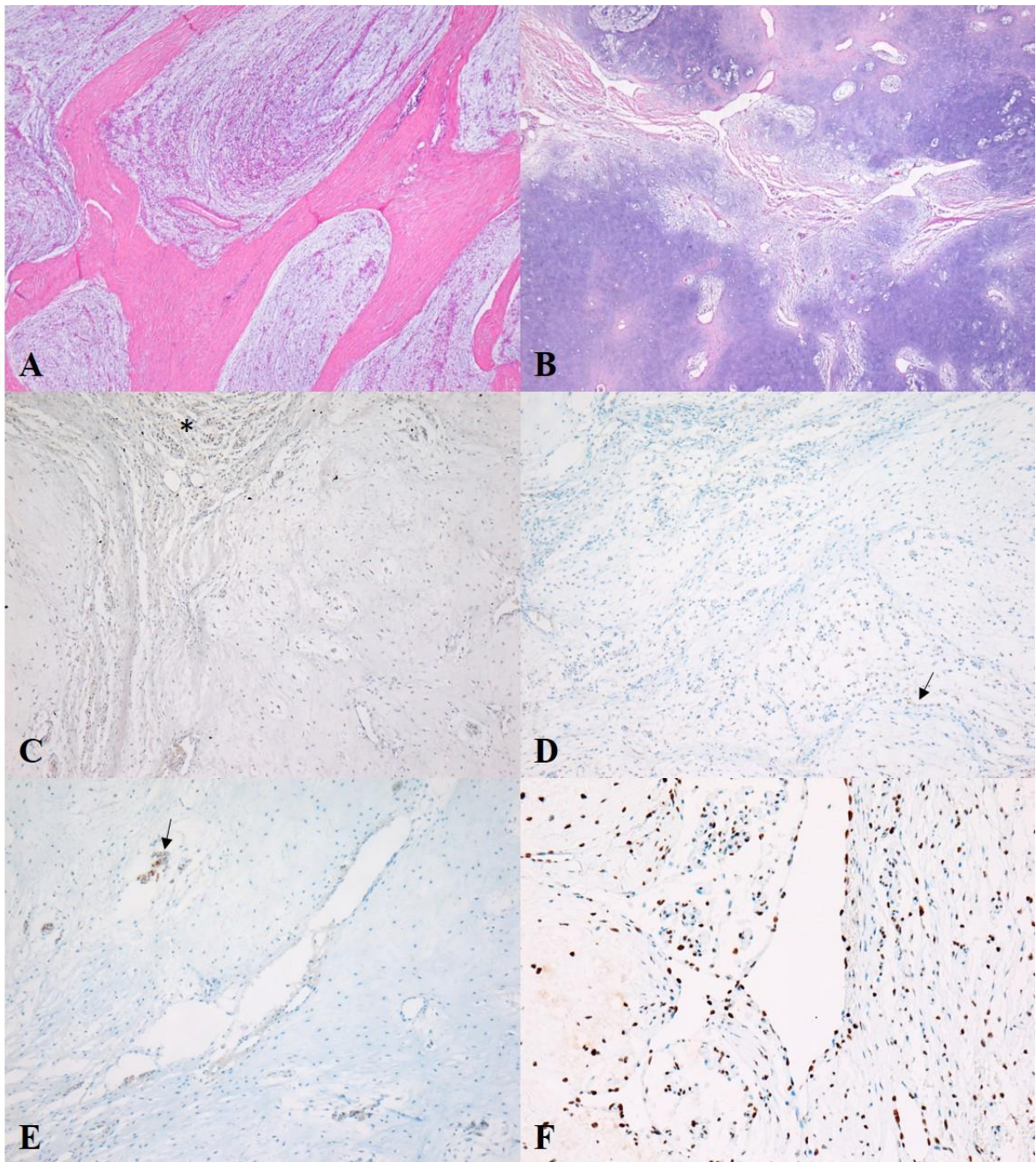


**Figure 14:** Histopathological and immunohistochemical characteristics of nerve sheath myxoma. **(A)** Nerve sheath myxoma consisting of myxoid lobules separated by distinct collagenous septa (case no. 59). HE, 40x. **(B)** Nerve sheath myxoma with large areas of cartilaginous metaplasia (case no. 14). HE, 40x. **(C, D, E, F)** Same case as **(B)**. **(C)** Mild multifocal positivity for Sox10 (black asterisk). Sox10, 100x. **(D)** Mild multifocal positivity for claudin-1 (arrow). Claudin-1, 100x. **(E)** Mild multifocal positivity for GFAP. GFAP, 100x. **(F)** Loss of H3K27me3 expression in 5-49% of tumor cells (loss in the minority). H3K27me3, 200x.

## 4.2.2 Malignant nerve sheath tumors

The majority of NSTs in our study were malignant (67/79; 84.8%). Based on their histopathologic features and IHC staining results for Sox10, claudin-1, GFAP, CNPase, and Ki-67, we diagnosed 56 MNSTs (83.6%) as conventional variants (**Figures 15, 16, and 17**), six MNSTs with divergent differentiation (9.0%) (**Figure 18**), four MNSTs with perineural differentiation/perineural MNSTs (6.0%) (**Figure 19**), and one MNST with epithelioid differentiation/epithelioid MNST (1.5%) (**Figure 20**). Based on the grading scale used, we histopathologically classified 15 MNSTs (22.4%) as grade I MNSTs, all of which represented a conventional variant, 28 MNSTs (41.8%) as grade II, including 25 conventional, two perineural, and one epithelioid MNST, and 24 MNSTs (35.8%) as grade III, including 16 conventional, two perineural, and all six MNSTs with divergent differentiation (**Table 6**).

### 4.2.2.1 Histopathological features of MNSTs

Most MNSTs presented as poorly circumscribed, non-encapsulated, infiltrative masses. Usually, infiltrative growth was pronounced longitudinally along the nerve and occasionally extended into the spinal cord and/or through the epineurium into surrounding tissues – fat, connective tissue, or muscle. Overall, the MNSTs were highly cellular tumors with a small to moderate amount of collagenous or myxoid stroma. In five conventional MNSTs (nos. 26, 41, 44, 48, 54), only portions of the tumor exhibited malignancy, suggesting a transition from a neurofibroma.

Necrotic areas of varying extent were noted in 65.7% of MNSTs (44/67); in all but one conventional MNST (no. 73), in which more than 50% of the tumor was necrotic, necrosis was equal to or less than 50% of the tumor. The difference in the presence of necrosis between MNSTs and BNSTs was statistically significant (Fisher's Exact Test,  $p = 0.0379$ ).

Herniation of tumor cells into vessels was observed in 35.9% of MNSTs (24/67) and was statistically significant for MNSTs compared to BNSTs (Fisher's Exact Test,  $p = 0.0355$ ). No invasion into lymphatic vessels was observed while invasion into blood vessels was observed in a conventional grade III MNST (no. 13), which was also the only case with confirmed metastases to the lung and brain.

In numerous cases of MNSTs (44/67, 65.7%), we detected intra- and/or peritumoral inflammatory infiltrates composed mainly of lymphocytes. However, they were not statistically significant more numerous or larger in MNSTs compared to BNSTs (Fisher's Exact Test,  $p = 0.4866$ ).

Tumor cells that formed fascicles, interlacing bundles, and concentric whorls were dominant components of conventional and perineural MNSTs as well as parts of MNSTs with divergent differentiation. Tumor cells were generally spindle-shaped, fusiform, or oval and exhibited various degrees of cellular pleomorphism and atypia. The degree of anisocytosis, anisokaryosis, nuclear pleomorphism, and the number of nucleoli were statistically significantly higher in MNSTs compared with BNSTs (Fisher's Exact Test,  $p < 0.0001$ ). The difference in cellular atypia was also statistically significant in higher-grade MNSTs compared to lower histopathological grade (Fisher's Exact Test,  $p < 0.05$ ). Multinucleated cells were detected in 27 MNSTs (40.3%), and the difference in the presence of multinucleated cells between MNSTs and BNSTs was marginally statistically significant (Fisher's Exact Test,  $p = 0.0999$ ).

The number of mitoses varied among MNSTs; four MNSTs, of which two were grade I and two were grade II, had a mitotic count of 1/10 HPF, whereas 19 grade III MNSTs had a mitotic count greater than 20/10 HPF. The mitotic count in one conventional grade III MNST was 105 mitoses/10 HPF. The mean mitotic count in MNSTs was  $17 \pm 21$  mitoses/10 HPF. MNSTs had a statistically significant higher mitotic count compared to BNSTs (Wilcoxon rank sum test,  $p < 0.0001$ ).

Bony tissue was a component in all six MNSTs with divergent differentiation, and five of them also contained cartilaginous tissue. The osseous component in case no. 43, which was the only one without cartilaginous differentiation, and the osseous and cartilaginous components in cases nos. 60 and 61 showed marked atypia, leading to the diagnosis of osteosarcomatous and chondrosarcomatous differentiation.

One morphologically distinctive case (no. 64) was diagnosed as epithelioid MNST and consisted of round and oval tumor cells with round, oval, or bean-shaped nuclei. The nuclei were slightly eccentric in numerous cells.

#### 4.2.2.2 Immunohistochemical features of MNSTs

Sixty-seven percent (44/66) of MNSTs expressed Sox10, with 35% of tumors (23/66) showing mild expression (+) and 29% of tumors (19/66) showing moderate expression (++). As stated previously, staining for Sox10 in one MNST (no. 58) was considered unreliable because the internal positive control (non-neoplastic Schwann cells) was negative. Two MNSTs strongly expressed Sox10; an epithelioid MNST (no. 64) that was negative for claudin-1, CNPase, and GFAP, and one conventional grade II MNST (no. 20) that also weakly expressed claudin-1.

Seventy-one percent of MNSTs (48/67) differentially expressed claudin-1, with predominantly moderate immunoreactivity. Seven MNSTs strongly expressed claudin-1 (+++), and four of them were negative for Sox10, GFAP, and CNPase (nos. 9, 33, 34, and 37). Accordingly, we classified them as MNSTs with perineural differentiation. GFAP was expressed in 33% of MNSTs (22/79), with weak expression in the majority of MNSTs (17/22) and moderate expression in five MNSTs. No MNST expressed CNPase.

Twelve MNSTs (18%) were immunonegative for Sox10, claudin-1, GFAP, and CNPase. According to their histopathological features, ten of these MNSTs were conventional (nos. 1, 7, 13, 17, 22, 36, 42, 44, 74, 75) and two were MNSTs with divergent differentiation (nos. 4, 5) but with osseous and cartilaginous components without atypia. One immunonegative MNST was a grade I, four a grade II, and seven a grade III MNSTs.

The proliferation index Ki-67 was calculated in 46 MNSTs and was as high as 71.4% in one MNST with divergent differentiation (no. 60). The mean Ki-67 proliferation index in MNSTs was  $24.41 \pm 15.07\%$  and was statistically significantly higher compared to BNSTs (Wilcoxon rank sum test,  $p = 0.0001$ ), as shown in **Figure 21a**. While the difference in proliferation index Ki-67 between different grades of MNSTs was marginally statistically significant (**Figure 21b**, Kruskal-Wallis rank sum test,  $p = 0.0907$ ). Higher mitotic count was associated with a higher Ki-67 proliferation index, which was confirmed with Spearman's rank correlation coefficient that showed a high correlation between Ki-67 and the number of mitoses/10 HPF ( $p < 0.0001$ , **Figure 22**).

Of 59 MNSTs successfully stained for H3K27me3, we detected complete loss of expression in 27% of MNSTs (16/59). Including one BNST, complete loss of H3K27me3 expression was thus detected in 25% of all NSTs (17/68). The staining of two MNSTs was scored as geographic

loss of staining, which was considered a complete loss of expression. Fifty-one percent of MNSTs (30/59) had a mosaic loss of expression, and 22% (13/59) had completely retained expression, including epithelioid MNST and MNST with proven metastases. One of the cases with complete loss of H3K27me3 expression was also immunonegative for Sox10, claudin-1, GFAP, and CNPase and had a proliferation index Ki-67 of 43.6%. No statistically significant association was found between H3K27me3 expression and clinical data, type or grade of MNST, histopathologic features of the tumors, and IHC results of staining with Sox10, claudin-1, GFAP, CNPase, or Ki-67 for any of the three scoring scales (**Figures 23 and 24**).

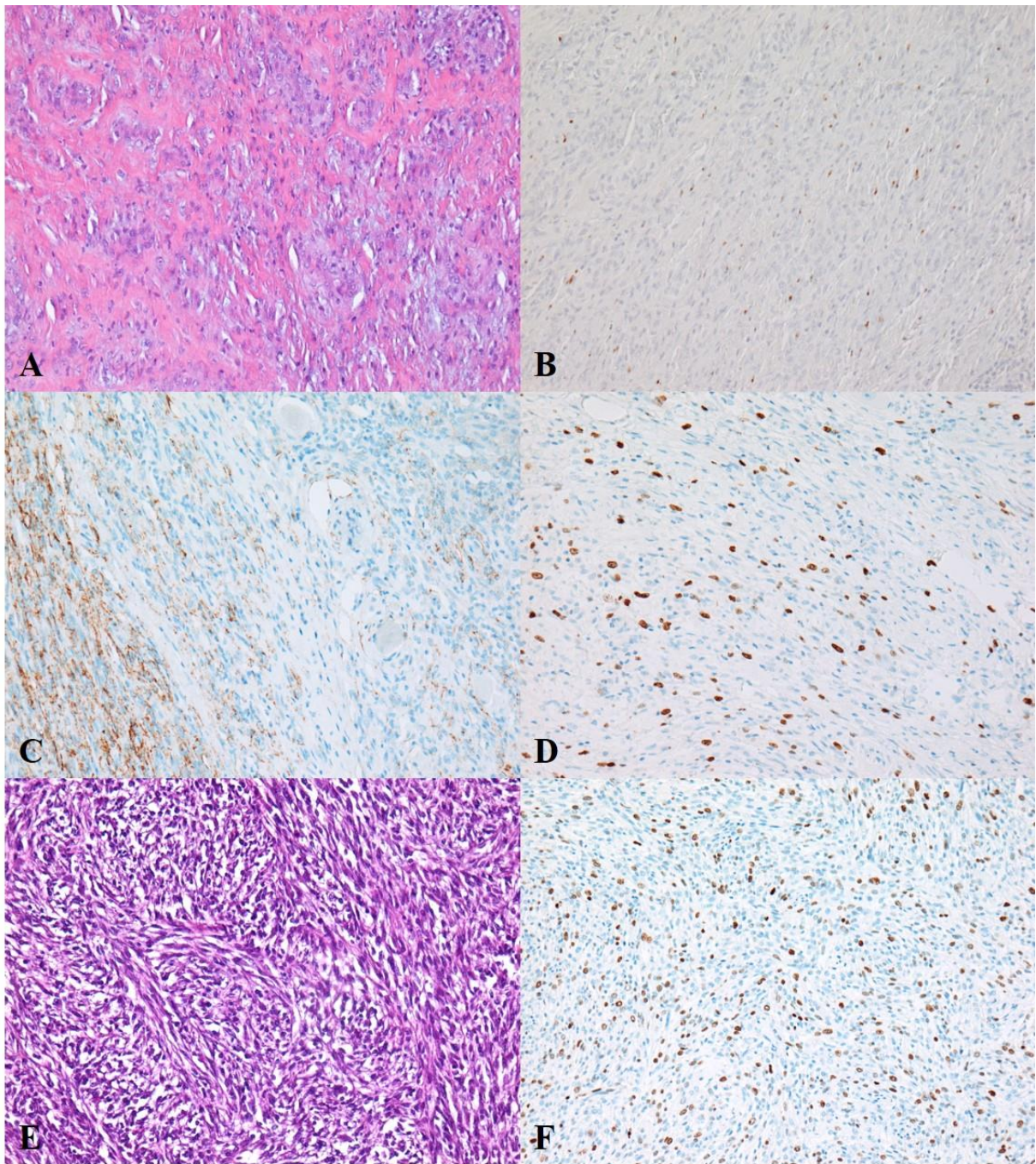


**Figure 15:** Histopathological and immunohistochemical characteristics of conventional MNST. (A, B, C, D) Grade I (case no. 50). (A) HE, 200x. (B) Moderate expression (++) of Sox10. Sox10, 200x. (C) Moderate expression (++) of claudin-1. Claudin-1, 200x. (D) The proliferation index Ki-67 was 16.4% in this case. Ki-67, 200x. (E, F) Grade II (case no. 49). (E) HE, 200x. (F) The proliferation index Ki-67 was 23.5% in this case. Ki-67, 200x.

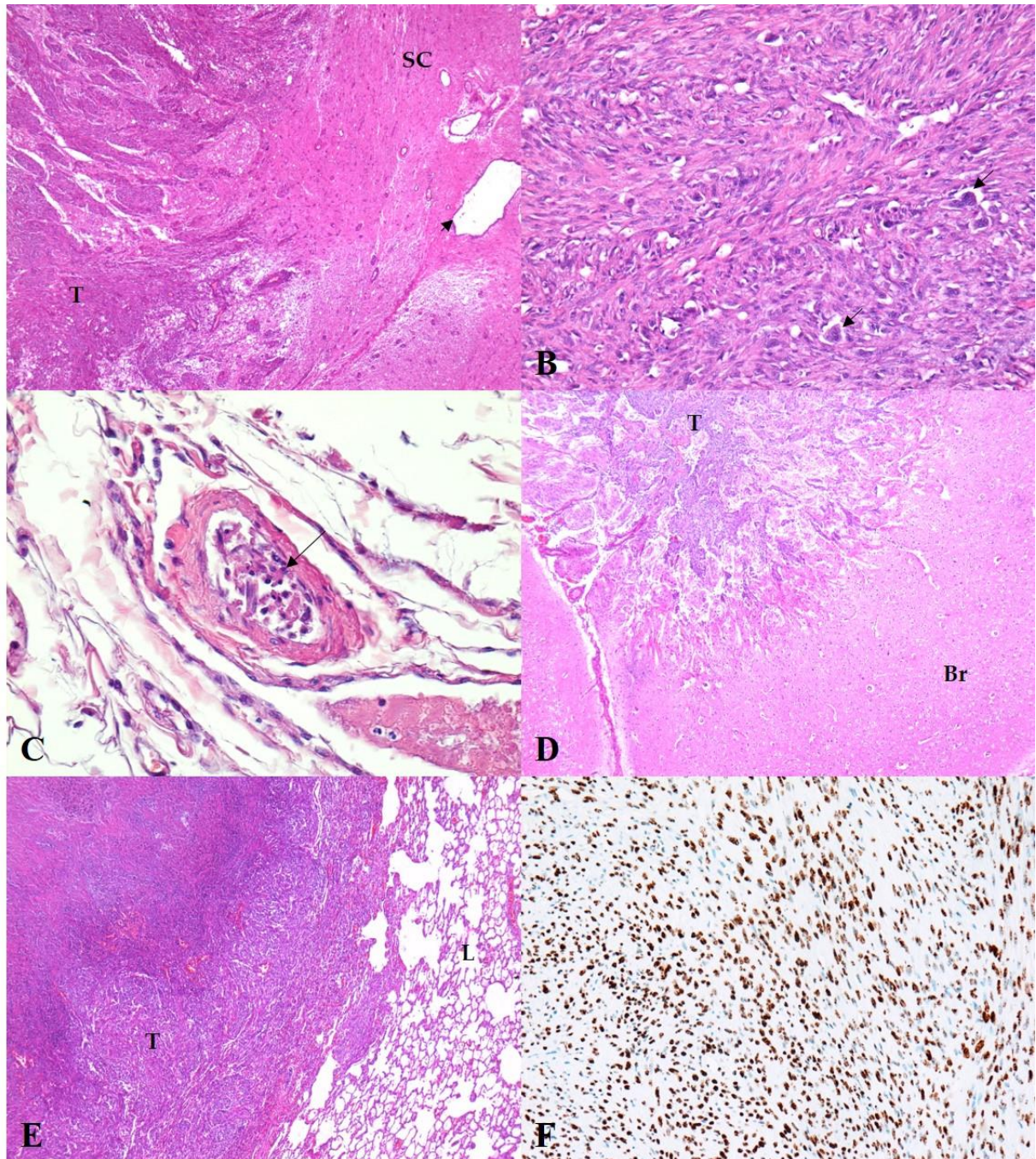


**Figure 16:** Histopathological and immunohistochemical characteristics of conventional MNST. (A) Marked infiltrative growth of high-cellular MNST into the spinal cord (case no. 6). T: tumor, SC: spinal cord, arrowhead: spinal cord canal. HE, 40x. (B, C, D, E, F) Grade III metastatic MNST (case no. 13). (B) High-cellular tumor with numerous multinucleated tumor cells. Few multinucleated cells are indicated by arrows. HE, 200x. (C) Numerous spindloid cells in the lumen of a blood vessel are consistent with blood vessel invasion (arrow). HE, 400x. (D) Metastasis of MNST in the brain. T: tumor. Br: brain. HE, 40x. (E) Metastasis of MNST in the lungs. T: tumor. L: lungs. HE, 40x. (F) Metastatic MNST exhibited complete retention of H3K27me3 expression. H3K27me3, 200x.

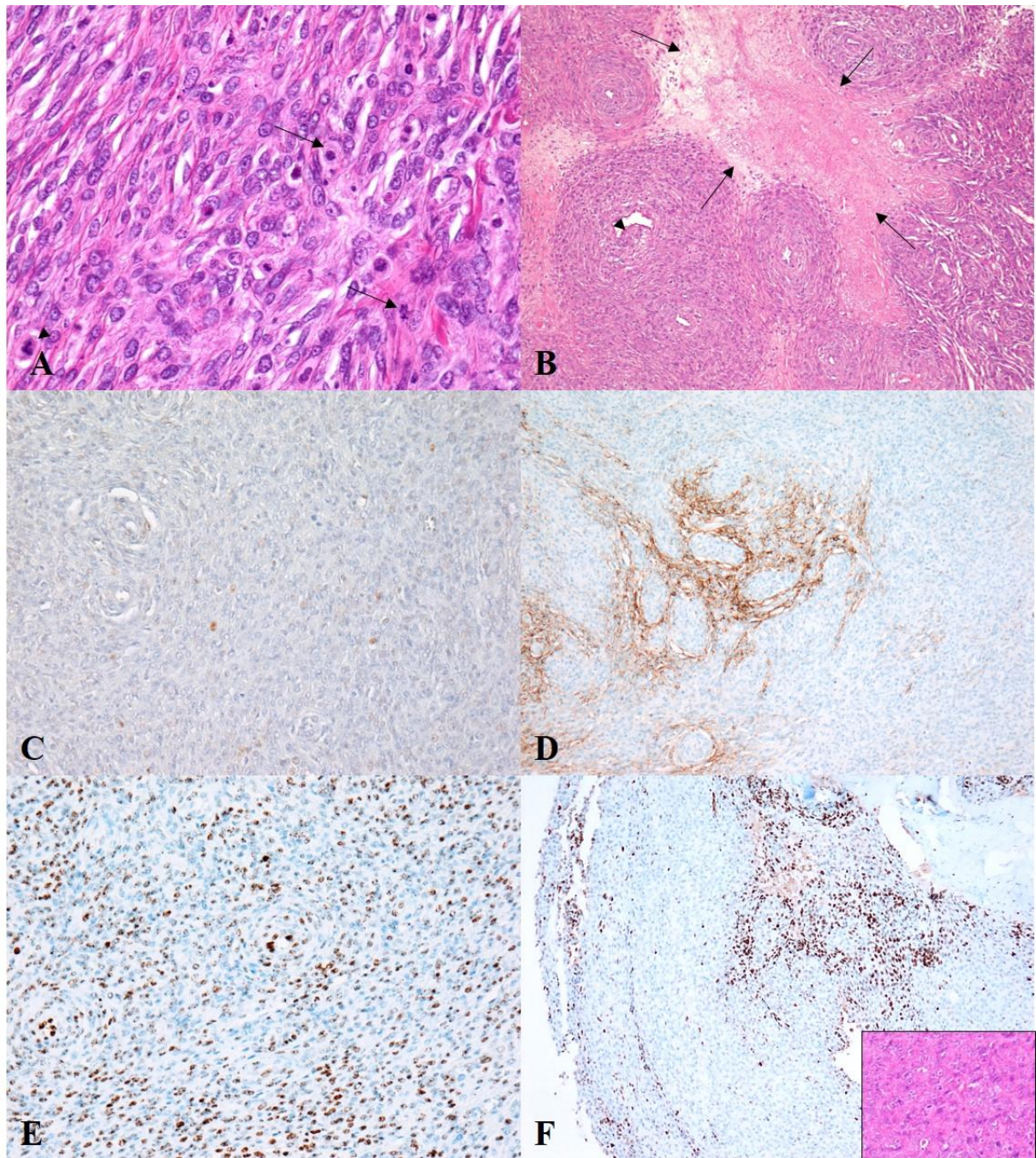


**Figure 17:** Histopathological and immunohistochemical characteristics of conventional MNST. **(A)** Brisk mitotic activity; few mitoses are indicated by an arrow. Occasionally, atypical mitoses are seen (arrowhead) (case no. 55) HE, 400x. **(B, C, D, E)** Conventional MNST, grade III (case no. 56). **(B)** Well-demarcated geographic necrosis (arrows). Slight intraluminal vascular herniation (arrowhead) is shown. HE, 100x. **(C)** Mild expression (+) of Sox10. Sox10, 200x. **(D)** Moderate expression (++) of claudin-1. Claudin-1, 100x. **(E)** Loss of H3K27me3 expression in 5-49% of tumor cells (loss in the minority). H3K27me3, 200x. **(F)** Conventional MNST, grade III (case no. 74) with geographic loss – complete loss of H3K27me3 expression. H3K27me3, 100x. Insert image: HE, 100x.

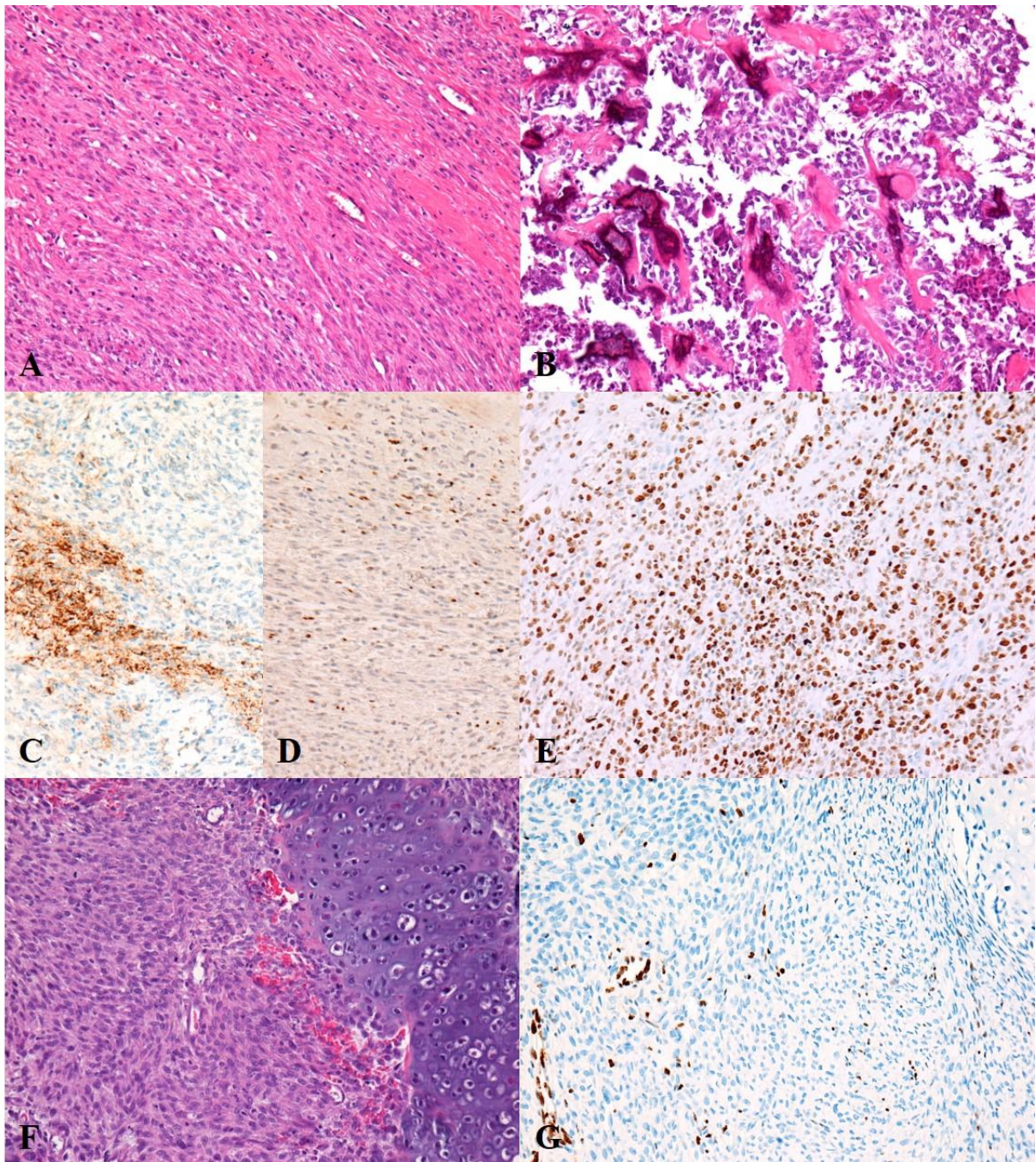


**Figure 18:** Histopathological and immunohistochemical characteristics of MNST with divergent differentiation. (A, B, C, D, E) MNST with osteosarcomatous differentiation (case no. 60). (A) Spindle cell component. HE, 200x. (B) Osteosarcomatous component. HE, 200x. (C) Moderate immunoreactivity (++) for claudin-1. Claudin-1, 200x. (D) Moderate immunoreactivity (++) for Sox10. Sox10, 200x. (E) The proliferation index Ki67 was 71.4% in this case. Ki67, 200x. (F, G) MNST with osteosarcomatous and chondrosarcomatous differentiation (case no. 61). (F) The spindle cell component is on the left and the chondrosarcomatous component is on the right of the image. HE, 200x. (G) The tumor exhibited complete loss of H3K27me3 expression. Only endothelial cells and scattered lymphocytes expressed the marker. H3K27me3, 200x.

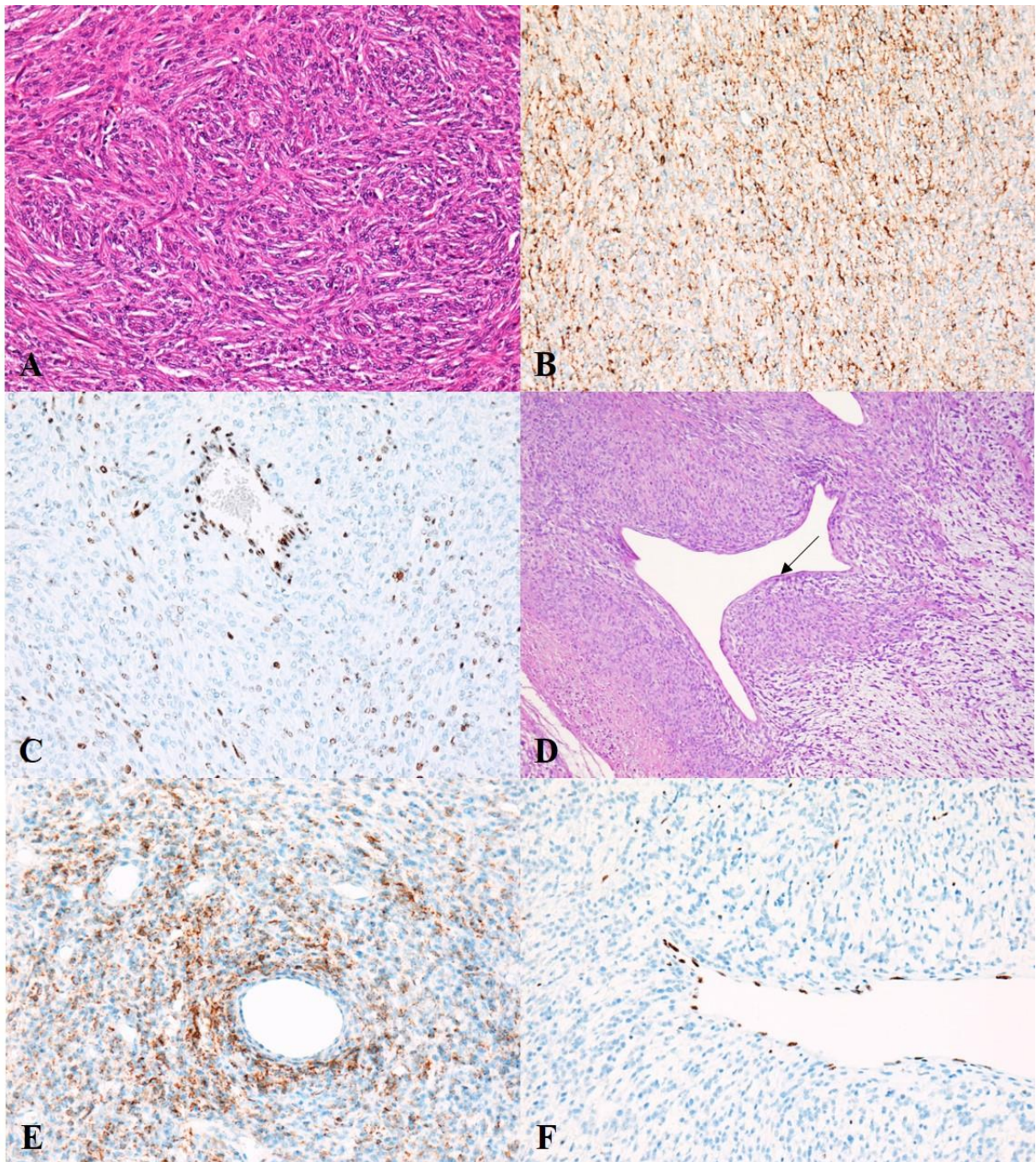


**Figure 19:** Histopathological and immunohistochemical characteristics of MNST with perineurial differentiation. **(A, B, C)** Case no. 33. **(A)** HE, 200x. **(B)** Strong diffuse immunopositivity (+++) for claudin-1. Claudin-1, 200x. **(C)** Mosaic loss of H3K27me3 expression with retained expression in 5-49% of tumor cells (+) – loss in the majority. H3K27me3, 200x. **(D, E, F)** Case no. 37. **(D)** Perivascular hypercellularity with distinct herniation of the tumor into the vessels (arrow). HE, 100x. **(E)** Strong diffuse immunopositivity (+++) for claudin-1. Claudin-1, 200x. **(F)** Complete loss of H3K27me3 expression. Only endothelial cells and scattered lymphocytes express the marker. H3K27me3, 200x.

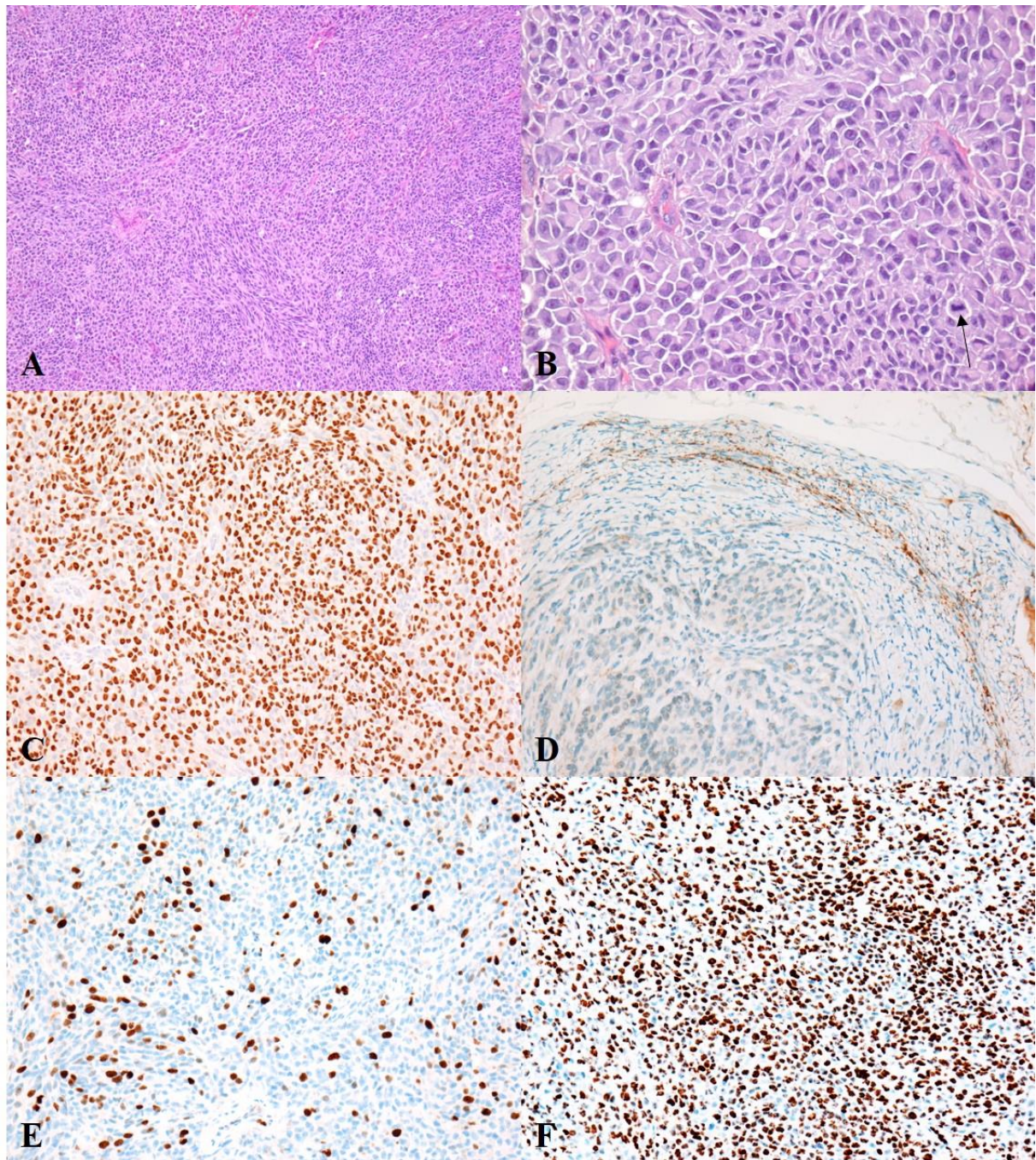


**Figure 20:** Histopathological and immunohistochemical characteristics of epithelioid MNST (case no. 64). (A) HE, 100x. (B) The arrow indicates mitosis. HE, 400x. (C) Strong diffuse immunoreactivity (+++) for Sox10. Sox10, 200x. (D) Tumor cells are negative for claudin-1. Claudin-1 is expressed in non-neoplastic perineurial cells. Claudin-1, 200x. (E) The proliferative index Ki-67 was 20.4% in this case. Ki67, 200x. (F) The tumor exhibited complete retention of H3K27me3. H3K27me3, 200x.

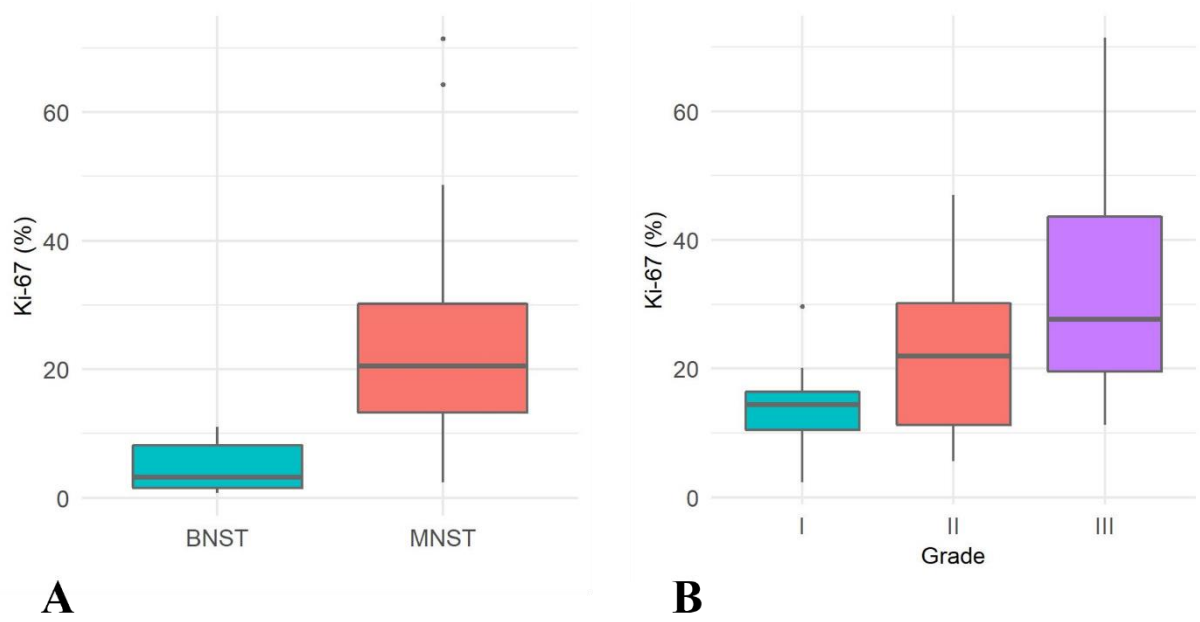


**Figure 21:** (A) Comparison of proliferation index Ki-67 between malignant nerve sheath tumors (MNST) and benign nerve sheath tumors (BNST). (B) Comparison of proliferation index Ki-67 between different grades of malignant nerve sheath tumors.

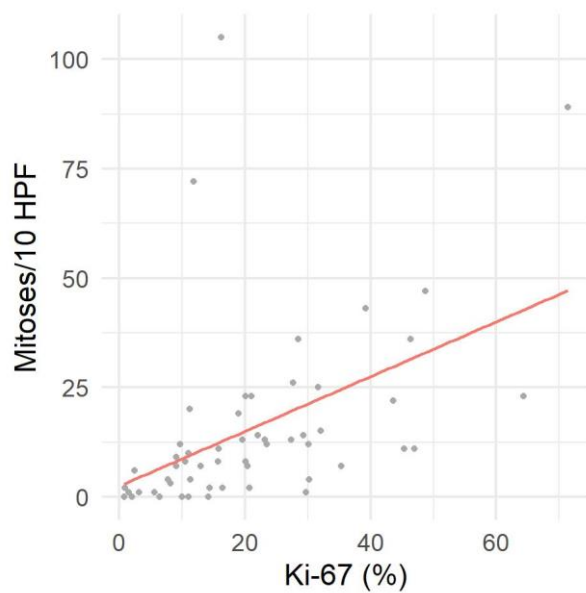


**Figure 22:** Correlation between proliferation index Ki-67 and mitotic count per 10 high power fields.

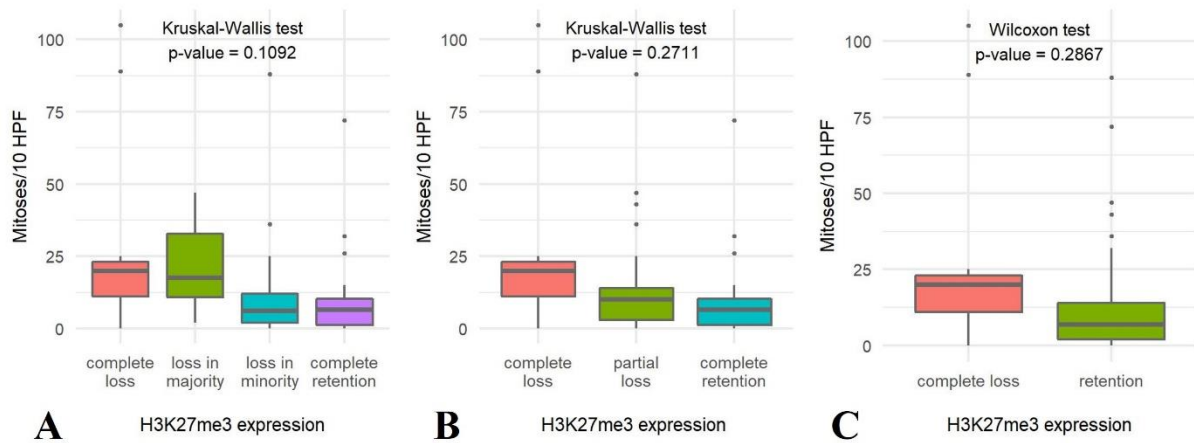


**Figure 23:** Comparison of the number of mitoses per ten high-power fields based on H3K27me3 expression using a 4-tier scoring scale (A), a 3-tier scoring scale (B), and a 2-tier scoring scale (C), indicating the statistical test used and the corresponding *p*-value.

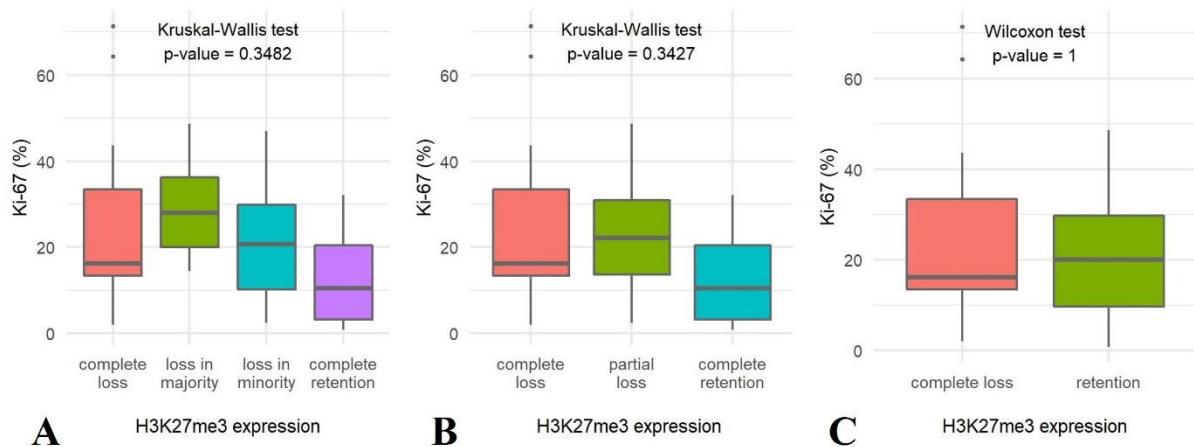


**Figure 24:** Comparison of the Ki-67 proliferation index fields based on H3K27me3 expression using a 4-tier scoring scale (A), a 3-tier scoring scale (B), and a 2-tier scoring scale (C), indicating the statistical test used and the corresponding *p*-value.

**Table 4:** Tumor types and results of immunohistochemical stainings for each examined case.

| No. | Tumor type                                 | Histological grade<br>(if malignant) | Sox10<br>expression | Claudin-1<br>expression | GFAP<br>expression | CNPase<br>expression | Proliferation<br>index Ki-67 (%) | H3K27me3 expression                |
|-----|--|--------------------------------------|---------------------|-------------------------|--------------------|----------------------|----------------------------------|------------------------------------|
| 1   | MNST – conventional                        | III                                  | –                   | –                       | –                  | –                    | ND                               | Mosaic loss – loss in the minority |
| 2   | MNST – conventional                        | I                                    | +                   | ++                      | –                  | –                    | ND                               | ND                                 |
| 3   | MNST – conventional                        | II                                   | ++                  | ++                      | +                  | –                    | ND                               | Complete loss                      |
| 4   | MNST – divergent                           | III                                  | –                   | –                       | –                  | –                    | ND                               | ND                                 |
| 5   | MNST – divergent                           | III                                  | –                   | –                       | –                  | –                    | ND                               | ND                                 |
| 6   | MNST – conventional                        | II                                   | +                   | +                       | –                  | –                    | ND                               | Mosaic loss – loss in the majority |
| 7   | MNST – conventional                        | II                                   | –                   | –                       | –                  | –                    | ND                               | ND                                 |
| 8   | MNST – conventional                        | III                                  | (++)                | (++)                    | (++)               | –                    | ND                               | Complete loss                      |
| 9   | MNST – perineural                          | II                                   | –                   | +++                     | –                  | –                    | ND                               | Complete loss                      |
| 10  | MNST – conventional                        | I                                    | ++                  | ++                      | ++                 | –                    | ND                               | Complete retention                 |
| 11  | Hybrid BNST –<br>perineurioma/neurofibroma | NA                                   | ND                  | ++                      | ND                 | –                    | ND                               | ND                                 |
| 12  | MNST – conventional                        | II                                   | +                   | +                       | +                  | –                    | ND                               | Complete loss                      |
| 13  | MNST – conventional                        | III                                  | –                   | –                       | –                  | –                    | ND                               | Complete retention                 |
| 14  | Nerve sheath myxoma                        | NA                                   | +                   | +                       | +                  | –                    | ND                               | Mosaic loss – loss in the minority |
| 15  | MNST – conventional                        | I                                    | ++                  | ++                      | (+)                | –                    | ND                               | Mosaic loss – loss in the minority |
| 16  | MNST – conventional                        | II                                   | –                   | +                       | –                  | –                    | ND                               | Complete retention                 |

|    |  |     |     |     |    |   |      |                                    |
|----|--|-----|-----|-----|----|---|------|------------------------------------|
| 17 | MNST – conventional                      | I   | –   | –   | –  | – | ND   | Mosaic loss – loss in the minority |
| 18 | MNST – conventional                      | I   | ++  | –   | –  | – | ND   | Complete loss                      |
| 19 | MNST – conventional                      | III | +   | +   | –  | – | ND   | Mosaic loss – loss in the majority |
| 20 | MNST – conventional                      | II  | +++ | +   | –  | – | ND   | Complete retention                 |
| 21 | MNST – conventional                      | I   | +   | +++ | +  | – | ND   | Complete retention                 |
| 22 | MNST – conventional                      | II  | –   | –   | –  | – | ND   | ND                                 |
| 23 | MNST – conventional                      | III | +   | +   | –  | – | ND   | Complete loss                      |
| 24 | Hybrid BNST –<br>perineurioma/schwannoma | NA  | ++  | ++  | +  | – | ND   | ND                                 |
| 25 | MNST – conventional                      | III | +   | +   | +  | – | 11.8 | Complete retention                 |
| 26 | MNST – conventional                      | I   | ++  | ++  | +  | – | 9.1  | Complete retention                 |
| 27 | MNST – conventional                      | II  | ++  | ++  | +  | – | 23.2 | Complete loss                      |
| 28 | MNST – conventional                      | II  | +   | –   | –  | – | 15.8 | Complete loss                      |
| 29 | Neurofibroma                             | NA  | ++  | +++ | ++ | – | 11.0 | ND                                 |
| 30 | MNST – conventional                      | I   | +   | +   | +  | – | 14.4 | Mosaic loss – loss in the majority |
| 31 | MNST – conventional                      | I   | ++  | ++  | ++ | – | 10.5 | Complete retention                 |
| 32 | MNST – conventional                      | III | +   | +   | –  | – | 28.5 | Mosaic loss – loss in the majority |
| 33 | MNST – perineural                        | III | –   | +++ | –  | – | 20.1 | Mosaic loss – loss in the majority |
| 34 | MNST – perineural                        | II  | –   | +++ | –  | – | 35.3 | Mosaic loss – loss in the majority |

|    |                      |     |     |     |    |   |      |                                    |
|----|----------------------|-----|-----|-----|----|---|------|------------------------------------|
| 35 | MNST – conventional  | III | ++  | +   | –  | – | 21.0 | Complete loss                      |
| 36 | MNST – conventional  | III | –   | –   | –  | – | 27.7 | Complete retention                 |
| 37 | MNST – perineural    | III | –   | +++ | –  | – | 64.3 | Complete loss                      |
| 38 | Schwannoma – classic | NA  | +++ | –   | ++ | + | 1.5  | Complete retention                 |
| 39 | MNST – conventional  | I   | +   | –   | –  | – | 15.7 | Complete loss                      |
| 40 | MNST – conventional  | II  | +   | +   | –  | – | 9.1  | Mosaic loss – loss in the minority |
| 41 | MNST – conventional  | I   | ++  | ++  | +  | – | 14.2 | Mosaic loss – loss in the minority |
| 42 | MNST – conventional  | II  | –   | –   | –  | – | 27.4 | Mosaic loss – loss in the majority |
| 43 | MNST – divergent     | III | –   | ++  | –  | – | 22.1 | Mosaic loss – loss in the minority |
| 44 | MNST – conventional  | II  | –   | –   | –  | – | 19.0 | ND                                 |
| 45 | Nerve sheath myxoma  | NA  | ++  | ++  | ++ | – | 3.2  | Complete retention                 |
| 46 | MNST – conventional  | II  | ++  | ++  | +  | – | 45.3 | Mosaic loss – loss in the minority |
| 47 | MNST – conventional  | II  | –   | ++  | –  | – | 7.8  | Mosaic loss – loss in the minority |
| 48 | MNST – conventional  | I   | +   | ++  | –  | – | 29.7 | Mosaic loss – loss in the minority |
| 49 | MNST – conventional  | II  | +   | +   | +  | – | 23.5 | Mosaic loss – loss in the minority |
| 50 | MNST – conventional  | I   | ++  | ++  | –  | – | 16.4 | Mosaic loss – loss in the minority |
| 51 | MNST – conventional  | II  | –   | ++  | –  | – | 9.7  | ND                                 |
| 52 | MNST – conventional  | II  | ++  | ++  | –  | – | 30.2 | Complete retention                 |

|    |                          |     |     |     |     |   |      |                                    |
|----|--------------------------|-----|-----|-----|-----|---|------|------------------------------------|
| 53 | MNST – conventional      | III | –   | +   | –   | – | 39.2 | Mosaic loss – loss in the majority |
| 54 | MNST – conventional      | II  | +   | ++  | –   | – | 11.1 | Complete loss                      |
| 55 | MNST – conventional      | III | –   | +   | –   | – | 16.2 | Complete loss                      |
| 56 | MNST – conventional      | III | +   | ++  | –   | – | 46.4 | Mosaic loss – loss in the minority |
| 57 | MNST – conventional      | II  | +   | –   | –   | – | 5.6  | ND                                 |
| 58 | MNST – conventional      | I   | ND  | (+) | (+) | – | 2.4  | Mosaic loss – loss in the minority |
| 59 | Nerve sheath myxoma      | NA  | ++  | ++  | +   | – | 8.2  | Mosaic loss – loss in the minority |
| 60 | MNST – divergent         | III | ++  | ++  | +   | – | 71.4 | Complete loss                      |
| 61 | MNST – divergent         | III | ++  | –   | –   | – | 11.2 | Complete loss                      |
| 62 | Neurofibroma             | NA  | –   | ++  | +   | – | 0.8  | Complete retention                 |
| 63 | Neurofibroma – plexiform | NA  | ++  | ++  | ++  | – | 0.9  | Complete retention                 |
| 64 | MNST – epithelioid       | II  | +++ | –   | –   | – | 20.4 | Complete retention                 |
| 65 | MNST – conventional      | I   | ++  | ++  | –   | – | 20.1 | Complete retention                 |
| 66 | MNST – conventional      | III | ++  | +++ | –   | – | 48.7 | Mosaic loss – loss in the majority |
| 67 | MNST – divergent         | III | ++  | ++  | ++  | – | 31.7 | Mosaic loss – loss in the minority |
| 68 | MNST – conventional      | II  | +   | –   | –   | – | 11.3 | Mosaic loss – loss in the minority |
| 69 | Neurofibroma             | NA  | ++  | +   | ++  | – | 2.0  | Complete loss                      |
| 70 | MNST – conventional      | II  | ++  | +   | +   | – | 30.1 | Mosaic loss – loss in the minority |

|    |                     |     |    |     |    |   |      |                                    |
|----|---------------------|-----|----|-----|----|---|------|------------------------------------|
| 71 | MNST – conventional | II  | +  | ++  | +  | – | 20.7 | Mosaic loss – loss in the minority |
| 72 | MNST – conventional | II  | +  | +   | +  | – | 47.0 | Mosaic loss – loss in the minority |
| 73 | MNST – conventional | III | +  | +   | +  | – | 13.0 | Mosaic loss – loss in the minority |
| 74 | MNST – conventional | III | –  | –   | –  | – | 43.6 | Complete loss                      |
| 75 | MNST – conventional | III | –  | –   | –  | – | 19.6 | Mosaic loss – loss in the majority |
| 76 | Neurofibroma        | NA  | ++ | +++ | ++ | – | 10.0 | Complete retention                 |
| 77 | MNST – conventional | II  | +  | +   | –  | – | 32.1 | Complete retention                 |
| 78 | Neurofibroma        | NA  | ++ | ++  | +  | – | 6.4  | Mosaic loss – loss in the minority |
| 79 | MNST - conventional | II  | +  | +++ | ++ | – | 29.3 | Mosaic loss – loss in the minority |

MNST: malignant nerve sheath tumor; BNST: benign nerve sheath tumor; –: negative reaction; +: weak positive reaction; ++: moderate positive reaction; +++: strong positive reaction; ND: no data; NA: not applicable. The results in the brackets indicate that the reaction may be limited to the nerve residues.

**Table 5:** Results of immunohistochemical staining for Sox10, claudin-1, GFAP, and CNPase in different subtypes and variants of canine NSTs.

|                     | <b>Sox10<br/>expression</b> | <b>Claudin-1<br/>expression</b> | <b>GFAP<br/>expression</b> | <b>CNPase<br/>expression</b> |
|---------------------|-----------------------------|---------------------------------|----------------------------|------------------------------|
| <b>BNST</b>         |                             |                                 |                            |                              |
| Neurofibroma*       | -/++                        | +/+/+++                         | +/++                       | -                            |
| Schwannoma*         | +++                         | -                               | +/++                       | -/+                          |
| Perineurioma*       | -                           | +/+/+++                         | -                          | -                            |
| Nerve sheath myxoma | +/++                        | +/++                            | +/++                       | -                            |
| <b>MNST</b>         |                             |                                 |                            |                              |
| Conventional        | -/+/+/+++                   | -/+/+/+++                       | -/+/++                     | -                            |
| Divergent           | -/++                        | -/++                            | -/+/++                     | -                            |
| Perineural          | -                           | +++                             | -                          | -                            |
| Epithelioid         | +++                         | -                               | -                          | -                            |

BNST: benign nerve sheath tumor; MNST: malignant nerve sheath tumor; -: negative reaction; +: weak positive reaction; ++: moderate positive reaction; +++: strong positive reaction.

\* Each component of hybrid nerve sheath tumors is considered separately in the table.

**Table 6:** Results of immunohistochemical analysis for Sox10, Claudin-1, GFAP, CNPase, and proliferation index Ki-67 in each subtype and variant of NSTs.

|                        | <i>N</i> | Sox10<br>expression,<br><i>n</i> (%) | Claudin-1<br>expression,<br><i>n</i> (%) | GFAP<br>expression,<br><i>n</i> (%) | CNPase<br>expression,<br><i>n</i> (%) | Proliferation<br>index Ki-67 (%)<br>Range ****<br>(Mean, SD) |
|------------------------|----------|--------------------------------------|--|-------------------------------------|---------------------------------------|--|
| <b>NST</b>             | 79       | 54/77 (68.4) **                      | 59/79 (74.7)                             | 33/78 (43.0) *                      | 1/79 (0.1)                            | 0.8 – 71.4<br>(21.2 ± 15.6)                                  |
| <b>BNST</b>            | 12       | 10/11 (90.9) *                       | 11/12 (91.7)                             | 11/11 (100) *                       | 1/12 (0.8)                            | 0.8 – 11.0<br>(4.9 ± 4.1)                                    |
| Neurofibroma***        | 7        | 5/6 (83.3) *                         | 7/7 (100)                                | 6/6 (100) *                         | 0/7 (0)                               | 0.8 – 11.0<br>(5.1 ± 4.6)                                    |
| Schwannoma***          | 2        | 2/2 (100)                            | 0/2 (0)                                  | 2/2 (100)                           | 1/2 (50.0)                            | 1.5  |
| Perineurioma***        | 2        | 0/1 (0) *                            | 2/2 (100)                                | 0/1 (0) *                           | 0/2 (0)                               | ND   |
| Nerve sheath<br>myxoma | 3        | 3/3 (100)                            | 3/3 (100)                                | 3/3 (100)                           | 0/3 (0)                               | 3.2 – 8.2<br>(5.7 ± 3.5)                                     |
| <b>MNST</b>            | 67       | 44/66 (66.7) *                       | 48/67 (71.6)                             | 22/67 (32.8)                        | 0/67 (0)                              | 2.4 – 71.4<br>(24.4 ± 15.1)                                  |
| Conventional           | 56       | 40/55 (72.7) *                       | 41/56 (73.2)                             | 20/56 (35.7)                        | 0/56 (0)                              | 2.4 – 48.7<br>(22.3 ± 12.6)                                  |
| <i>Grade I</i>         | 15       | 13/14 (91.7) *                       | 12/15 (76.9)                             | 8/15 (46.2)                         | 0/15 (0)                              | 2.4 – 29.7<br>(14.7 ± 7.6)                                   |
| <i>Grade II</i>        | 25       | 18/25 (72.0)                         | 18/25 (72.0)                             | 9/25 (36.0)                         | 0/25 (0)                              | 5.6 – 47.0<br>(22.1 ± 12.3)                                  |
| <i>Grade III</i>       | 16       | 9/16 (56.3)                          | 11/16 (68.8)                             | 3/16 (18.8)                         | 0/16 (0)                              | 11.8 – 48.7<br>(28.7 ± 13.7)                                 |
| Divergent              | 6        | 3/6 (50.0)                           | 3/6 (50.0)                               | 2/6 (33.3)                          | 0/6 (0)                               | 11.2 – 71.4<br>(34.1 ± 26.2)                                 |
| <i>Grade III</i>       | 6        | 3/6 (50.0)                           | 3/6 (50.0)                               | 2/6 (33.3)                          | 0/6 (0)                               | 11.2 – 71.4<br>(34.1 ± 26.2)                                 |
| Perineural             | 4        | 0/4 (0)                              | 4/4 (100)                                | 0/4 (0)                             | 0/4 (0)                               | 20.1 – 64.3<br>(39.9 ± 22.5)                                 |
| <i>Grade II</i>        | 2        | 0/2 (0)                              | 2/2 (100)                                | 0/2 (0)                             | 0/2 (0)                               | 35.3   |
| <i>Grade III</i>       | 2        | 0/2 (0)                              | 2/2 (100)                                | 0/2 (0)                             | 0/2 (0)                               | 20.1 – 64.3<br>(45.2 ± 31.3)                                 |
| Epithelioid            | 1        | 1 (100)                              | 0/1 (0)                                  | 0/1 (0)                             | 0/1 (0)                               | 20.4   |
| <i>Grade II</i>        | 1        | 1 (100)                              | 0/1 (0)                                  | 0/1 (0)                             | 0/1 (0)                               | 20.4   |

*N*: number of all samples that match the diagnosis/variant/grade. *n*: number of samples expressing the IHC marker relative to the number of samples evaluated. NST: nerve sheath tumor. BNST: benign nerve sheath tumor. MNST: malignant nerve sheath tumor. \* Staining for one sample was unreliable. \*\* Staining for two samples was unreliable. \*\*\* Each component of hybrid nerve sheath tumors is considered separately in the table. \*\*\*\* The value includes samples for which evaluation of the Ki-67 proliferation index was possible (cases no. 25 - 79). ND: no data.

**Table 7:** Immunohistochemical analysis of H3K27me3 expression in 68 canine NSTs divided by type, subtype, and histological grade using the 4-tier scoring scale.

| Type       | Subtype             | Histological grade* | <i>N</i>        | Complete loss ( <i>n</i> ) | Loss in majority ( <i>n</i> ) | Loss in minority ( <i>n</i> ) | Complete retention ( <i>n</i> ) |
|------------|---------------------|---------------------|-----------------|----------------------------|-------------------------------|-------------------------------|---------------------------------|
| BNST       | Neurofibroma        | /                   | 5               | 1                          | 0                             | 1                             | 3                               |
|            | Schwannoma          | /                   | 1               | 0                          | 0                             | 0                             | 1                               |
|            | Nerve sheath myxoma | /                   | 3               | 0                          | 0                             | 2                             | 1                               |
|            | sum                 | /                   | 9               | 1                          | 0                             | 3                             | 5                               |
| MNST       | Conventional        | <i>Grade I</i>      | 14              | 2                          | 1                             | 6                             | 5                               |
|            |                     | <i>Grade II</i>     | 20              | 5                          | 2                             | 9                             | 4                               |
|            |                     | <i>Grade III</i>    | 16              | 5                          | 5                             | 3                             | 3                               |
|            |                     | <i>sum</i>          | 50              | 12                         | 8                             | 18                            | 12                              |
|            | Divergent           | <i>Grade III</i>    | 4               | 2                          | 0                             | 2                             | 0                               |
|            |                     | <i>Grade II</i>     | 2               | 1                          | 1                             | 0                             | 0                               |
|            |                     | <i>Grade III</i>    | 2               | 1                          | 1                             | 0                             | 0                               |
|            | Perineural          | <i>sum</i>          | 4               | 2                          | 2                             | 0                             | 0                               |
|            |                     | Epithelioid         | <i>Grade II</i> | 1                          | 0                             | 0                             | 0                               |
|            | sum                 | /                   | 59              | 16                         | 10                            | 20                            | 13                              |
| <b>sum</b> | /                   | /                   | <b>68</b>       | <b>17</b>                  | <b>10</b>                     | <b>23</b>                     | <b>18</b>                       |

*N*: number of all samples of a certain type/subtype/histological grade; *n*: number of tumors with the indicated expression; H3K27me3: trimethylation at lysine 27 of histone 3; NST: nerve sheath tumor; BNST: benign nerve sheath tumor; MNST: malignant nerve sheath tumor.

\*Histological grade only applies to MNSTs.

## 5 DISCUSSION

In our study, we examined 79 canine tumors previously diagnosed as NSTs based on their localization and histopathologic and IHC characteristics. Considering the morphologic features of the tumors and the results of IHC staining of Sox-10, claudin-1, GFAP, CNPase, H3K27me3, and Ki-67, we classified the tumors according to the latest human WHO Classification of Tumors of the Central Nervous System. At the same time, we investigated the potential significance of the markers used for the diagnosis of NSTs in dogs.

### 5.1 CLASSIFICATION AND GRADING OF CANINE NERVE SHEATH TUMORS

We recognized histopathological and IHC features of NSTs in dogs that resemble their human counterparts. Our findings were consistent with the ones from Schöniger and Summers, who studied neurofibromas in dogs, horses, and a chicken and found the same growth patterns and several histopathologic variants similar to human neurofibromas. Based on growth patterns, they distinguished between localized, plexiform, and diffuse neurofibromas. The latter were poorly demarcated and infiltrative and must necessarily be distinguished from MNST. Microscopic subtypes of neurofibromas included classic, cellular, collagenous, myxoid, and pigmented neurofibromas. The study cases even included a hybrid neurofibroma/schwannoma (Schöniger and Summers, 2009).

Among BNSTs, we diagnosed schwannoma, neurofibroma, nerve sheath myxoma, and hybrid BNST, the latter consisting of a perineurioma in combination with neurofibroma or schwannoma areas. Our study included perineurioma only as part of hybrid BNSTs but few cases of intraneural perineuriomas in dogs have been reported in the literature (Higgins et al., 2006; Martins et al., 2010; Cornelis et al., 2012). The findings in one case of intraneural perineurioma in a dog showed many similarities in clinical and pathologic features to its human counterpart although cytogenetic analysis of this canine tumor was not performed and would be required for a definitive diagnosis (Higgins et al., 2006). The second case also describes no abnormalities on clinical examination of a dog one month after the removal of an intraneural perineurioma. Five years later, the dog was euthanized for reasons unrelated to the previously removed tumor (Cornelis et al., 2012). In the absence of specific immunohistochemical

markers, some authors suggested ultrastructural examination to confirm the diagnosis of perineurioma, since the formation of pseudo-onion bulbs is not completely specific to it (Martins et al., 2010). In hypertrophic neuropathies, onion bulb formation results from the non-neoplastic proliferation of Schwann cells after repeated demyelination and remyelination due to different causes (Higgins et al., 2006; Higgins et al., 2016). The latter may be associated with generalized diseases, such as inflammatory polyneuropathies, diabetic neuropathy, globoid cell leukodystrophy, neurofibromatosis type I, and chronic lead poisoning, or with localized lesions, such as local hypertrophic neuropathy, hypertrophic interstitial neuritis, intraneural neurofibromas, and hypertrophic neurofibromatosis (Higgins et al., 2006). The gold standard for diagnosis of perineurioma is TEM but because it is expensive and not available in all institutions with histopathological diagnostics, it is not routinely used. A more accessible alternative is IHC (Cornelis et al., 2012).

We diagnosed three BNSTs as nerve sheath myxomas although this diagnosis may not be entirely appropriate. In human pathology, nerve sheath myxoma is characterized as a cutaneous neoplasm arising from the nerve sheath and is classified as a subtype of soft tissue tumor in the WHO Classification of Soft Tissue Tumors and Bone (Ahlawat and Fayad, 2020). Because they originate from Schwann cells, their main feature confirming their origin is diffuse IHC expression of S100 (Khashaba et al., 2020; Tafti et al., 2021). Accordingly, we would expect that canine tumors with abundant myxoid stroma, which we diagnosed as nerve sheath myxomas, would strongly express Sox-10 as a marker of Schwann cell differentiation but our results show only mild to moderate positivity for Sox-10 and GFAP. In addition, they also expressed claudin-1 mildly to moderately. Although the morphology fits the diagnosis of a nerve sheath myxoma, this variant in a dog can be considered a benign myxoid NST for now (Schöniger and Summers, 2009). Further immunohistochemical and ultrastructural studies of this histopathologic variant in dogs would be required to define it more precisely.

The majority of NSTs included in our study were diagnosed as MNSTs. We recognized similar histopathologic variants described in humans: conventional, perineural, epithelioid MNST, and MNST with divergent differentiation. Using the STS grading system, we classified them into low-grade (grade I), intermediate-grade (grade II), and high-grade (grade III) MNSTs.

In addition to the obvious histopathological features of malignancy (infiltrative growth, severe cellular, and nuclear atypia, higher mitotic count, intratumoral necrosis, ...), we used a high Ki-

67 proliferation index as an indicator of malignancy. In humans, it has been described as an important prognostic marker, with an elevated index indicating a worse prognosis (Watanabe et al., 2001; Lucas et al., 2020; Martin et al., 2020). However, the Ki-67 index of MNSTs and cellular schwannomas may overlap, so care should be taken not to misclassify a tumor as malignant. In the study by Pekmezci et al., the Ki-67 index of MNST in humans started at 1%, whereas it reached 36% in cellular schwannomas, which were considered benign due to their lack of metastatic potential and disease-related death (Pekmezci et al., 2015). In our study, IHC staining for proliferation index Ki-67 was unfortunately unsuccessful in 24 specimens submitted for histopathologic examination between 2000 and 2008. Ki-67 is a highly problematic nuclear marker characterized by marked antigen degradation leading to a reduction of immunosignal intensity in archived tissues (Grillo et al., 2017), which we believe is the reason for the unreliable staining of our oldest 24 samples. Grillo et al. presented two strategies that were shown to be effective for antigen recovery: prolonged heat pretreatment and deep sections (Grillo et al., 2017). Deeper sections resulted in successful IHC staining for some of our samples, except for these 24. However, we did not use prolonged antigen retrieval, because it already took 60 minutes and would have most likely destroyed the sample.

The majority of MNSTs in our study (83.6%) were conventional variants. About half of the conventional MNSTs (44.6%) were grade II, whereas slightly less than one-third were grade I (26.8%) and grade III (28.6%). A conventional grade III MNST metastasized to the lung and brain. Although metastases have not been detected in any other MNST, they also cannot be excluded with certainty because follow-up for these dogs is unknown. In higher grades of conventional MNST, we found a slight decrease in the expression of the IHC markers Sox-10, claudin-1, and GFAP. We speculate that this may be the result of poorer tumor cell differentiation in higher-grade tumors. The Ki-67 index increases with the grade of malignancy, consistent with the presumed more malignant nature of the higher-grade tumors although the difference between the different histologic grades was only marginally statistically significant. A statistically significant higher Ki-67 proliferation index was found in MNSTs compared with BNSTs.

Nine percent of MNSTs in our study were with divergent differentiation and were all classified as grade III MNST. They contained osseous and/or cartilaginous tissue, which in some cases exhibited criteria of malignancy. MNSTs with divergent differentiation are associated with a

poor prognosis (Patnaik et al., 2002). In humans, their prognosis is similar to the prognosis of conventional high-grade MNST, and they are frequently associated with NF1. They may involve areas of neoplastic bone, cartilage, smooth or skeletal muscle, or angiosarcoma-like areas. MNST with rhabdomyosarcomatous differentiation is also referred to as a malignant Triton tumor. In addition to mesenchymal tissue, it may also contain glandular epithelium, neuroendocrine epithelium, or rarely squamous epithelium (Louis et al., 2016a). The reason for the divergent differentiation of MNST remains unclear. One possible reason could be the pluripotency of the cells of the neural crest, which are highly migratory cells that give rise to various derivatives, including glia and neurons of the sensory, sympathetic, and enteric nervous systems, melanocytes, and cartilaginous, bony, and connective tissues of the head and neck (Chijiwa et al., 2004; Adams and Bronner-Fraser, 2009). In dogs, few cases of MNSTs with divergent differentiation have been described in the literature, including cartilaginous and bony tissue that may or may not be malignant, rhabdomyosarcomatous and myxomatous differentiation, and glandular or pseudoglandular differentiation (Anderson et al., 1999; Patnaik et al., 2002; Kim et al., 2003; Chijiwa et al., 2004; Volmer et al., 2010). Nevertheless, MNSTs with divergent differentiation may actually represent a histopathological pattern rather than a variant. The latter are considered to have potential clinical utility, whereas no clear clinicopathologic significance has been demonstrated in such cases as Triton malignant tumors or glandular MNST (Louis et al., 2016a).

Although the divergent differentiation is more often indicative of the malignant nature of the tumor, cartilage and bone are common metaplastic elements found in both benign and malignant NSTs (Patnaik et al., 2002). In humans, also glandular structures were found in BNSTs (Woodruff and Christensen, 1993; Yoshida and Toot, 1993; Joshi et al., 2008; Saggini et al., 2019) but it is not entirely clear whether they are a true metaplastic element or merely the entrapped adjacent glands (Saggini et al., 2019).

Strong reactivity for claudin-1 and negative reaction for Sox-10 and GFAP in four MNSTs (6.0%) led to the diagnosis of MNST with perineurial differentiation or malignant perineurioma. Malignant perineurioma is considered a less aggressive variant in humans although it can metastasize (Louis et al., 2016a). MNSTs with perineurial differentiation have not yet been reported in dogs. Jakab et al. who investigated claudin-1 expression in canine NSTs did not detect claudin-1-positive and S100-negative malignant tumors, which would be

consistent with a diagnosis of malignant perineurioma (Jakab et al., 2012). The same authors hypothesized that the three S-100-negative MNSTs in dogs from the study by Chijiwa et al. might be MNSTs with perineurial differentiation but this was never demonstrated (Chijiwa et al., 2004; Jakab et al., 2012).

We diagnosed one epithelioid MNST (1.5%) with a specific tumor cell morphology similar to those reported in humans. In humans, epithelioid MNSTs are described as possibly arising from the malignant transformation of a schwannoma. They do not appear to be associated with NF1 and have a lower risk of recurrence, metastasis, and disease-related death compared to conventional MNSTs (Louis et al., 2016a). Occasionally, epithelioid MNSTs in dogs have been described in the literature (Pumarola et al., 1996; García et al., 2004), with one case even metastasizing to the liver, kidneys, lungs, and lymph nodes (García et al., 2004). Two previously reported epithelioid MNSTs were composed of a spindle-shaped and an epithelioid cell component, and the tumor cells exhibited numerous criteria of malignancy (Pumarola et al., 1996; García et al., 2004). Immunohistochemical staining for S-100 was also mostly restricted to the spindle cell component, whereas epithelioid cells were negative (Pumarola et al., 1996) or only slightly positive (García et al., 2004). In contrast, our case of epithelioid MNST consisted exclusively of epithelioid cells that were diffuse and strongly positive for Sox-10, clearly confirming the Schwann cell origin of the tumor cells.

The most recent human WHO classification represents the renaming of the former melanotic schwannoma to malignant melanotic NST. This specific entity has been recognized as a frequently aggressive tumor type with a unique genetic basis (Louis et al., 2021). Although no melanotic tumor was found in our study, six cases of melanotic NSTs in dogs have been described in the literature. All six cases were described as invasive NSTs composed of pigmented Schwann cells expressing numerous criteria for malignancy (Patnaik et al., 1984; Warren et al., 2020). We believe that designating such a tumor as a malignant melanotic NST rather than a melanotic schwannoma is appropriate and consistent with its recognized nature and may help with the interpretation of such tumors in the future. Especially in cutaneous tumors, this variant can easily be misdiagnosed as melanoma. In such cases, the useful immunohistochemical markers are laminin and collagen IV, which are expressed in neoplastic cells derived from Schwann cells but not in melanomas (Higgins et al., 2016; Lanigan et al., 2021).

Another change in the latest human WHO classification was including paraganglioma in the group of nerve tumors under the explanation that paraganglioma involves specialized neuroendocrine cells of the sympathetic and parasympathetic nervous systems (Louis et al., 2021). In humans, paragangliomas in the head and neck are usually nonproducing, whereas those arising in the thoracic and abdominal cavities are more prone to produce catecholamines. The classification of paragangliomas in dogs is not clear because of a lack of data which is mostly limited to case reports. Reported cases in dogs commonly occur in the aorta or carotid body (Treggiari et al., 2017; Park and Minamoto, 2021). We believe that adding paraganglioma to the group of NSTs in dogs could be considered but a deeper insight into this particular entity would be required.

While NSTs in humans is often associated with genetic mutations and may also occur after radiotherapy in a small percentage of cases, no such association has been demonstrated in dogs (Louis et al., 2016a; Lanigan et al., 2021). The available anamnestic data of the cases included in our study did not indicate the previous radiotherapy that could influence tumor growth. On the other hand, no genetic tests were performed in our study to conclude genetic mutations in these particular cases.

## 5.2 SOX-10, CLAUDIN-1, GFAP, CNPase, AND Ki-67 IN THE DIAGNOSIS OF CANINE NERVE SHEATH TUMORS

Based on the results obtained, we consider Sox10, claudin-1, GFAP, and Ki-67 to be useful markers and H3K27me3 to be a potentially useful marker, whereas CNPase was negative in almost all cases and proved not to be useful for the diagnosis of NSTs in dogs.

The majority of BNSTs (90.9%) and two-thirds of MNSTs (66.7%) in our study expressed Sox-10. Overall, 68.4% of all NSTs examined in our study expressed this transcriptional marker, confirming the origin of tumor cells from the neural crest. Strong expression of Sox10 was restricted to tumors composed entirely of Schwann cells, such as schwannoma, which also had a classic phenotype and left no doubt about the correctness of the diagnosis, and epithelioid MNST, which is also derived from Schwann cells (Louis et al., 2016a). Of the BNSTs, one neurofibroma and perineurioma areas of a hybrid perineurioma-schwannoma were completely negative for Sox10. In the case of perineurioma, such a result was expected and was consistent with the uniform population of neoplastic perineurial cells that have recently been shown to be

non-neural crest-derived and possibly neuroectoderm-derived (Kucenas, 2015). In neurofibroma, where the main component is thought to originate from Schwann cells, we expected the opposite (Schöniger and Summers, 2009). An unsuccessful staining reaction is still possible in this case because there were no obvious nerve remnants that could serve as an internal positive control. The proportion of MNSTs in our study that expressed Sox10 to varying degrees is consistent with the results of human studies, such as those of Kang et al. (67%) (Kang et al., 2014), Ersen et al. (54%) (Ersen et al., 2017) and Nonaka et al. (49%) (Nonaka et al., 2008), and is slightly higher than the results of Karamchandani et al. (27%) (Karamchandani et al., 2012). We detected lower expression of Sox10 in MNSTs compared with BNSTs, and also in higher-grade MNSTs compared with low-grade MNSTs, which may reflect the lower degree of Schwann cell differentiation in more malignant tumors. In humans, the difference in expression is also associated with NF1, whereas there are no known familial genetic mutations for NSTs in dogs (Ersen et al., 2017).

Claudin-1 was expressed in 74.7% of NSTs, 91.7% of BNSTs, and 71.6% of MNSTs in our study. Moderate to strong immunopositivity was detected in perineurioma regions of hybrid BNSTs and MNSTs, which were classified as MNSTs with perineurial differentiation based on the overall IHC results. Schwannoma and epithelioid MNST that were diffusely positive for Sox10, confirming their Schwann cell origin, were completely negative for claudin-1. Based on the results obtained, we agree with previous studies in human and veterinary medicine describing claudin-1 as one of the useful markers to distinguish NSTs from other spindle cell tumors and to further subclassify NSTs (Folpe et al., 2002; Cornelis et al., 2012; Jakab et al., 2012). Considering claudin-1 and S100 expression, Jakab et al. subdivided BNSTs into claudin-1-negative/S100-positive schwannomas, claudin-1-positive/S100-positive neurofibromas, and claudin-1-positive/S100-negative perineuriomas. All MNSTs in their study were claudin-1- and S100-positive with variable expression of both markers. Nevertheless, they reported claudin-1 positivity also in canine hemangiopericytomas and myopericytomas, highlighting the importance of using an IHC panel to rule out differential diagnoses (Jakab et al., 2012).

Less than 50% of the NSTs in our study expressed GFAP. While it was mildly to moderately expressed in all BNSTs (100%), it was mostly mildly expressed in one-third of MNSTs (32.8%). According to data from human and veterinary pathology, the expression of GFAP varies in NSTs (Tascos et al., 1982; Memoli et al., 1984; Kawahara et al., 1988; Gray et al.,

1989; Chijiwa et al., 2004; Gaitero et al., 2008). Gray et al. considered that the reason for the difference in expression could be differences in methodology and the specificity and sensitivity of the different antibodies used. Moreover, sequential changes in the expression of IF during tumorigenesis may explain some apparent variations in the IF of NSTs and other neoplasms; during the phylogenetic ascent from lower to higher vertebrates, some cells appear to lose their ability to express some IF (Gray et al., 1989). The results of Stanton et al., who examined GFAP expression in human NSTs, suggest that NSTs contain cells with polypeptides that share epitopes with GFAP but differ from astrocytic GFAP by at least one epitope. They suggested an influence of tumor location on GFAP immunoreactivity (Stanton et al., 1987). Wallerian degeneration leads to greater expression of this marker, confirming the fact that it is the nonmyelinated Schwann cells that express GFAP. Therefore, NSTs expressing GFAP may arise from or involve nerves with more nonmyelinated Schwann cells. The results of the study by Kawahara et al. also suggest that GFAP is more frequently expressed by tumors located deeper in the spinal canal, mediastinum, and other organs where nonmyelinated fibers are present although this cannot be considered certain (Kawahara et al., 1988). Another interesting finding by Kawahara et al. was the perivascular enhancement of GFAP expression in schwannoma. They related this phenomenon to the enhanced GFAP expression of subpial and perivascular glia limitans in the normal brain (Kawahara et al., 1988). Although GFAP is expressed by only a relatively small percentage of MNSTs in our study, we believe that it nevertheless has some potential to distinguish NSTs arising outside the CNS from other spindle cell tumors. It is not very useful in the CNS in this context because neoplasms of glial and Schwann cell origin can express both markers (Gray et al., 1989).

Classical schwannoma was the only NST in our study that expressed CNPase, and immunoreactivity was only mild. Our results differ from those of Nielsen et al, who described CNPase as a sensitive marker for bovine NSTs (Nielsen et al., 2011). Recently, CNPase also proved useful for the identification and characterization of NSTs in goldfish (Armando et al., 2021). There is no doubt about the immunoreactivity of this marker for canine tissues, since the brain, which served as a positive control in our study, showed an appropriate positive reaction. The results may be related, in part, to the fact that the amount of CNPase tends to be lower in PNS myelin compared with CNS myelin, as reported in the literature (Reddy et al., 1982). Nielsen et al., who found weaker CNPase immunoreactivity in tumors with a fascicular pattern,

suggest that a possible explanation for the decreased CNPase expression is that cells with a fascicular pattern tend to produce less myelin (Nielsen et al., 2011). Based on our results, we do not consider CNPase useful for the diagnosis of NSTs in dogs.

### 5.3 LOSS OF H3K27me3 EXPRESSION IN CANINE NERVE SHEATH TUMORS

Of the 68 NSTs in our study that was successfully stained with H3K27me3, 25% of the tumors (17/68) showed complete loss of H3K27me3 expression. Sixteen of them were MNSTs and one was classified as BNST - neurofibroma. In two MNSTs, we detected a geographic loss of staining, which we consider a variant of complete loss according to the interpretation of Asano et al. Namely, they assumed that complete loss of H3K27me3 expression in well-defined areas on a background of preserved expression indicates PRC2 inactivation (Asano et al., 2017). In our study, we found no significant association between the loss of H3K27me3 and other variables, such as histopathological features and IHC staining for other markers tested. We found a slightly higher Ki-67 proliferation index and mitotic count in NSTs with loss of H3K27me3 expression compared with tumors with partial or complete retention of the marker but the results were not statistically significant. Unfortunately, 17 of the NSTs successfully stained with H3K27me3 did not exhibit immunoreactivity for Ki-67.

Previous studies from human pathology have found a loss of H3K27me3 expression in a higher proportion of MNSTs but results vary from study to study. Cleven et al. reported the loss of H3K27me3 expression in 34% (55/162) of MNSTs (Cleven et al., 2016) while Le Guellec et al. found 72% (88/122) of MNSTs with loss of expression in their study (Le Guellec et al., 2017). The results of other studies belong somewhere in between (Prieto-Granada et al., 2016; Röhrich et al., 2016; Asano et al., 2017; Ersen et al., 2017). Lu et al. performed a meta-analysis of available data from the literature and estimated the frequency of H3K27me3 loss in MNSTs to be 53% (Lu et al., 2019). In humans, loss of H3K27me3 expression is common in MNSTs induced by radiotherapy, with loss of expression occurring in 86-100% of cases (Lu et al., 2019). Some authors reported a higher incidence of H3K27me3 loss in NF-1-associated tumors (Röhrich et al., 2016; Schaefer et al., 2016; Ersen et al., 2017) while others found the loss to be more common in sporadic MNSTs (Prieto-Granada et al., 2016; Asano et al., 2017). Based on the processed data, Lu et al. estimated H3K27me3 loss as a feature of approximately 50% of

sporadic and NF-1-associated tumors (Lu et al., 2019). In the absence of data in veterinary medicine on genetic disorders associated with the occurrence of neoplasms, no such assessments could be made for NSTs in dogs.

As far as we know, no study from human pathology has reported a complete loss of H3K27me3 expression in neurofibroma. In fact, they describe this marker as potentially useful for distinguishing between MNSTs and BNSTs (Cleven et al., 2016; Röhrich et al., 2016; Asano et al., 2017). Concerning BNSTs, there is only one report in the literature of a complete loss of H3K27me3 expression in a schwannoma (Cleven et al., 2016). These findings raise questions about the diagnosis of neurofibroma with H3K27me3 loss in our study although the diagnosis was made based on histopathologic and IHC features suggestive of a benign character of the tumor. Because we lack data on the clinical course of the disease and the survival of the dog, we cannot completely exclude the possibility of low-grade MNST. However, until a larger prospective study of NST in dogs is performed, we also cannot be sure that the interpretation of the results of NSTs in dogs can fully follow those in human medicine.

Because no other tumor type was included in our study, we could not evaluate the specificity of H3K27me3 loss. The majority of human pathology studies report specificity above 90%, except for the study by Le Guellec et al. who also detected H3K27me3 loss in 25% (7/29) melanomas and reported specificity of 75% (Le Guellec et al., 2017; Lu et al., 2019). There are also single reports of some other non-MNSTs with complete loss of H3K27me3 expressions, such as undifferentiated pleomorphic sarcoma, radiation-induced osteosarcoma (Asano et al., 2017), dedifferentiated chondrosarcoma (Makise et al., 2018), synovial sarcoma, fibrosarcomatous dermatofibrosarcoma protuberans, angiosarcoma, and clear cell sarcoma (Cleven et al., 2016).

Some human pathology studies have described a complete loss of H3K27me3 expression in 89-100% of MNSTs with divergent differentiation, suggesting that this may be a useful marker to distinguish these tumors from osteosarcomas and rhabdomyosarcomas when location and morphology are nonspecific (Prieto-Granada et al., 2016; Röhrich et al., 2016; Asano et al., 2017). Nevertheless, caution should be exercised in interpretation; Makise et al. reported the loss of H3K27me3 expression in 6% (3/47) of cases of dedifferentiated chondrosarcomas, all of which had heterologous differentiation (Makise et al., 2018). PRC2 and H3K27me3 play an important role in maintaining and reprogramming cell identity during normal development, and

epigenetic alteration caused by deficiency of H3K27me3 could lead to heterologous differentiation, regardless of tumor type (Makise et al., 2018). On the contrary, Cleven et al. found retention of H3K27me3 in all MNSTs with divergent differentiation (Cleven et al., 2016). In the study by Ersen et al. loss was also not a feature of MNSTs with rhabdomyoblastic differentiation, and in MNSTs with glandular differentiation, expression was retained in the malignant glandular component (Ersen et al., 2017). In our study, four MNSTs were successfully stained with H3K27me3, and two of them showed complete loss of expression while two showed partial loss of expression in less than 50% of tumor cells.

Seven NSTs in our study were negative for Sox10, claudin-1, GFAP, and CNPase, and of these, one also exhibited complete loss of H3K27me3 expression. However, to date, there is insufficient evidence to take this finding as confirmatory of MNST in dogs.

Twenty-six percent of NSTs stained for H3K27me3 in our study showed complete retention of staining (18/68), 56% of BNSTs, and 22% of MNSTs. Among others, intact expression was detected in epithelioid MNST. This finding is consistent with the results of previous studies in human pathology, in which epithelioid MNSTs were consistently found to have intact H3K27me3 expression, again demonstrating their distinct morphological, IHC, and molecular characteristics compared with non-epithelioid MNSTs (Cleven et al., 2016; Prieto-Granada et al., 2016; Röhrich et al., 2016; Schaefer et al., 2016; Asano et al., 2017).

Nearly half of all stained NSTs in our study showed mosaic loss of H3K27me3 expression, 33% of BNSTs, and 51% of MNSTs. Originally, the mosaic loss of H3K27me3 expression was thought to be specific to MNSTs but subsequent studies have shown otherwise. The mosaic loss of staining was also found in neurofibromas, and it has been demonstrated in other tumor types (Röhrich et al., 2016; Asano et al., 2017). According to the authors, such a result cannot be associated with a PRC2 mutation and should not be considered diagnostic for MNSTs. Only complete loss of staining, whether global or geographic, should be considered for evaluating the usefulness of H3K27me3 loss in diagnosing MNSTs (Asano et al., 2017). It also needs to be used as part of a broad IHC panel to aid in the diagnosis of MNSTs (Mito et al., 2017).

In humans, loss of H3K27me3 expression was associated with a worse prognosis in patients with breast, ovarian, and pancreatic cancers (Wei et al., 2008). Cleven et al. associated loss of H3K27me3 with shorter survival (Cleven et al., 2016), whereas Pekmezci et al. found no

significant association between the loss of H3K27me3 and clinical outcome in MNSTs (Pekmezci et al., 2015). Most other studies in human medicine have not performed survival analysis based on H3K27me3 loss (Lu et al., 2019). In our retrospective study, we, unfortunately, lack data on disease progression and survival of the dogs, and therefore we cannot relate H3K27me3 expression to tumor prognosis. According to our results, we believe that IHC for H3K27me3 may add some value to the diagnosis of NST in dogs and that this marker may prove useful if included in the prospective study.

## 6 CONCLUSIONS

This dissertation provides insight into the existing knowledge of NSTs, particularly from canine and human pathology, and adds some data to a possible IHC panel that could aid in the diagnosis of NSTs in dogs in practice.

Given our findings and incorporating data from the literature, we believe that an updated classification of NSTs in dogs could largely follow the recent human WHO classification of tumors of the cranial and paraspinal nerves.

We identified Sox10, claudin-1, GFAP, and Ki-67 as useful IHC markers whereas CNPase has no value for the diagnosis and classification of NST in dogs according to the results of our study.

We demonstrated a complete loss of H3K27me3 expression in a subset of canine NSTs but found no significant association between H3K27me3 expression and histopathological or IHC features of the included tumors. We believe that loss of H3K27me3 expression in combination with other IHC markers may be useful for the diagnosis of NSTs.

However, a larger prospective study is needed to investigate the significance of classifying MNSTs into different histopathological variants and the applicability of grading and to further evaluate the expression of different IHC markers about disease progression and survival to determine their prognostic utility. In addition, our study only investigated the sensitivity but not the specificity of IHC markers. Additional IHC studies that include other tumor types would be needed, particularly those that are most common differential diagnoses for NSTs. More detailed insight into genetics is needed to identify potential genetic alterations associated with NSTs in dogs.

## 7 REFERENCES

- Adams, E.J., Green, J.A., Clark, A.H., and Youngson, J.H. (1999). Comparison of different scoring systems for immunohistochemical staining. *J Clin Pathol* 52(1), 75-77. doi: 10.1136/jcp.52.1.75.
- Adams, M.S., and Bronner-Fraser, M. (2009). Review: the role of neural crest cells in the endocrine system. *Endocr Pathol* 20(2), 92-100. doi: 10.1007/s12022-009-9070-6.
- Ahlawat, S., and Fayad, L.M. (2020). Revisiting the WHO classification system of soft tissue tumours: emphasis on advanced magnetic resonance imaging sequences. Part 1. *Pol J Radiol* 85, e396-e408. doi: 10.5114/pjr.2020.98685.
- Al-Daraji, W.I. (2008). Granular perineurioma: the first report of a rare distinctive subtype of perineurioma. *Am J Dermatopathol* 30(2), 163-168. doi: 10.1097/DAD.0b013e3181639288.
- Anderson, G.M., Dallaire, A., Miller, L.M., and Miller, C.W. (1999). Peripheral nerve sheath tumor of the diaphragm with osseous differentiation in a one-year-old dog. *J Am Anim Hosp Assoc* 35(4), 319-322. doi: 10.5326/15473317-35-4-319.
- Armando, F., Pigoli, C., Gambini, M., Ghidelli, A., Ghisleni, G., Corradi, A., et al. (2021). Peripheral Nerve Sheath Tumors Resembling Human Atypical Neurofibroma in Goldfish (*Carassius auratus*, Linnaeus, 1758). *Animals (Basel)* 11(9). doi: 10.3390/ani11092621.
- Asano, N., Yoshida, A., Ichikawa, H., Mori, T., Nakamura, M., Kawai, A., et al. (2017). Immunohistochemistry for trimethylated H3K27 in the diagnosis of malignant peripheral nerve sheath tumours. *Histopathology* 70(3), 385-393. doi: 10.1111/his.13072.
- Bacigaluppi, S., Fiaschi, P., Prior, A., Bragazzi, N.L., Merciadri, P., and Gennaro, S. (2020). Intraneural haemangioma of peripheral nerves. *Br J Neurosurg* 34(5), 480-486. doi: 10.1080/02688697.2018.1449803.
- Basa, R.M., Crowley, A.M., and Johnson, K.A. (2020). Neurofibroma of the ulnar nerve in the carpal canal in a dog: treatment by marginal neurectomy. *J Small Anim Pract* 61(8), 512-515. doi: 10.1111/jsap.12945.

- Bergmann, W., Burgener, I.A., Roccabianca, P., Rytz, U., and Welle, M. (2009). Primary splenic peripheral nerve sheath tumour in a dog. *J Comp Pathol* 141(2-3), 195-198. doi: 10.1016/j.jcpa.2009.03.009.
- Bourque, P.R., Sampaio, M.L., Warman-Chardon, J., Samaan, S., and Torres, C. (2019). Neurolymphomatosis of the lumbosacral plexus and its branches: case series and literature review. *BMC Cancer* 19(1), 1149. doi: 10.1186/s12885-019-6365-y.
- Brocca, G., Zamparo, S., Quaglio, F., and Verin, R. (2021). Metastatic myxoid nerve sheath tumor of the dorsal fin in a rainbow trout, *Oncorhynchus mykiss* (Walbaum). *J Fish Dis* 44(11), 1875-1878. doi: 10.1111/jfd.13517.
- Buza, E.L., Menzies, R.A., Goldschmidt, M.H., and Durham, A.C. (2012). Malignant peripheral nerve sheath tumor in a cat with nodal and pulmonary metastases. *J Vet Diagn Invest* 24(4), 781-784. doi: 10.1177/1040638712445775.
- Campos, L.C., Silva, J.O., Santos, F.S., Araújo, M.R., Lavalle, G.E., Ferreira, E., et al. (2015). Prognostic significance of tissue and serum HER2 and MUC1 in canine mammary cancer. *J Vet Diagn Invest* 27(4), 531-535. doi: 10.1177/1040638715592445.
- Chijiwa, K., Uchida, K., and Tateyama, S. (2004). Immunohistochemical evaluation of canine peripheral nerve sheath tumors and other soft tissue sarcomas. *Vet Pathol* 41(4), 307-318. doi: 10.1354/vp.41-4-307.
- Cleven, A.H., Sannaa, G.A., Briaire-de Bruijn, I., Ingram, D.R., van de Rijn, M., Rubin, B.P., et al. (2016). Loss of H3K27 tri-methylation is a diagnostic marker for malignant peripheral nerve sheath tumors and an indicator for an inferior survival. *Mod Pathol* 29(6), 582-590. doi: 10.1038/modpathol.2016.45.
- Coindre, J.M. (2006). Grading of soft tissue sarcomas: review and update. *Arch Pathol Lab Med* 130(10), 1448-1453. doi: 10.5858/2006-130-1448-gostsr.
- Cornelis, I., Chiers, K., Maes, S., Kramer, M., Ducatelle, R., De Decker, S., et al. (2012). Claudin-1 and glucose transporter 1 immunolabelling in a canine intraneural perineurioma. *J Comp Pathol* 147(2-3), 186-190. doi: 10.1016/j.jcpa.2011.12.005.
- de Lahunta, A. (2010). Feline nerve sheath tumors versus feline peripheral nerve sheath tumors. *Vet Pathol* 47(4), 758. doi: 10.1177/0300985810363489.

- de Oliveira, J.T., Pinho, S.S., de Matos, A.J., Hespanhol, V., Reis, C.A., and Gärtner, F. (2009). MUC1 expression in canine malignant mammary tumours and relationship to clinicopathological features. *Vet J* 182(3), 491-493. doi: 10.1016/j.tvjl.2008.09.007.
- Denesvre, C. (2013). Marek's disease virus morphogenesis. *Avian Dis* 57(2 Suppl), 340-350. doi: 10.1637/10375-091612-Review.1.
- Dennis, M.M., McSporran, K.D., Bacon, N.J., Schulman, F.Y., Foster, R.A., and Powers, B.E. (2011). Prognostic factors for cutaneous and subcutaneous soft tissue sarcomas in dogs. *Vet Pathol* 48(1), 73-84. doi: 10.1177/0300985810388820.
- DeSano, J., 2nd, Gardner, P., Hart, J.W., Samuel, S., and Williams, K. (2021). Intraneural Lipoma of the Digital Nerve: A Case Report and Literature Review. *Cureus* 13(2), e13074. doi: 10.7759/cureus.13074.
- Dracham, C.B., Shankar, A., and Madan, R. (2018). Radiation induced secondary malignancies: a review article. *Radiat Oncol J* 36(2), 85-94. doi: 10.3857/roj.2018.00290.
- Eng, L.F., Ghirnikar, R.S., and Lee, Y.L. (2000). Glial fibrillary acidic protein: GFAP-thirty-one years (1969-2000). *Neurochem Res* 25(9-10), 1439-1451. doi: 10.1023/a:1007677003387.
- Erlandson, R.A., and Woodruff, J.M. (1982). Peripheral nerve sheath tumors: an electron microscopic study of 43 cases. *Cancer* 49(2), 273-287. doi: 10.1002/1097-0142(19820115)49:2<273::aid-cnrcr2820490213>3.0.co;2-r.
- Ersen, A., Pekmezci, M., Folpe, A.L., and Tihan, T. (2017). Comparison of New Diagnostic Tools for Malignant Peripheral Nerve Sheath Tumors. *Pathol Oncol Res* 23(2), 393-398. doi: 10.1007/s12253-016-0125-y.
- Fetsch, J.F., and Miettinen, M. (1997). Sclerosing perineurioma: a clinicopathologic study of 19 cases of a distinctive soft tissue lesion with a predilection for the fingers and palms of young adults. *Am J Surg Pathol* 21(12), 1433-1442. doi: 10.1097/00000478-199712000-00005.
- Fine, S.W., McClain, S.A., and Li, M. (2004). Immunohistochemical staining for calretinin is useful for differentiating schwannomas from neurofibromas. *Am J Clin Pathol* 122(4), 552-559. doi: 10.1309/agbg-tbrj-4w0b-c7ln.

- Folpe, A.L., Billings, S.D., McKenney, J.K., Walsh, S.V., Nusrat, A., and Weiss, S.W. (2002). Expression of claudin-1, a recently described tight junction-associated protein, distinguishes soft tissue perineurioma from potential mimics. *Am J Surg Pathol* 26(12), 1620-1626. doi: 10.1097/00000478-200212000-00010.
- Foo, T.L., Yak, R., and Puhaindran, M.E. (2017). Peripheral Nerve Lymphomatosis. *J Hand Surg Asian Pac Vol* 22(1), 104-107. doi: 10.1142/s0218810417720042.
- Gaitero, L., Añor, S., Fondevila, D., and Pumarola, M. (2008). Canine cutaneous spindle cell tumours with features of peripheral nerve sheath tumours: a histopathological and immunohistochemical study. *J Comp Pathol* 139(1), 16-23. doi: 10.1016/j.jcpa.2008.03.003.
- Galatian, A.A., Crowson, A.N., Fischer, R.J., Yob, E.H., and Shendrik, I. (2013). Malignant peripheral nerve sheath tumor with glandular differentiation in a patient with neurofibromatosis type 1. *Am J Dermatopathol* 35(8), 859-863. doi: 10.1097/DAD.0b013e318284a611.
- García, P., Sánchez, B., Sánchez, M.A., González, M., Rollán, E., and Flores, J.M. (2004). Epithelioid malignant peripheral nerve sheath tumour in a dog. *J Comp Pathol* 131(1), 87-91. doi: 10.1016/j.jcpa.2003.12.012.
- Gillette, S.M., Gillette, E.L., Powers, B.E., and Withrow, S.J. (1990). Radiation-induced osteosarcoma in dogs after external beam or intraoperative radiation therapy. *Cancer Res* 50(1), 54-57.
- Gómez-Mateo Mdel, C., Compañ-Quilis, A., and Monteagudo, C. (2015). Microcystic pseudoglandular plexiform cutaneous neurofibroma. *J Cutan Pathol* 42(11), 884-888. doi: 10.1111/cup.12572.
- Graadt van Roggen, J.F., McMenamin, M.E., Belchis, D.A., Nielsen, G.P., Rosenberg, A.E., and Fletcher, C.D. (2001). Reticular perineurioma: a distinctive variant of soft tissue perineurioma. *Am J Surg Pathol* 25(4), 485-493. doi: 10.1097/00000478-200104000-00008.
- Gray, M.H., Rosenberg, A.E., Dickersin, G.R., and Bhan, A.K. (1989). Glial fibrillary acidic protein and keratin expression by benign and malignant nerve sheath tumors. *Hum Pathol* 20(11), 1089-1096. doi: 10.1016/0046-8177(89)90228-1.

- Grillo, F., Bruzzone, M., Pigozzi, S., Prosapio, S., Migliora, P., Fiocca, R., et al. (2017). Immunohistochemistry on old archival paraffin blocks: is there an expiry date? *J Clin Pathol* 70(11), 988-993. doi: 10.1136/jclinpath-2017-204387.
- Guo, X., Ma, S., Han, Y., Lan, Z., Tian, G., Zhang, X., et al. (2021). Intraneural hemangioma of spinal nerve roots: a Case Report and literature review. *Br J Neurosurg*, 1-3. doi: 10.1080/02688697.2020.1849550.
- Higgins, M.A., Rossmeisl, J.H., Jr., Saunders, G.K., Hayes, S., and Kiupel, M. (2008). B-cell lymphoma in the peripheral nerves of a cat. *Vet Pathol* 45(1), 54-57. doi: 10.1354/vp.45-1-54.
- Higgins, R.J., Bollen, A.W., Dickinson, P.J., and Sisó-Llonch, S. (2016). "Tumors of the Nervous System," in *Tumors in Domestic Animals.*, 834-891.
- Higgins, R.J., Dickinson, P.J., Jimenez, D.F., Bollen, A.W., and Lecouteur, R.A. (2006). Canine intraneural perineurioma. *Vet Pathol* 43(1), 50-54. doi: 10.1354/vp.43-1-50.
- Hirose, T., Hasegawa, T., Kudo, E., Seki, K., Sano, T., and Hizawa, K. (1992). Malignant peripheral nerve sheath tumors: an immunohistochemical study in relation to ultrastructural features. *Hum Pathol* 23(8), 865-870. doi: 10.1016/0046-8177(92)90396-k.
- Hirose, T., Tani, T., Shimada, T., Ishizawa, K., Shimada, S., and Sano, T. (2003). Immunohistochemical demonstration of EMA/Glut1-positive perineurial cells and CD34-positive fibroblastic cells in peripheral nerve sheath tumors. *Mod Pathol* 16(4), 293-298. doi: 10.1097/01.Mp.0000062654.83617.B7.
- Holliday, A.C., Mazloom, S.E., Coman, G.C., Kolodney, M.S., Chavan, R.N., and Grider, D.J. (2017). Benign Glandular Schwannoma With Ancient Change. *Am J Dermatopathol* 39(4), 300-303. doi: 10.1097/dad.0000000000000739.
- Hosoya, K., Poulson, J.M., and Azuma, C. (2008). Osteoradionecrosis and radiation induced bone tumors following orthovoltage radiation therapy in dogs. *Vet Radiol Ultrasound* 49(2), 189-195. doi: 10.1111/j.1740-8261.2008.00349.x.

- Hsueh, C.S., Tsai, C.Y., Lee, J.C., Kao, C.L., Wang, F.I., Jeng, C.R., et al. (2019). CD56(+) B-cell Neurolymphomatosis in a Cat. *J Comp Pathol* 169, 25-29. doi: 10.1016/j.jcpa.2019.03.004.
- Ichikawa, M., Suzuki, S., Tei, M., Nibe, K., Uchida, K., Ono, K., et al. (2018). Malignant peripheral nerve sheath tumor originating from the adrenal gland in a dog. *J Vet Med Sci* 80(10), 1572-1575. doi: 10.1292/jvms.18-0431.
- Jakab, C., Gálfi, P., Jerzsele, Á., Szabó, Z., Németh, T., Sterczer, Á., et al. (2012). Expression of claudin-1 in canine peripheral nerve sheath tumours and perivascular wall tumours. Immunohistochemical study. *Histol Histopathol* 27(7), 905-917. doi: 10.14670/hh-27.905.
- Jessen, K.R., and Mirsky, R. (2019). Schwann Cell Precursors; Multipotent Glial Cells in Embryonic Nerves. *Front Mol Neurosci* 12, 69. doi: 10.3389/fnmol.2019.00069.
- Jo, V.Y., and Fletcher, C.D. (2015). Epithelioid malignant peripheral nerve sheath tumor: clinicopathologic analysis of 63 cases. *Am J Surg Pathol* 39(5), 673-682. doi: 10.1097/pas.0000000000000379.
- Jokinen, C.H., Dadras, S.S., Goldblum, J.R., van de Rijn, M., West, R.B., and Rubin, B.P. (2008). Diagnostic implications of podoplanin expression in peripheral nerve sheath neoplasms. *Am J Clin Pathol* 129(6), 886-893. doi: 10.1309/m7d5ktvyeye51xyqa.
- Joshi, D., Gangane, N., Kishore, S., and Vagha, S. (2008). Unusual histological presentation in neurofibromas: Two case reports. *Cases J* 1(1), 188. doi: 10.1186/1757-1626-1-188.
- Kang, Y., Pekmezci, M., Folpe, A.L., Ersen, A., and Horvai, A.E. (2014). Diagnostic utility of SOX10 to distinguish malignant peripheral nerve sheath tumor from synovial sarcoma, including intraneural synovial sarcoma. *Mod Pathol* 27(1), 55-61. doi: 10.1038/modpathol.2013.115.
- Karamchandani, J.R., Nielsen, T.O., van de Rijn, M., and West, R.B. (2012). Sox10 and S100 in the diagnosis of soft-tissue neoplasms. *Appl Immunohistochem Mol Morphol* 20(5), 445-450. doi: 10.1097/PAI.0b013e318244ff4b.
- Kawahara, E., Oda, Y., Ooi, A., Katsuda, S., Nakanishi, I., and Umeda, S. (1988). Expression of glial fibrillary acidic protein (GFAP) in peripheral nerve sheath tumors. A

- comparative study of immunoreactivity of GFAP, vimentin, S-100 protein, and neurofilament in 38 schwannomas and 18 neurofibromas. *Am J Surg Pathol* 12(2), 115-120. doi: 10.1097/00000478-198802000-00004.
- Kelsh, R.N. (2006). Sorting out Sox10 functions in neural crest development. *Bioessays* 28(8), 788-798. doi: 10.1002/bies.20445.
- Khanna, L., Prasad, S.R., Yedururi, S., Parameswaran, A.M., Marcal, L.P., Sandrasegaran, K., et al. (2021). Second Malignancies after Radiation Therapy: Update on Pathogenesis and Cross-sectional Imaging Findings. *Radiographics* 41(3), 876-894. doi: 10.1148/rg.2021200171.
- Khashaba, H., Hafez, E., and Burezq, H. (2020). Nerve Sheath Myxoma: A rare tumor, a case report and literature review. *Int J Surg Case Rep* 73, 183-186. doi: 10.1016/j.ijscr.2020.07.030.
- Kim, D.Y., Cho, D.Y., Kim, D.Y., Lee, J., and Taylor, H.W. (2003). Malignant peripheral nerve sheath tumor with divergent mesenchymal differentiations in a dog. *J Vet Diagn Invest* 15(2), 174-178. doi: 10.1177/104063870301500214.
- Kim, Y.C., Park, H.J., Cinn, Y.W., and Vandersteen, D.P. (2001). Benign glandular schwannoma. *Br J Dermatol* 145(5), 834-837. doi: 10.1046/j.1365-2133.2001.04476.x.
- Kochat, V., Raman, A.T., Landers, S.M., Tang, M., Schulz, J., Terranova, C., et al. (2021). Enhancer reprogramming in PRC2-deficient malignant peripheral nerve sheath tumors induces a targetable de-differentiated state. *Acta Neuropathol* 142(3), 565-590. doi: 10.1007/s00401-021-02341-z.
- Koestner A. Armed Forces Institute of Pathology (U.S.) American Registry of Pathology & WHO Collaborating Center for Worldwide Reference on Comparative Oncology. (1999). *Histological classification of tumors of the nervous system of domestic animals*. Armed Forces Institute of Pathology in cooperation with the American Registry of Pathology and the World Health Organization Collaborating Center for Worldwide Reference on Comparative Oncology.
- Kostov, M., Mijovic, Z., Visnjic, M., Mihailovic, D., Stojanovic, M., and Zdravkovic, M. (2008). Malignant peripheral nerve sheath tumour in a dog presenting as a pseudo aneurysm of the left jugular vein: a case report. *Veterinarni Medicina* 53(12).

- Krause, G., Winkler, L., Mueller, S.L., Haseloff, R.F., Piontek, J., and Blasig, I.E. (2008). Structure and function of claudins. *Biochim Biophys Acta* 1778(3), 631-645. doi: 10.1016/j.bbamem.2007.10.018.
- Kuberappa, P.H., Bagalad, B.S., Ananthaneni, A., Kiresur, M.A., and Srinivas, G.V. (2016). Certainty of S100 from Physiology to Pathology. *J Clin Diagn Res* 10(6), Ze10-15. doi: 10.7860/jcdr/2016/17949.8022.
- Kucenas, S. (2015). Perineurial glia. *Cold Spring Harb Perspect Biol* 7(6). doi: 10.1101/cshperspect.a020511.
- Kwong, S., Seeger, L.L., Motamedi, K., Nelson, S.D., and Golshani, B. (2018). Intraneural Hemangioma: Case Report of a Rare Tibial Nerve Lesion. *Cureus* 10(12), e3784. doi: 10.7759/cureus.3784.
- Lanigan, L.G., Russell, D.S., Woolard, K.D., Pardo, I.D., Godfrey, V., Jortner, B.S., et al. (2021). Comparative Pathology of the Peripheral Nervous System. *Vet Pathol* 58(1), 10-33. doi: 10.1177/0300985820959231.
- Le Guellec, S., Macagno, N., Velasco, V., Lamant, L., Lae, M., Filleron, T., et al. (2017). Loss of H3K27 trimethylation is not suitable for distinguishing malignant peripheral nerve sheath tumor from melanoma: a study of 387 cases including mimicking lesions. *Mod Pathol* 30(12), 1677-1687. doi: 10.1038/modpathol.2017.91.
- Lee, S.W., Baek, S.M., Lee, A.R., Kim, T.U., Kim, D., Kwon, Y.S., et al. (2020). Malignant Peripheral Nerve Sheath Tumour in the Urinary Bladder of a Dog. *J Comp Pathol* 175, 64-68. doi: 10.1016/j.jcpa.2019.12.005.
- Lee, W., Teckie, S., Wiesner, T., Ran, L., Prieto Granada, C.N., Lin, M., et al. (2014). PRC2 is recurrently inactivated through EED or SUZ12 loss in malignant peripheral nerve sheath tumors. *Nat Genet* 46(11), 1227-1232. doi: 10.1038/ng.3095.
- Li, L.T., Jiang, G., Chen, Q., and Zheng, J.N. (2015). Ki67 is a promising molecular target in the diagnosis of cancer (review). *Mol Med Rep* 11(3), 1566-1572. doi: 10.3892/mmr.2014.2914.
- Li, X., Kaur, H., Xu, W., and Wang, X. (2017). Benign Glandular Schwannoma in Basal Ganglia. *World Neurosurg* 97, 762.e761-762.e764. doi: 10.1016/j.wneu.2016.09.073.

- Louis, D.N., Ohgaki, H., Wiestler, O.D., and Cavenee, W.K. (eds.). (2016a). *World Health Organization Histological Classification of Tumours of the Central Nervous System*. Lyon, France: International Agency for Research on Cancer.
- Louis, D.N., Perry, A., Reifenberger, G., von Deimling, A., Figarella-Branger, D., Cavenee, W.K., et al. (2016b). The 2016 World Health Organization Classification of Tumors of the Central Nervous System: a summary. *Acta Neuropathol* 131(6), 803-820. doi: 10.1007/s00401-016-1545-1.
- Louis, D.N., Perry, A., Wesseling, P., Brat, D.J., Cree, I.A., Figarella-Branger, D., et al. (2021). The 2021 WHO Classification of Tumors of the Central Nervous System: a summary. *Neuro Oncol* 23(8), 1231-1251. doi: 10.1093/neuonc/noab106.
- Lu, V.M., Marek, T., Gilder, H.E., Puffer, R.C., Raghunathan, A., Spinner, R.J., et al. (2019). H3K27 trimethylation loss in malignant peripheral nerve sheath tumor: a systematic review and meta-analysis with diagnostic implications. *J Neurooncol* 144(3), 433-443. doi: 10.1007/s11060-019-03247-3.
- Lucas, C.G., Vasudevan, H.N., Chen, W.C., Magill, S.T., Braunstein, S.E., Jacques, L., et al. (2020). Histopathologic findings in malignant peripheral nerve sheath tumor predict response to radiotherapy and overall survival. *Neurooncol Adv* 2(1), vdaa131. doi: 10.1093/noajnl/vdaa131.
- Lyskjaer, I., Lindsay, D., Tirabosco, R., Steele, C.D., Lombard, P., Strobl, A.C., et al. (2020). H3K27me3 expression and methylation status in histological variants of malignant peripheral nerve sheath tumours. *J Pathol* 252(2), 151-164. doi: 10.1002/path.5507.
- Magaki, S., Hojat, S.A., Wei, B., So, A., and Yong, W.H. (2019). An Introduction to the Performance of Immunohistochemistry. *Methods Mol Biol* 1897, 289-298. doi: 10.1007/978-1-4939-8935-5\_25.
- Makise, N., Sekimizu, M., Kubo, T., Wakai, S., Hiraoka, N., Komiyama, M., et al. (2018). Clarifying the Distinction Between Malignant Peripheral Nerve Sheath Tumor and Dedifferentiated Liposarcoma: A Critical Reappraisal of the Diagnostic Utility of MDM2 and H3K27me3 Status. *Am J Surg Pathol* 42(5), 656-664. doi: 10.1097/pas.0000000000001014.

- Mandara, M.T., Foiani, G., Silvestri, S., and Chiaradia, E. (2021). Immunoexpression of epithelial membrane antigen in canine meningioma: Novel results for perspective considerations. *Vet Comp Oncol* 19(1), 115-122. doi: 10.1111/vco.12648.
- Mandrioli, L., Morini, M., Biserni, R., Gentilini, F., and Turba, M.E. (2012). A case of feline neurolymphomatosis: pathological and molecular investigations. *J Vet Diagn Invest* 24(6), 1083-1086. doi: 10.1177/1040638712460674.
- Marek, T., Amrami, K.K., Mahan, M.A., and Spinner, R.J. (2018). Intraneural lipomas: institutional and literature review. *Acta Neurochir (Wien)* 160(11), 2209-2218. doi: 10.1007/s00701-018-3677-7.
- Martin, E., Acem, I., Grünhagen, D.J., Bovée, J., and Verhoef, C. (2020). Prognostic Significance of Immunohistochemical Markers and Genetic Alterations in Malignant Peripheral Nerve Sheath Tumors: A Systematic Review. *Front Oncol* 10, 594069. doi: 10.3389/fonc.2020.594069.
- Martins, T.B., Ramos, A.T., Viott, A.d.M., Adeodato, A.G., and Graça, D.L. (2010). Canine intraneural perineurioma. *Brazilian Journal of Veterinary Pathology* 3, 66-69.
- Memoli, V.A., Brown, E.F., and Gould, V.E. (1984). Glial fibrillary acidic protein (GFAP) immunoreactivity in peripheral nerve sheath tumors. *Ultrastruct Pathol* 7(4), 269-275. doi: 10.3109/01913128409141487.
- Mentzel, T., and Katenkamp, D. (1999). Intraneural angiosarcoma and angiosarcoma arising in benign and malignant peripheral nerve sheath tumours: clinicopathological and immunohistochemical analysis of four cases. *Histopathology* 35(2), 114-120. doi: 10.1046/j.1365-2559.1999.00714.x.
- Miettinen, M., McCue, P.A., Sarlomo-Rikala, M., Biernat, W., Czapiewski, P., Kopczynski, J., et al. (2015). Sox10--a marker for not only schwannian and melanocytic neoplasms but also myoepithelial cell tumors of soft tissue: a systematic analysis of 5134 tumors. *Am J Surg Pathol* 39(6), 826-835. doi: 10.1097/pas.0000000000000398.
- Mito, J.K., Qian, X., Doyle, L.A., Hornick, J.L., and Jo, V.Y. (2017). Role of Histone H3K27 Trimethylation Loss as a Marker for Malignant Peripheral Nerve Sheath Tumor in Fine-Needle Aspiration and Small Biopsy Specimens. *Am J Clin Pathol* 148(2), 179-189. doi: 10.1093/ajcp/aqx060.

- Muthiah, S., Hussain, R., Stefanos, N., and Husain, A. (2018). An incidental finding of an asymptomatic intraneural glomus tumor: A case report and review of the literature. *J Cutan Pathol* 45(4), 269-273. doi: 10.1111/cup.13097.
- Naber, U., Friedrich, R.E., Glatzel, M., Mautner, V.F., and Hagel, C. (2011). Podoplanin and CD34 in peripheral nerve sheath tumours: focus on neurofibromatosis 1-associated atypical neurofibroma. *J Neurooncol* 103(2), 239-245. doi: 10.1007/s11060-010-0385-4.
- Nielsen, A.B., Jensen, H.E., and Leifsson, P.S. (2011). Immunohistochemistry for 2',3'-cyclic nucleotide-3'-phosphohydrolase in 63 bovine peripheral nerve sheath tumors. *Vet Pathol* 48(4), 796-802. doi: 10.1177/0300985810388521.
- Nonaka, D., Chiriboga, L., and Rubin, B.P. (2008). Sox10: a pan-schwannian and melanocytic marker. *Am J Surg Pathol* 32(9), 1291-1298. doi: 10.1097/PAS.0b013e3181658c14.
- Ochi, A., Ochiai, K., Hatai, H., and Umemura, T. (2008). Naturally occurring multiple perineuriomas in a chicken (*Gallus domesticus*). *Vet Pathol* 45(5), 685-689. doi: 10.1354/vp.45-5-685.
- Olga, K., Yulia, B., and Vassilios, P. (2020). The Functions of Mitochondrial 2',3'-Cyclic Nucleotide-3'-Phosphodiesterase and Prospects for Its Future. *Int J Mol Sci* 21(9). doi: 10.3390/ijms21093217.
- Osum, S.H., Watson, A.L., and Largaespada, D.A. (2021). Spontaneous and Engineered Large Animal Models of Neurofibromatosis Type 1. *Int J Mol Sci* 22(4). doi: 10.3390/ijms22041954.
- Park, J.W., Woo, G.H., Jee, H., Jung, D.W., Youn, H.Y., Choi, M.C., et al. (2011). Malignant peripheral nerve sheath tumour in the liver of a dog. *J Comp Pathol* 144(2-3), 223-226. doi: 10.1016/j.jcpa.2010.08.009.
- Park, Y.T., and Minamoto, T. (2021). Laparoscopic resection of retroperitoneal paraganglioma close to caudal vena cava in a dog. *Vet Med Sci* 7(6), 2191-2197. doi: 10.1002/vms3.588.

- Patnaik, A.K., Erlandson, R.A., and Lieberman, P.H. (1984). Canine malignant melanotic schwannomas: a light and electron microscopic study of two cases. *Vet Pathol* 21(5), 483-488. doi: 10.1177/030098588402100505.
- Patnaik, A.K., Zachos, T.A., Sams, A.E., and Aitken, M.L. (2002). Malignant nerve-sheath tumor with divergent and glandular differentiation in a dog: a case report. *Vet Pathol* 39(3), 406-410. doi: 10.1354/vp.39-3-406.
- Pekmezci, M., Cuevas-Ocampo, A.K., Perry, A., and Horvai, A.E. (2017). Significance of H3K27me3 loss in the diagnosis of malignant peripheral nerve sheath tumors. *Mod Pathol* 30(12), 1710-1719. doi: 10.1038/modpathol.2017.97.
- Pekmezci, M., Reuss, D.E., Hirbe, A.C., Dahiya, S., Gutmann, D.H., von Deimling, A., et al. (2015). Morphologic and immunohistochemical features of malignant peripheral nerve sheath tumors and cellular schwannomas. *Mod Pathol* 28(2), 187-200. doi: 10.1038/modpathol.2014.109.
- Pfaff, A.M., March, P.A., and Fishman, C. (2000). Acute bilateral trigeminal neuropathy associated with nervous system lymphosarcoma in a dog. *J Am Anim Hosp Assoc* 36(1), 57-61. doi: 10.5326/15473317-36-1-57.
- Piña-Oviedo, S., Del Valle, L., Baquera-Heredia, J., and Ortiz-Hidalgo, C. (2009). Immunohistochemical characterization of Renaut bodies in superficial digital nerves: further evidence supporting their perineurial cell origin. *J Peripher Nerv Syst* 14(1), 22-26. doi: 10.1111/j.1529-8027.2009.00202.x.
- Piña-Oviedo, S., and Ortiz-Hidalgo, C. (2008). The normal and neoplastic perineurium: a review. *Adv Anat Pathol* 15(3), 147-164. doi: 10.1097/PAP.0b013e31816f8519.
- Piunti, A., and Shilatifard, A. (2021). The roles of Polycomb repressive complexes in mammalian development and cancer. *Nat Rev Mol Cell Biol* 22(5), 326-345. doi: 10.1038/s41580-021-00341-1.
- Poli, F., Calistri, M., Mandara, M.T., and Baroni, M. (2019). Central nervous system metastasis of an intradural malignant peripheral nerve sheath tumor in a dog. *Open Vet J* 9(1), 49-53. doi: 10.4314/ovj.v9i1.9.

- Prater, M.C., and Janz, B.A. (2017). Mixed Lymphangioma and Cavernous Hemangioma Within the Ulnar Nerve: A Case Report. *Hand (N Y)* 12(5), Np145-np147. doi: 10.1177/1558944717703738.
- Prieto-Granada, C.N., Wiesner, T., Messina, J.L., Jungbluth, A.A., Chi, P., and Antonescu, C.R. (2016). Loss of H3K27me3 Expression Is a Highly Sensitive Marker for Sporadic and Radiation-induced MPNST. *Am J Surg Pathol* 40(4), 479-489. doi: 10.1097/pas.0000000000000564.
- Pumarola, M., Añor, S., Borràs, D., and Ferrer, I. (1996). Malignant epithelioid schwannoma affecting the trigeminal nerve of a dog. *Vet Pathol* 33(4), 434-436. doi: 10.1177/030098589603300411.
- Ramírez, G.A., Herráez, P., Rodríguez, F., Godhino, A., Andrada, M., and Espinosa de los Monteros, A. (2007). Malignant peripheral nerve sheath tumour (malignant schwannoma) in the diaphragm of a goat. *J Comp Pathol* 137(2-3), 137-141. doi: 10.1016/j.jcpa.2007.05.003.
- Ramis, A., Pumarola, M., Fernandez-Morán, J., Añor, S., Majó, N., and Zidan, A. (1998). Malignant peripheral nerve sheath tumor in a water moccasin (*Agkistrodon piscivorus*). *J Vet Diagn Invest* 10(2), 205-208. doi: 10.1177/104063879801000222.
- Ramos-Vara, J.A., and Borst, L.B. (2016). "Immunohistochemistry," in *Tumors in Domestic Animals.*, 44-87.
- Rank, J.P., and Rostad, S.W. (1998). Perineurioma with ossification: a case report with immunohistochemical and ultrastructural studies. *Arch Pathol Lab Med* 122(4), 366-370.
- Rankine, A.J., Filion, P.R., Platten, M.A., and Spagnolo, D.V. (2004). Perineurioma: a clinicopathological study of eight cases. *Pathology* 36(4), 309-315. doi: 10.1080/00313020410001721663.
- Ravanbod, H., Motififard, M., Aliakbari, M., Zolfaghari, M., and Hatami, S. (2021). Intraneural cavernous hemangioma: a rare case of extrafascicular left ulnar nerve tumor. *Am J Blood Res* 11(1), 72-76.

- R Core Team. R: *A Language and Environment for Statistical Computing*. R Foundation for Statistical Computing, Vienna, Austria, 2021. Available online: <https://www.R-project.org/> (accessed on March 8, 2022).
- Reddy, N.B., Askanas, V., and Engel, W.K. (1982). Demonstration of 2',3'-cyclic nucleotide 3'-phosphohydrolase in cultured human Schwann cells. *J Neurochem* 39(3), 887-889. doi: 10.1111/j.1471-4159.1982.tb07977.x.
- Resende, T.P., Pereira, C.E., Vannucci, F.A., Araujo, F.S., dos Santos, J.L., Cassali, G.D., et al. (2015). Malignant peripheral nerve sheath tumour in a sow. *Acta Vet Scand* 57, 56. doi: 10.1186/s13028-015-0150-y.
- Reynolds, R., Carey, E.M., and Herschkowitz, N. (1989). Immunohistochemical localization of myelin basic protein and 2',3'-cyclic nucleotide 3'-phosphohydrolase in flattened membrane expansions produced by cultured oligodendrocytes. *Neuroscience* 28(1), 181-188. doi: 10.1016/0306-4522(89)90242-x.
- Rodriguez, F.J., Folpe, A.L., Giannini, C., and Perry, A. (2012). Pathology of peripheral nerve sheath tumors: diagnostic overview and update on selected diagnostic problems. *Acta Neuropathol* 123(3), 295-319. doi: 10.1007/s00401-012-0954-z.
- Röhrich, M., Koelsche, C., Schimpf, D., Capper, D., Sahm, F., Kratz, A., et al. (2016). Methylation-based classification of benign and malignant peripheral nerve sheath tumors. *Acta Neuropathol* 131(6), 877-887. doi: 10.1007/s00401-016-1540-6.
- Rosenberg, A.S., Langee, C.L., Stevens, G.L., and Morgan, M.B. (2002). Malignant peripheral nerve sheath tumor with perineurial differentiation: "malignant perineurioma". *J Cutan Pathol* 29(6), 362-367. doi: 10.1034/j.1600-0560.2001.290607.x.
- Rothwell, T.L., Papadimitriou, J.M., Xu, F.N., and Middleton, D.J. (1986). Schwannoma in the testis of a dog. *Vet Pathol* 23(5), 629-631. doi: 10.1177/030098588602300515.
- Saggini, A., Di Prete, M., D'Amico, F., Lora, V., and Orlandi, A. (2019). Glandular Schwannoma: An Uncommon Variant of Schwannoma with Controversial Histogenesis. *Dermatopathology (Basel)* 6(4), 206-212. doi: 10.1159/000503599.

- Sakurai, M., Azuma, K., Nagai, A., Fujioka, T., Sunden, Y., Shimada, A., et al. (2016). Neurolymphomatosis in a cat. *J Vet Med Sci* 78(6), 1063-1066. doi: 10.1292/jvms.15-0553.
- Sato, H., Hiroshima, S., Anei, R., and Kamada, K. (2019). Primary neurolymphomatosis of the trigeminal nerve. *Br J Neurosurg*, 1-4. doi: 10.1080/02688697.2019.1568391.
- Sato, T., Yamamoto, A., Shibuya, H., Sudo, H., Shirai, W., and Amemori, T. (2005). Intraocular peripheral nerve sheath tumor in a dog. *Vet Ophthalmol* 8(4), 283-286. doi: 10.1111/j.1463-5224.2005.00398.x.
- Schaefer, I.M., Fletcher, C.D., and Hornick, J.L. (2016). Loss of H3K27 trimethylation distinguishes malignant peripheral nerve sheath tumors from histologic mimics. *Mod Pathol* 29(1), 4-13. doi: 10.1038/modpathol.2015.134.
- Schaffer, P.A., Charles, J.B., Tzipory, L., Ficociello, J.E., Marvel, S.J., Barrera, J., et al. (2012). Neurolymphomatosis in a dog with B-cell lymphoma. *Vet Pathol* 49(5), 771-774. doi: 10.1177/0300985811419531.
- Scholzen, T., and Gerdes, J. (2000). The Ki-67 protein: from the known and the unknown. *J Cell Physiol* 182(3), 311-322. doi: 10.1002/(sici)1097-4652(200003)182:3<311::Aid-jcp1>3.0.Co;2-9.
- Schöniger, S., and Summers, B.A. (2009). Localized, plexiform, diffuse, and other variants of neurofibroma in 12 dogs, 2 horses, and a chicken. *Vet Pathol* 46(5), 904-915. doi: 10.1354/vp.08-VP-0322-S-FL.
- Schöniger, S., Valentine, B.A., Fernandez, C.J., and Summers, B.A. (2011). Cutaneous schwannomas in 22 horses. *Vet Pathol* 48(2), 433-442. doi: 10.1177/0300985810377072.
- Schulman, F.Y., Johnson, T.O., Facemire, P.R., and Fanburg-Smith, J.C. (2009). Feline peripheral nerve sheath tumors: histologic, immunohistochemical, and clinicopathologic correlation (59 tumors in 53 cats). *Vet Pathol* 46(6), 1166-1180. doi: 10.1354/vp.08-VP-0327-S-FL.

- Shimada, S., Tsuzuki, T., Kuroda, M., Nagasaka, T., Hara, K., Takahashi, E., et al. (2007). Nestin expression as a new marker in malignant peripheral nerve sheath tumors. *Pathol Int* 57(2), 60-67. doi: 10.1111/j.1440-1827.2006.02059.x.
- Silva, E.O., Goiozo, P.F.I., Pereira, L.G., Headley, S.A., and Bracarense, A. (2017). Concomitant Malignant Pulmonary Peripheral Nerve Sheath Tumour and Benign Cutaneous Peripheral Nerve Sheath Tumour in a Dog. *J Comp Pathol* 157(1), 46-50. doi: 10.1016/j.jcpa.2017.05.002.
- Snyder, L.A., Linder, K.E., and Neel, J.A. (2007). Malignant peripheral nerve sheath tumor in a hamster. *J Am Assoc Lab Anim Sci* 46(6), 55-57.
- Sprinkle, T.J. (1989). 2',3'-cyclic nucleotide 3'-phosphodiesterase, an oligodendrocyte-Schwann cell and myelin-associated enzyme of the nervous system. *Crit Rev Neurobiol* 4(3), 235-301.
- Stanton, C., Perentes, E., Collins, V.P., and Rubinstein, L.J. (1987). GFA protein reactivity in nerve sheath tumors: a polyvalent and monoclonal antibody study. *J Neuropathol Exp Neurol* 46(6), 634-643. doi: 10.1097/00005072-198711000-00003.
- Stilwell, J.M., and Rissi, D.R. (2019). Pathology and immunohistochemistry of a malignant nerve sheath tumor in a pig: case report and brief review of the literature. *J Vet Diagn Invest* 31(1), 122-127. doi: 10.1177/1040638718820949.
- Stoica, G., Tasca, S.I., and Kim, H.T. (2001). Point mutation of neu oncogene in animal peripheral nerve sheath tumors. *Vet Pathol* 38(6), 679-688. doi: 10.1354/vp.38-6-679.
- Sugita, S., Aoyama, T., Emori, M., Kido, T., Takenami, T., Sakuraba, K., et al. (2021). Assessment of H3K27me3 immunohistochemistry and combination of NF1 and p16 deletions by fluorescence in situ hybridization in the differential diagnosis of malignant peripheral nerve sheath tumor and its histological mimics. *Diagn Pathol* 16(1), 79. doi: 10.1186/s13000-021-01140-0.
- Sundberg, J.P., Burnstein, T., Page, E.H., Kirkham, W.W., and Robinson, F.R. (1977). Neoplasms of Equidae. *J Am Vet Med Assoc* 170(2), 150-152.
- Suzuki, S., Uchida, K., and Nakayama, H. (2014). The effects of tumor location on diagnostic criteria for canine malignant peripheral nerve sheath tumors (MPNSTs) and the markers

- for distinction between canine MPNSTs and canine perivascular wall tumors. *Vet Pathol* 51(4), 722-736. doi: 10.1177/0300985813501336.
- Tafti, D.A., Dearborn, M.C., Ornoff, A., Moeck, A.R., and Cecava, N.D. (2021). Nerve Sheath Myxoma in the Lower Extremity: A Rare Case with Description of Magnetic Resonance Imaging and Sonographic Findings. *Am J Case Rep* 22, e927922. doi: 10.12659/ajcr.927922.
- Tascos, N.A., Parr, J., and Gonatas, N.K. (1982). Immunocytochemical study of the glial fibrillary acidic protein in human neoplasms of the central nervous system. *Hum Pathol* 13(5), 454-458. doi: 10.1016/s0046-8177(82)80028-2.
- Tekavec, K., Švara, T., Knific, T., Gombač, M., and Cantile, C. (2022a). Histopathological and Immunohistochemical Evaluation of Canine Nerve Sheath Tumors and Proposal for an Updated Classification. *Veterinary Sciences* 9(5), 204.
- Tekavec, K., Švara, T., Knific, T., Mlakar, J., Gombač, M., and Cantile, C. (2022b). Loss of H3K27me3 expression in canine nerve sheath tumors. *Frontiers in Veterinary Science* 9. doi: 10.3389/fvets.2022.921720.
- Thomason, J.D., Rapoport, G., Fallaw, T., Calvert, C.A., and Sakamoto, K. (2015). Pulmonary edema secondary to a cardiac schwannoma in a dog. *J Vet Cardiol* 17(2), 149-153. doi: 10.1016/j.jvc.2015.01.006.
- Thway, K., and Fisher, C. (2014). Malignant peripheral nerve sheath tumor: pathology and genetics. *Ann Diagn Pathol* 18(2), 109-116. doi: 10.1016/j.anndiagpath.2013.10.007.
- Treggiari, E., Pedro, B., Dukes-McEwan, J., Gelzer, A.R., and Blackwood, L. (2017). A descriptive review of cardiac tumours in dogs and cats. *Vet Comp Oncol* 15(2), 273-288. doi: 10.1111/vco.12167.
- Trojer, P., and Reinberg, D. (2007). Facultative heterochromatin: is there a distinctive molecular signature? *Mol Cell* 28(1), 1-13. doi: 10.1016/j.molcel.2007.09.011.
- Ueno, H., Miyoshi, K., Fukui, S., Kondo, Y., Matsuda, K., and Uchide, T. (2014). Extranodal lymphoma with peripheral nervous system involvement in a dog. *J Vet Med Sci* 76(5), 723-727. doi: 10.1292/jvms.13-0159.

- Val-Bernal, J.F., and González-Vela, M.C. (2005). Cutaneous lipomatous neurofibroma: characterization and frequency. *J Cutan Pathol* 32(4), 274-279. doi: 10.1111/j.0303-6987.2005.00311.x.
- Vandavelde, M., Higgins, R.J., and Oevermann, A. (2012). *Veterinary neuropathology: essentials of theory and practice*. Oxford: Wiley-Blackwell.
- Veazey, R.S., Angel, K.L., Snider, T.G., 3rd, Lopez, M.K., and Taylor, H.W. (1993). Malignant schwannoma in a goat. *J Vet Diagn Invest* 5(3), 454-458. doi: 10.1177/104063879300500330.
- Vogel, U.S., and Thompson, R.J. (1988). Molecular structure, localization, and possible functions of the myelin-associated enzyme 2',3'-cyclic nucleotide 3'-phosphodiesterase. *J Neurochem* 50(6), 1667-1677. doi: 10.1111/j.1471-4159.1988.tb02461.x.
- Volmer, C., Caplier, L., Reyes-Gomez, E., Huet, H., Owen, R.A., and Fontaine, J.J. (2010). An atypical peripheral nerve sheath tumour with pseudoglandular architecture in a dog. *J Vet Med Sci* 72(2), 249-251. doi: 10.1292/jvms.09-0362.
- Vom Hagen, F., Romkes, G., Kershaw, O., and Eule, J.C. (2015). Malignant peripheral nerve sheath tumor of the third eyelid in a 3-year-old Rhodesian Ridgeback. *Clin Case Rep* 3(1), 50-56. doi: 10.1002/ccr3.146.
- Warren, A.L., Miller, A.D., de Lahunta, A., Kortz, G., and Summers, B.A. (2020). Four Cases of the Melanotic Variant of Malignant Nerve Sheath Tumour: a Rare, Aggressive Neoplasm in Young Dogs with a Predilection for the Spinal Cord. *J Comp Pathol* 178, 1-8. doi: 10.1016/j.jcpa.2020.03.010.
- Watanabe, T., Oda, Y., Tamiya, S., Kinukawa, N., Masuda, K., and Tsuneyoshi, M. (2001). Malignant peripheral nerve sheath tumours: high Ki67 labelling index is the significant prognostic indicator. *Histopathology* 39(2), 187-197. doi: 10.1046/j.1365-2559.2001.01176.x.
- Watrous, B.J., Lipscomb, T.P., Heidel, J.R., and Normal, L.M. (1999). Malignant peripheral nerve sheath tumor in a cat. *Vet Radiol Ultrasound* 40(6), 638-640. doi: 10.1111/j.1740-8261.1999.tb00892.x.

- Wei, Y., Xia, W., Zhang, Z., Liu, J., Wang, H., Adsay, N.V., et al. (2008). Loss of trimethylation at lysine 27 of histone H3 is a predictor of poor outcome in breast, ovarian, and pancreatic cancers. *Mol Carcinog* 47(9), 701-706. doi: 10.1002/mc.20413.
- Woodhoo, A., and Sommer, L. (2008). Development of the Schwann cell lineage: from the neural crest to the myelinated nerve. *Glia* 56(14), 1481-1490. doi: 10.1002/glia.20723.
- Woodruff, J.M., and Christensen, W.N. (1993). Glandular peripheral nerve sheath tumors. *Cancer* 72(12), 3618-3628. doi: 10.1002/1097-0142(19931215)72:12<3618::aid-ncr2820721212>3.0.co;2-#.
- Yamaguchi, U., Hasegawa, T., Hirose, T., Fugo, K., Mitsuhashi, T., Shimizu, M., et al. (2003). Sclerosing perineurioma: a clinicopathological study of five cases and diagnostic utility of immunohistochemical staining for GLUT1. *Virchows Arch* 443(2), 159-163. doi: 10.1007/s00428-003-0849-4.
- Yamanaka, R., and Hayano, A. (2017). Radiation-Induced Malignant Peripheral Nerve Sheath Tumors: A Systematic Review. *World Neurosurg* 105, 961-970.e968. doi: 10.1016/j.wneu.2017.06.010.
- Yang, Z., and Wang, K.K. (2015). Glial fibrillary acidic protein: from intermediate filament assembly and gliosis to neurobiomarker. *Trends Neurosci* 38(6), 364-374. doi: 10.1016/j.tins.2015.04.003.
- Yoshida, S.O., and Toot, B.V. (1993). Benign glandular schwannoma. *Am J Clin Pathol* 100(2), 167-170. doi: 10.1093/ajcp/100.2.167.
- Zamecnik, M. (2003). Perineurioma with adipocytes (lipomatous perineurioma). *Am J Dermatopathol* 25(2), 171-173; author reply 173-174. doi: 10.1097/00000372-200304000-00018.

## 8 OTHER ACTIVITIES

Activities related to the Ph.D. research project:

- Studying neuropathology; a review of the current literature and participation in the diagnostic procedure of neurological cases.
- Performing autopsies on animals with neurological clinical signs in collaboration with veterinary clinics.
- Discussion on neuropathological cases in small and large animals.
- Discussion on recent peer-reviewed publications in veterinary and human neuropathology.

General activities on veterinary pathology:

- Performing histopathological and cytological diagnostics in various animal species.
- Performing immunohistochemistry; from the selection of appropriate primary antibodies and positive controls to staining procedures and interpretation.
- Training for the deputy and appointment of the deputy of the head of the National Reference Laboratory for Transmissible Spongiform Encephalopathies in Slovenia.

Teaching activity:

- Practical classes of Pathology with 2<sup>nd</sup>- and 3<sup>rd</sup>-year students of the Veterinary Faculty of the University of Ljubljana (necropsy and histopathology).
- Practical classes of elective courses Pathomorphological practice and Cytopathological practice with 4<sup>th</sup>-, 5<sup>th</sup>-, and 6<sup>th</sup>-year students of the Veterinary Faculty of the University of Ljubljana (necropsy and histopathology, clinical pathology).

Attendance at congresses, conferences, symposia, workshops, and seminars:

- Annual seminar of the French Society of Veterinary Pathology: “Update on gastrointestinal biopsies and clinicopathological correlations” (12. 12. – 14. 12. 2019, SFAPV, Maisons-Alfort).

- Symposium: “Tumors with NTRK fusion – diagnosis and treatment” (14. 11. 2019, Institute of Pathology, Faculty of Medicine, University of Ljubljana, Slovenia).
- International conference: “Brain tumors: from bench to clinic” (26. 11. 2019, University Medical Center, Interreg Italia-Slovenija, Trans-Glioma. University Medical Center, Ljubljana, Slovenia).
- Workshop “Getting the Hang of Hematology” by Dr. Kate Schlicher Baker (28. 4. – 2. 5. 2020, *online workshop*).
- Free Friday Webinar: “Tumors of the Peripheral Nervous System” by Dr. Kevin Woolard (12. 6. 2020, Davis-Thompson DVM Foundation, *online meeting*).
- Annual Meeting of the National Reference Laboratories for Mollusc Diseases (7. 7. 2020, *online meeting*).
- Meeting of the EURL for TSE: 2019 round of TSE EURL EQAs: Results feedback. Turin, Italy (16. 9. 2020 – 18. 9. 2020, *online meeting*).
- Free Friday Webinar: “Examine the “fresh” brain” by Dr. Raquel Rech (25. 9. 2020, Davis-Thompson DVM Foundation, *online meeting*).
- The II. Seminar of the Mexican Subdivision of the Davis-Thompson Foundation: “Congenital lesions of the central nervous system & Infectious diseases of the CNS – viral and protozoal” by Dr. Kevin Woolard (30. 9. – 1. 1. 2020, Davis-Thompson DVM Foundation, *online meeting*).
- Seminar: “Innovative evaluation of knowledge of science students” by Iztok Devetak (13. 11. 2021, *online meeting*. University of Ljubljana, Ljubljana, Slovenia).
- Seminar: “The importance of necropsy and additional investigations in the work of the clinical veterinarian” (2. 3. 2021, Institute of Pathology, Wild Animals, Fish and Bees, Veterinary Faculty, University of Ljubljana, *online meeting*. Lecturers: Mitja Gombač, Tanja Švara, Kristina Tekavec).
- 2021 Annual Meeting & Workshop of NRLs for Mollusc Diseases (16. 3. – 19. 3. 2021, *online meeting*).
- Seminar: “Questions for encouraging greater student activity” by Andreja Lavrič (22. 4. 2021, *online meeting*. University of Ljubljana, Ljubljana, Slovenia).
- Seminar: “Didactic structure of a student-centered teaching method” by Assoc. Prof. Sonja Rutar (5. 11. 2022, *online meeting*. University of Primorska, Slovenia).

- 2022 Annual Meeting of NRLs for Mollusc Diseases (28. 3. – 29. 3. 2022, *online meeting*).
- Seminars: “Remyelination of the CNS; is it useful and how can it be achieved?” and “From muscle to the CNS; a personal tour of what can go wrong in dogs and cats.” by Prof. Ian Duncan from the University of Wisconsin (20. 05. 2022, Department of Veterinary Sciences, University of Pisa, Pisa).
- Virtual Neuropathology Rotation at Mount Sinai School of Medicine, New York, US. Attendings: Dr. Nadejda Tsankova, Dr. Melissa Umphlett, Dr. John Crary (6. 6. – 30. 6. 2022, *virtual observership*).
- 28<sup>th</sup> Ljudevit Jurak International Symposium on Comparative Pathology with One Health Session (10. 6. – 11. 6. 2022, Zagreb, Croatia).
- 19th TSE EURL/NRL Annual Meeting (17. 10. – 18. 10. 2022, Turin, Italy).

Course participation:

- Academic English I – English for Research Publication and Presentation Purposes. Lecturer: Joanne Spataro, *Il Centro Linguistico dell'Università di Pisa* (January – April 2020, Scuola Medica, via Roma n. 55, Dipar. Anatomia & online CLI website).
- Italian Language Course A1. Lecturer: Kaja Katarina Breclj, The Faculty of Arts, University of Ljubljana, Slovenia (October 2019 – June 2020, The Faculty of Arts, University of Ljubljana, Ljubljana, Slovenia & online Zoom platform).
- Veterinary Clinical Neuropathology, lectures in Master’s degree program. Lecturer: Prof. Dr. Carlo Cantile, Department of Veterinary Sciences, University of Pisa (March – April 2020, online – MS Teams).
- C1+ English for Research Purposes. Lecturer: Joanne Spataro, *Il Centro Linguistico dell'Università di Pisa* (October – December 2020, online CLI website).
- Statistical methods for data analysis. Lecturer: Katarina Košmelj. University of Ljubljana, Biotechnical Faculty (January – February 2021, online platform).
- Veterinary Clinical Neuropathology, lectures in Master’s degree program. Lecturer: Prof. Dr. Carlo Cantile, Department of Veterinary Sciences, University of Pisa (April – June 2021, online – MS Teams).

Study period abroad:

- During the COVID-19 epidemic, most of my study period was done at the Institute of Pathology, Wild Animals, Fish and Bees of the Veterinary Faculty, University of Ljubljana, Ljubljana, Slovenia, under the supervision of Assist. Prof. Dr. Tanja Švara and in constant contact with my supervisor, Prof. Dr. Carlo Cantile.
- 14. 2. – 20. 4. 2022: Visiting the Department of Pathology and Forensic Veterinary Medicine and Ethics, Faculty of Veterinary Medicine of the University "Ss. Cyril and Methodius", Skopje, Republic of North Macedonia.
- 15. 8. – 16. 9. 2022: Externship in the Clinical Pathology Laboratory of the University of Pennsylvania, School of Veterinary Medicine, Philadelphia, Pennsylvania, United States of America.

Publications:

a) Articles in scientific journals:

- Gorazd Vengušt, Kristina Tekavec, Tina Pirš, Tanja Švara, Diana Žele Vengušt. Atypical actinomycotic pyogranuloma of the frontal and parietal region in a roe deer (*Capreolus capreolus*) – a case report. *Veterinarski Arhiv* 2020; 90(4): 429-434.
- Mitja Gombač, Marija Seničar, Tanja Švara, Sabina Šturm, Tamara Dolensšek, Kristina Tekavec, Vesna Cerkvenc Flajs, Heike Schmidt-Posthaus. Sudden outbreak of metastatic intestinal adenocarcinoma in rainbow trout *Oncorhynchus mykiss*. *Dis Aquat Organ*. 2021; 144: 237-244.
- Kristina Tekavec, Tanja Švara, Tanja Knific, Mitja Gombač, Carlo Cantile. Histopathological and immunohistochemical evaluation of canine nerve sheath tumors and proposal for an updated classification. *Vet Sci* 2022; 9(5): 204.
- Kristina Tekavec, Tanja Švara, Tanja Knific, Jernej Mlakar, Mitja Gombač, Carlo Cantile. Loss of H3K27me3 expression in canine nerve sheath tumors. *Front Vet Sci* 2022; 9.

b) Congress proceedings:

- Kristina Tekavec, Mitja Gombač, Carlo Cantile. Morphological features of high-grade canine gliomas/Caratteristiche morfologiche del glioma di alto grado del

cane (International conference “Brain tumors: from bench to clinic”. University Medical Center, Interreg Italia-Slovenia, Trans-Glioma, Ljubljana, 26. 11. 2019).

The abstract and poster presented at the conference are provided in the supplementary material (**Supplementary Figures 1 and 2**).

- Pavel Kvapil, Marjan Kastelic, Nika Kojc, Mitja Gombač, Sabina Šturm, Peter Kržan, Marko Cvetko, Kristina Tekavec, Tamara Dolenšek, Katarina Pavlin, Vesna Cerkvenc Flajs, Tanja Švara. Renal mixed epithelial and stromal tumor with widespread metastasis in a Siberian tiger (*Panthera tigris altaica*). In: Charlotte Kirk Baer (ed.). Proceedings 2021: Joint American association of ZOO veterinarians [and] European association of ZOO and wildlife veterinarians conference (4. 10. – 5. 11. 2021, *virtual conference*).
- Kristina Tekavec, Tanja Švara, Tanja Knific, Jernej Mlakar, Mitja Gombač, Carlo Cantile. Proposal for an update: Can the classification of canine nerve sheath tumors follow the human WHO classification? (28<sup>th</sup> Ljudevit Jurak International Symposium on Comparative Pathology with One Health Session. Zagreb, 10. – 11. 6. 2022).

The poster received the “Dr. Suzana Tkalčić ONE HEALTH award” for the best interprofessional student/resident teamwork (veterinary and human medicine students) poster presentation on the topic of comparative pathology/medicine.

The abstract and poster presented at the symposium are provided in the supplementary material (**Supplementary Figures 3 and 4**).

## 9 SUPPLEMENTARY MATERIAL

**Supplementary Table 1:** Evaluation of the tissue and cellular criteria of nerve sheath tumors.

| <b>TISSUE CRITERIA</b>  |  |
|---|--|
| Circumscription   | <ul style="list-style-type: none"> <li>• Well circumscribed</li> <li>• Ill-defined</li> </ul>  |
| Encapsulation   | <ul style="list-style-type: none"> <li>• Encapsulated</li> <li>• Capsule invaded</li> <li>• Incomplete fibrous pseudocapsule</li> <li>• Unencapsulated</li> </ul>  |
| Shape   | <ul style="list-style-type: none"> <li>• Nodular/multilobular/cystic/other:</li> </ul>   |
| Cellularity   | <ul style="list-style-type: none"> <li>• Low</li> <li>• Moderate</li> <li>• High</li> </ul>  |
| Growth pattern;<br>The proportion of each growth pattern<br>(0) absent, (1) <25%,<br>(2) 25 – 50%, (3) 50 – 75%, (4) > 75%) | <p><u>Overall microscopical appearance:</u></p> <ul style="list-style-type: none"> <li>- Heterogeneous</li> <li>- Uniform</li> </ul> <ul style="list-style-type: none"> <li>• Antoni type A (interlacing bundles, storiform, concentric)</li> <li>• Antoni type B (loose textured)</li> </ul> <p>Sheets/cords/meshwork of reticular fibers/rossettelike formations/sweeping fascicles/whorls/storiform pattern /plexiform pattern/other:</p> |
| Stroma  | <p><u>Amount:</u></p> <ul style="list-style-type: none"> <li>• Small</li> <li>• Moderate</li> <li>• Large</li> </ul> <p><u>Type of stroma:</u> collagenous/myxoid/fine/coarse/fibrovascular/fibrous/other:</p>   |
| Necrosis  | <ul style="list-style-type: none"> <li>• Absent</li> <li>• Present, ≤50%</li> <li>• Present, &gt;50%</li> </ul>  |
| Hemorrhages   | <ul style="list-style-type: none"> <li>• Absent</li> <li>• Present</li> </ul>  |
| Vascular invasion   | <ul style="list-style-type: none"> <li>• Absent</li> <li>• Blood vessel invasion</li> <li>• Lymphatic vessel invasion</li> <li>• Blood and lymphatic vessel invasion</li> </ul>  |
| Herniation into vessels   | <ul style="list-style-type: none"> <li>• Absent</li> <li>• Present</li> </ul>  |
| Inflammatory infiltrates  | <ul style="list-style-type: none"> <li>• Absent</li> <li>• Present</li> <li>- Type: _____</li> <li>- The extent of inflammation</li> <li>- Location (perivascular, within the capsule, etc.):</li> </ul>   |
| Hyalinization   | <ul style="list-style-type: none"> <li>• Absent</li> <li>• Present</li> </ul>  |

|   |  |   |
|---|--|---|
| Osteoid components  | <ul style="list-style-type: none"> <li>• Absent</li> <li>• Present</li> </ul>  |   |
| Cartilaginous components                                      | <ul style="list-style-type: none"> <li>• Absent</li> <li>• Present</li> </ul>  |   |
| <b>CELLULAR CRITERIA</b>                                      |  |   |
| Cellular morphology   | Spindle/oval/polygonal/fusiform/onion-bulb-like formations/signet ring-like/epithelioid/other:   |   |
| Anisocytosis  | <ul style="list-style-type: none"> <li>• Mild</li> <li>• Moderate</li> <li>• Strong</li> </ul>   |   |
| Anisokaryosis   | <ul style="list-style-type: none"> <li>• Mild</li> <li>• Moderate</li> <li>• Strong</li> </ul>   |   |
| Nuclear characteristics                                       | <u>Nuclear pleomorphism:</u> <ul style="list-style-type: none"> <li>• Absent</li> <li>• Present:                             <ul style="list-style-type: none"> <li>- Mild</li> <li>- Moderate</li> <li>- Strong</li> </ul> </li> </ul> <u>Nuclear shape:</u> oval/round/elongated/bean-shaped/vesicular/hyperchromatic/other: |   |
| Nucleoli  | <ul style="list-style-type: none"> <li>• Not evident</li> <li>• Prominent</li> <li>- Number of nucleoli – up to _____</li> <li>- Shape of nucleoli</li> </ul>  |   |
| Cytoplasm   | <u>Amount:</u> <ul style="list-style-type: none"> <li>• Small</li> <li>• Moderate</li> <li>• Large</li> </ul>  | <u>Color:</u><br><u>Character:</u> <ul style="list-style-type: none"> <li>• <i>Homogenous</i></li> <li>• <i>Granular</i></li> <li>• <i>Containing pigment</i></li> <li>• <i>Other:</i></li> </ul> |
| Cell borders  | <ul style="list-style-type: none"> <li>• Distinct</li> <li>• Indistinct</li> </ul>   |   |
| Mitoses<br>((1) 0-9/10 HPF, (2) 10-19/10 HPF, (3) >19/10 HPF) | 1/    2/    3/    4/    5/<br>6/    7/    8/    9/    10/<br>MC = _____/10 HPF<br>Max. number of mitoses per HPF:<br>Presence of atypical mitotic figures:   |   |
| Multinucleated cells  | <ul style="list-style-type: none"> <li>• Absent</li> <li>• Present → Up to _____ nuclei</li> </ul>   |   |

## Morphological features of high-grade canine gliomas

Kristina Tekavec<sup>1</sup>, Mitja Gombač<sup>1</sup>, Carlo Cantile<sup>2</sup>

<sup>1</sup>*Veterinary faculty, University of Ljubljana;* <sup>2</sup>*Department of Veterinary Science, University of Pisa*

Domestic canine patients with spontaneous high-grade gliomas provide us with a unique opportunity to study naturally-occurring disease in higher-order mammals whose brain and body often differ only moderately in size and complexity from human patients. Because these dogs live in close physical proximity to their owners, they often encounter many of the same indoor and outdoor environmental exposures as well.

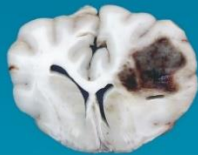
Some studies report the incidence of primary brain tumors ranging from 20 per 100,000 (0.02%) in a population of dogs in the United Kingdom in a single year, to 1.9% of a population of 6,175 dogs necropsied in a multi-year single-center study in the United States, with 70% of those being gliomas.

In this study we retrieved the clinical data and neuropathological reports of a 10-year record of high-grade canine gliomas collected at the Department of Veterinary Science of the University of Pisa from 2009 to 2018. In 51 affected dogs, tumors included 13 glioblastomas, 2 gliosarcomas, 16 gliomatosis cerebri, and 20 anaplastic oligodendrogliomas. The mean age was 7.8 years and the incidence rate ratio was 1.55 for males/females. Brachycephalic canine breeds, such as Boxer and Bulldog, were overrepresented. Localization of the tumors was mainly supratentorial (34/51), and in 5 cases in the spinal cord. Diffuse and invasive growth, highly pleomorphic cell populations, high mitotic rates, areas of necrosis flanked by pseudopalisading cells, and peripheral tortuous to glomeruloid neovascularization were characteristic of high-grade canine tumors.

Dogs, in general, and certain breeds disproportionately, suffer from gliomas very similar in gross and histopathological appearance to their human counterparts. Appropriate investigation on canine high-grade glioma could serve as a valuable large-animal model for promising insights on the corresponding human disease.

**Supplementary Figure 1:** Abstract published in the abstract book of International conference »Brain tumors: from bench to clinic«. University Medical Center, Interreg Italia-Slovenia, Trans-Glioma, Ljubljana, 26. 11. 2019.

# Morphological features of high-grade canine gliomas



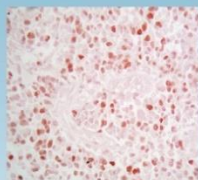
Gross picture of high-grade canine glioma.



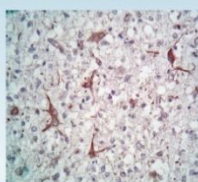
Giant cells displaying abundant cytoplasm and marked anisonucleosis (H&E, 400x)



Extensive necrosis and thrombosis (H&E, 100x)



Cell proliferation is immunolabeled with nuclear antigen Ki-67 (Ki-67 IHC, 400x)



A few neoplastic astrocytes express nestin (Nestin IHC, 400x)

Kristina Tekavec [1, 2], Mitja Gombač [1], Carlo Cantile [2]

1 Institute for Pathology, Wild Animals, Fish and Bees, Veterinary Faculty, University of Ljubljana, Ljubljana, Slovenia,  
2 Department of Veterinary Science, University of Pisa, Pisa, Italy

## INTRODUCTION

Domestic canine patients with spontaneous high-grade gliomas provide us with a unique opportunity to study naturally occurring disease in higher-order mammals whose brain and body often differ only moderately in size and complexity from human patients. Because these dogs live in close physical proximity to their owners, they often encounter many of the same indoor and outdoor environmental exposures as well [1, 2].

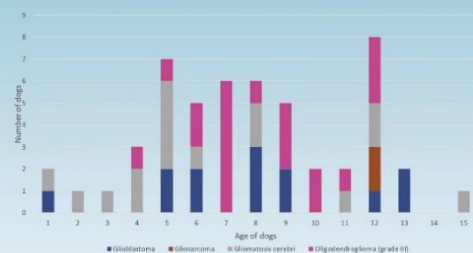
As the veterinary WHO classification system for nervous system tumors has not been updated since 1999 and the classic gross and histopathological features of canine gliomas appear very similar to their human counterparts, some veterinary pathologists often grade canine gliomas according to human diagnostic criteria [3, 4].

## MATERIAL AND METHODS

In this study we retrieved the clinical data and neuropathological reports of a 10-year record of high-grade canine gliomas collected at the Department of Veterinary Science of the University of Pisa from 2009 to 2018. Fifty-one dogs with different types of high-grade glioma were included in the study. Diagnoses were based on macroscopically and histopathological examination together with the immunohistochemical staining of the central nervous system lesions.

## RESULTS

In 51 affected dogs, tumors included 13 glioblastomas, 2 gliosarcomas, 16 gliomatosis cerebri, and 20 anaplastic oligodendrogliomas. The mean age was 7.8 years and the incidence rate ratio was 1.55 for males/females. Brachycephalic canine breeds, such as Boxer and Bulldog, were overrepresented. Localization of the tumors was mainly supratentorial (34/51), and in 5 cases in the spinal cord. Diffuse and invasive growth, highly pleomorphic cell populations, high mitotic rates, areas of necrosis flanked by pseudopalisading cells, and peripheral tortuous to glomeruloid neovascularization were characteristic of high-grade canine gliomas.



## CONCLUSION

Dogs, in general, and certain breeds disproportionately, suffer from gliomas very similar in gross and histopathological appearance to their human counterparts. Appropriate investigation on canine high-grade glioma could serve as a valuable large-animal model for promising insights on the corresponding human disease.



## REFERENCES

1. Parker HG, et al. Genetic structure of the purebred domestic dog. *Science*. 2004. 304(5674): 1160-1164.
2. Koehler JW, et al. A revised diagnostic classification of canine glioma: towards validation of the canine glioma patient as a naturally occurring preclinical model for human glioma. *J Neuropathol Exp Neurol*. 2018. 77(11): 1039-1054.
3. Koestner A, et al. *Histological classification of tumors of the central nervous system of domestic animals*. 2nd series, Vol. V, AFIP, Washington DC, 1999.
4. Louis DN, et al. The 2016 World Health Organization classification of tumors of the central nervous system: a summary. *Acta Neuropathol*. 2016. 131(6): 803-820.

CONTACT: kristina.tekavec@vf.uni-lj.si, carlo.cantile@unipi.it

Poster Presentations

**P50** **PROPOSAL FOR AN UPDATE:  
CAN THE CLASSIFICATION OF CANINE NERVE SHEATH  
TUMORS FOLLOW THE HUMAN WHO CLASSIFICATION?**

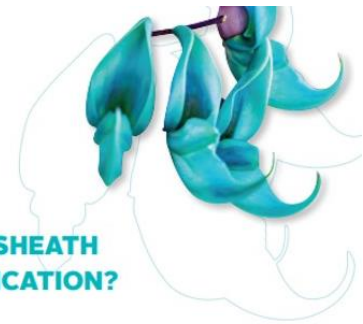
*Kristina Tekavec<sup>1,2</sup>, Tanja Švara<sup>2</sup>, Tanja Knific<sup>3</sup>, Jernej Mlakar<sup>4</sup>,  
Mitja Gombač<sup>2</sup>, Carlo Cantile<sup>1</sup>*

<sup>1</sup> Department of Veterinary Sciences, University of Pisa, Pisa, Italy

<sup>2</sup> Institute of Pathology, Wild Animals, Fish and Bees, Veterinary Faculty,  
University of Ljubljana, Ljubljana, Slovenia

<sup>3</sup> Institute of Food Safety, Feed and Environment, Veterinary Faculty,  
University of Ljubljana, Ljubljana, Slovenia

<sup>4</sup> Institute of Pathology, Faculty of Medicine, University of Ljubljana, Ljubljana, Slovenia



Nerve sheath tumors (NSTs) are a group of tumors arising from Schwann cells, perineurial cells, and/or endoneurial or epineurial fibroblasts. In veterinary pathology, the terminology of NSTs remains inconsistent and sometimes confusing, and many pathologists follow the human classification of such tumors in practice. In particular, malignant NSTs often lack specific histopathological and immunohistochemical (IHC) features, making it difficult to distinguish them from other neoplastic lesions. In our study, we histopathologically reevaluated 79 canine NSTs and assessed their reactivity for the IHC markers Sox10, claudin-1, GFAP, CNPase, H3K27me3, and Ki-67. Based on the results, we classified the tumors according to the latest human WHO classification and evaluated the potential diagnostic utility of the IHC markers tested. Twelve cases were diagnosed as benign nerve sheath tumors, including six neurofibromas, three nerve sheath myxomas, two hybrid nerve sheath tumors (perineurioma/neurofibroma and

perineurioma/schwannoma), and one schwannoma. Sixty-seven tumors were malignant nerve sheath tumors, including 56 conventional, four perineural, one epithelioid malignant nerve sheath tumor, and six malignant nerve sheath tumors with divergent differentiation. We identified Sox10, claudin-1, GFAP, and Ki-67 as useful IHC markers, whereas CNPase was found to be of no value in the diagnosis of canine NSTs. We found a complete loss of H3K27me3 expression in 25% of NSTs and believe that this marker, in combination with other IHC markers, may also be useful for the diagnosis of NSTs. Considering our results and incorporating data from the literature, we believe that an updated classification of NSTs in dogs using the proposed IHC panel could largely follow the recent human WHO classification of such tumors, but prospective studies monitoring the clinical course of the disease would be needed to assess its prognostic value.

81

# Proposal for an Update: Can the Classification of Canine Nerve Sheath Tumors Follow the Human WHO Classification?

Kristina Tekavec <sup>1,2\*</sup>, Tanja Švara <sup>2</sup>, Tanja Knific <sup>3</sup>, Jernej Mlakar <sup>4</sup>, Mitja Gombač <sup>2</sup>, Carlo Cantile <sup>1</sup>

<sup>1</sup> Department of Veterinary Sciences, University of Pisa, Pisa, Italy; \*kristina.tekavec@vf.uni-lj.si

<sup>2</sup> Institute of Pathology, Wild Animals, Fish and Bees, Veterinary Faculty, University of Ljubljana, Ljubljana, Slovenia

<sup>3</sup> Institute of Food Safety, Feed and Environment, Veterinary Faculty, University of Ljubljana, Ljubljana, Slovenia

<sup>4</sup> Institute of Pathology, Faculty of Medicine, University of Ljubljana, Ljubljana, Slovenia

## Introduction

Nerve sheath tumors (NSTs) are a group of tumors arising from Schwann cells, perineurial cells, and/or endoneurial or epineurial fibroblasts. In veterinary pathology, the terminology of NSTs remains inconsistent and sometimes confusing, and many pathologists follow the human classification of such tumors in practice [1]. Malignant NSTs (MNSTs) often lack specific histopathological and immunohistochemical (IHC) features, making it difficult to distinguish them from other neoplastic lesions [1, 2].

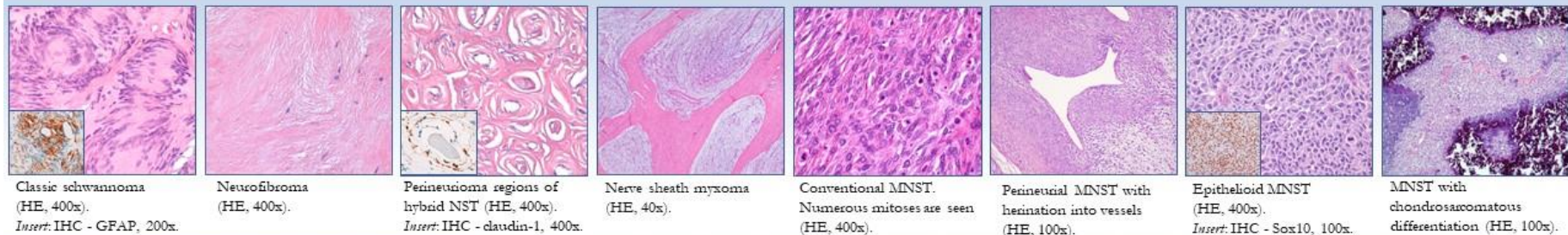
## Material and methods

We histopathologically reevaluated 79 canine NSTs and assessed their reactivity for the IHC markers Sox10, claudin-1, GFAP, CNPase, H3K27me3, and Ki-67. Based on the results, we classified the tumors according to the latest human WHO classification and evaluated the potential diagnostic utility of the IHC markers tested.

## Results

Twelve cases were diagnosed as benign NSTs, including 6 neurofibromas, 3 nerve sheath myxomas, 2 hybrid NSTs (perineurioma/neurofibroma and perineurioma/schwannoma), and 1 schwannoma. Sixty-seven tumors were MNSTs, including 56 conventional, 4 perineurial, 1 epithelioid MNST, and 6 MNSTs with divergent differentiation.

We identified Sox10, claudin-1, GFAP, and Ki-67 as useful IHC markers, whereas CNPase had no role in the diagnosis of NSTs in dogs. We found a complete loss of H3K27me3 expression in 25% of NSTs, but no statistically significant differences were found to confirm its diagnostic value.



## Conclusion

We believe that an updated classification of NSTs in dogs using the proposed IHC panel could largely follow the recent human WHO classification of such tumors, but prospective studies monitoring the clinical course of the disease would be needed to assess its prognostic value.

## References

- Higgins, R.J.; Bollen, A.W.; Dickinson, P.J.; Sisó-Llonch, S. Tumors of the Nervous System. In *Tumors in Domestic Animals*; 2016; pp. 834-891.
- Lanigan, L.G.; Russell, D.S.; Woolard, K.D.; Pardo, I.D.; Godfrey, V.; Jortner, B.S.; Burr, M.T.; Bolon, B. Comparative Pathology of the Peripheral Nervous System. *Vet Pathol* 2021, 58, 10-33.



## 10 ACKNOWLEDGMENTS

First and foremost, I would like to thank my supervisor Prof. Dr. Carlo Cantile and my co-supervisor Assist. Prof. Dr. Tanja Švara for their invaluable advice, continuous support, and patience throughout my doctoral studies.

Dr. Cantile, thank you for sharing all your knowledge, tissue archive, and enthusiasm for neuropathology with me. I am grateful for the opportunity to do my Ph.D. under your supervision.

Dr. Švara, thank you for your invaluable professional and moral support since the beginning of my career as a veterinary pathologist. I am grateful to have such a great teacher and mentor.

Sincere thanks to the members of the dissertation committee who took the time to read, comment, and improve my dissertation.

Sincere thanks to the University of Pisa for the opportunity and funding of my Ph.D. studies.

Thanks also to the Institute of Pathology, Wild Animals, Fish and Bees of the Veterinary Faculty of the University of Ljubljana, and the program group P4-0092 headed by Res. Couns. Dr. Matjaž Ocepek for the additional financial support.

Special thanks to Assoc. Prof. Dr. Mitja Gombač, Head of the Institute of Pathology, Wild Animals, Fish and Bees of the Veterinary Faculty, University of Ljubljana, who introduced me to veterinary pathology during my undergraduate studies, encouraged me in my professional career since then and contributed a lot to my professional development.

Special thanks to Assist. Dr. Tanja Knific for the statistical analysis and help in interpreting the results.

Sincere thanks to Prof. Dr. Jože Pižem and Assist. Dr. Jernej Mlakar from the Institute of Pathology, Faculty of Medicine, University of Ljubljana, for their collaboration and professional support.

Special thanks to the Laboratory of Immunohistochemistry of the Institute of Pathology, Faculty of Medicine, University of Ljubljana, especially Ajla Hajrlahović and Daniel Velkavrh, for their technical support.

Special thanks to Benjamin Cerk and Jurij Omahen from the Institute of Pathology, Wild Animals, Fish and Bees, Veterinary Faculty, University of Ljubljana, and Lisa Baroncini from

the Laboratory of Veterinary Neuropathology, Department of Veterinary Sciences, University of Pisa, for their technical support.

Thanks also to my co-workers at the Institute of Pathology, Wild Animals, Fish and Bees of the Veterinary Faculty of the University of Ljubljana for their support.

Sincere thanks to Prof. Dr. Trpe Ristoski of the Faculty of Veterinary Medicine, Department of Pathology and Forensic Veterinary Medicine and Ethics in Skopje, for his kindness and shared knowledge during my stay in North Macedonia.

Sincere thanks to Dr. Martina Piviani, Dr. Koranda Walsh, and Dr. Candice Chu, a great team of veterinary clinical pathologists in the Clinical Pathology Laboratory at the PennVet in Philadelphia, who hosted me for five weeks and shared their knowledge and advice with me. My special thanks to Martina, Paolo, and Francesco, as well as Maia, Mirtilla, Pippi, Pallino, and Vaniglia, who made me feel at home while I gained experience in the US.

Sincere thanks to my friends for their support and understanding.

Special thanks to my office mate Sabina for her friendship, help, encouragement, and great company since the beginning of our undergraduate studies.

Special thanks to Tamara, Tanja, Bojan, Jan, Katarina, and Marko for the discussions and positive energy.

Special thanks to Tea for her invaluable help with graphic designing.

Special thanks to Petra and Achille for help with bureaucratic matters, hospitality, and encouragement.

Special thanks to Malince, Gaspare, and Francesco for their friendship and company during my stay in Pisa.

My special thanks go to my parents Srečko and Marija, who have always supported my education, and to my siblings Sebastijan, Petra, Robert, Simon, and Jožica with their families. Thank you for your support and understanding.

A big thank you also goes to Andrej, Tatjana, Urška, Gašper, and Brina for their support and understanding.

Finally, I would like to give special thanks to my Jernej for his help, unwavering support, understanding, and belief in me. Thank you!